

**FACULTEIT
WETENSCHAPPEN**

Departement Chemie
Afdeling Biochemie



KATHOLIEKE
UNIVERSITEIT
LEUVEN
CAMPUS
KORTRIJK

Effects of heat and of near-UV irradiation on goat α -lactalbumin

Ann Vanhooren

Promotor :
PROF. DR. I. HANSSENS
2005

Proefschrift voorgedragen tot
het behalen van de graad van
Doctor in de Wetenschappen

“Life itself is the most wonderful fairy tale”

Hans Christian Andersen

Contents

ABBREVIATIONS

AIMS OF THE STUDY

CHAPTER 1: State of the art	1
CHAPTER 2: Structural basis for difference in heat capacity increments for Ca²⁺ binding to two α-lactalbumins	23
CHAPTER 3: Photo-excitation of tryptophan groups induces reduction of two disulfide bonds in goat α-lactalbumin	51
CHAPTER 4: Tryptophan to phenylalanine substitutions allow differentiation of short and long range conformational changes during denaturation of goat α-lactalbumin	77
CHAPTER 5: Selective mediation of tryptophan residues toward photolytic cleavage of disulfide bridges in goat α-lactalbumin	119
CHAPTER 6: Summary, conclusions and perspectives	145
CHAPTER 7: Samenvatting - Invloed van hitte en UV bestraling op geit α-lactalbumin	151

PUBLICATIONS

DANKWOORD

Abbreviations

A_1	fractional amplitude
$\alpha_{N(T)}$	fraction of native apo-LA
apo	cation depleted
BLA	bovine α -lactalbumin
c	concentration
Cam	carbamidomethylated
CD	circular dichroism
c_m	midpoint concentration of the GdnHCl-induced unfolding
ΔC_p	heat capacity change between two protein states
$\Delta C_{p, Ca^{2+}}$	heat capacity change for the binding of Ca^{2+}
$\Delta C_{p, Ca^{2+}, IN}$	heat capacity change for Ca^{2+} binding to intermediary unfolded apo-LA
$\Delta C_{p, Ca^{2+}, N}$	heat capacity change for Ca^{2+} binding to native apo-LA
$\Delta C_{p, NI}$	heat capacity change for the transition of the native to the intermediary unfolded state of apo-LA
ΔG	Gibbs free energy
ΔG_{NI}	free energy values for the transition of the native to the intermediary unfolded state of apo-LA
$\Delta G_{unf}^{5.05GdnHCl}$	free energies for unfolding in 5.05 M GdnHCl
$\Delta G_{unf}^{H_2O}$	free energie for unfolding in the absence of denaturant
$\Delta\Delta G_{unf}$	difference in the Gibbs free energy between the wild type and a particular mutant at a given GdnHCl concentration
$\Delta\Delta G_{unf}^{5.05GdnHCl}$	difference between the unfolding free energy of wild type and mutant GLA in 5.05 M GdnHCl.
$\Delta\Delta G_{unf}^\ddagger$	difference in activation free energy between the wild type and the mutant
ΔH	enthalpy exchange
$\Delta H_{Ca^{2+}, IN(T)}$	enthalpy exchange for Ca^{2+} binding to intermediary unfolded apo-LA
$\Delta H_{Ca^{2+}, exp(T)}$	molar heat exchange for Ca^{2+} binding
$-\Delta H_{Ca^{2+}, exp(T)}$	molar release of heat upon Ca^{2+} binding
$\Delta H_{Ca^{2+}, N(T)}$	enthalpy exchange for Ca^{2+} binding to native apo-LA
$\Delta H_{deprot(T)}$	deprotonation enthalpy of the buffer
ΔH_{exp}	observed enthalpy exchange

$\Delta H_{\text{NI}(298)}$	transition enthalpy at 298 K
$\Delta H_{\text{NI}(T)}$	enthalpy exchange for the transition of the native to the intermediary unfolded state of apo-LA
ΔH_{unf}	enthalpy exchange for unfolding
ΔS	entropy change
$\Delta S_{\text{NI}(298)}$	transition entropy at 298 K
ΔS_{unf}	entropy change for unfolding
DE-MALDI-TOF	delayed extraction matrix-assisted laser desorption-ionization time-of-flight
DSC	differential scanning calorimetry
DTNB	5,5'-dithiobis(2-nitrobenzoic acid)
DTT	1,4-dithiothreitol
EDTA	ethylenediaminetetra-acetate
EGTA	ethyleneglycoltetra-acetate
ESI-MS	electrospray ionization mass spectrometry
ϵ	molar absorption coefficient
f_{unf}	fraction of unfolded LA
$f_{\text{fl,int}}$	fractional change of the fluorescence intensity
$f_{\text{fl},\lambda}$	fractional change of the emission wavelength
F_{th}	the number of free thiol groups generated per protein molecule
GdnHCl	guanidine hydrochloride
GLA	goat α -lactalbumin
GT	bovine β -galactosyltransferase
HEPES	N-2-Hydroxyethylpiperazine-N'-ethane-sulfonic acid
h ν	energy of a photon
ITC	isothermal titration calorimetry
K	equilibrium constant
k_I	rate constant
$k_{\text{unf}}^{\text{mut}}$	unfolding rate constant of the mutant
$k_{\text{unf}}^{\text{wt}}$	unfolding rate constant of the wild type protein
$K_{\text{Ca}^{2+},\text{app}(T)}$	apparent Ca^{2+} -binding constant
$K_{\text{Ca}^{2+},\text{N}(T)}$	constant for Ca^{2+} binding to native apo-LA
$K_{\text{NI}(T)}$	constant for the equilibrium between native and intermediary unfolded apo-LA
LA	α -lactalbumin
λ	wavelength
λ_{max}	wavelength maximum

λ_N	wavelength of the emission maximum of native LA
λ_{obs}	observed wavelength of the emission maximum
λ_U	wavelength of the emission maximum of unfolded LA
MALDI-TOF MS	matrix-assisted laser desorption-ionization time-of-flight mass spectrometry
m_{unf}	cooperativity index
MOPS	3-(N-Morpholino)-2-hydroxypropane-sulfonic acid
M_r	molecular weight
MS/MS	tandem mass spectrometry
N	native state
n_{H^+}	number of protons released ($n_{\text{H}^+}>0$) or taken up ($n_{\text{H}^+}<0$) by the buffer
NMR	nuclear magnetic resonance
PDB	protein data bank
Q-TOF	quadrupole time-of-flight
S1	singlet state
SDS-PAGE	sodium dodecylsulfate-polyacrylamide gel electrophoresis
T_{exp}	observed temperature
$T_{\text{m,DSC}}$	transition temperature deduced from DSC
$T_{\text{m,Fl int}}$	transition temperature deduced from fluorescence intensity
$T_{\text{m,Fl } \lambda}$	transition temperature deduced from fluorescence wavelength shift
TNB ⁻	2-nitro-5-thiobenzoate ion
Tris	tris-(hydroxymethyl)-aminomethane
U	unfolded state
UV	ultraviolet
3SS-Cam-GLA	goat α -lactalbumin in which the 6-120 disulfide bond is selectively reduced and Cys6 and -120 are carbamidomethylated
3SS-GLA	goat α -lactalbumin in which the 6-120 disulfide bond is selectively reduced
^3Trp	triplet state

Aims of the study

The small, milk protein, α -lactalbumin (LA) has an important function in the mammary secretory cells as it is one of the components of lactose synthase. LA is very attractive for researchers interested in protein folding problems since it is a small molecule, easily purified and has a relative complex structure which converts to a molten globule state under conditions that are easily accessible. Recently it was found that some forms of the protein demonstrate bactericidal activity and that some of them cause apoptosis of tumor cells. The possible biological impact enlarges the importance of a good insight in the characteristics that determine structure, stability and conformational changes. One approach to solve this problem is to compare the unfolding behaviour of lactalbumins of closely related species.

Bovine α -lactalbumin (BLA) and goat α -lactalbumin (GLA) both consist of 123 amino acids and differ by only 7 amino-acids. The knowledge that the apo-form of BLA (the calcium depleted form of the protein) is less stable than apo-GLA, invited us to analyze and mutually compare their thermodynamic properties upon binding of Ca^{2+} (Chapter 2). The first goal of the present study was to find a structural basis for the difference in thermal stability.

During this physico-chemical study on native GLA, we observed some unusual fluorescence behaviour upon illumination of the protein with ultraviolet (UV) light. It is well known that UV irradiation may reduce or even abolish the biological activity of proteins and enzymes. Proteins are important targets for photo-induced degradation due to the presence of endogenous chromophores, such as aromatic amino acids. Some decades ago it was suggested that absorption of near-UV light by tryptophan can contribute to reductive splitting of disulfide bridges in proteins. Our second goal was to reveal the impact of this important phenomenon on the three-dimensional structure and function of α -lactalbumin (Chapter 3).

In order to reveal the impact of individual Trp residues on photolysis of disulfide bridges, recombinant proteins, with one or more Trp residues replaced by a phenylalanine, were produced. The influence of the mutations on the structural characteristics was defined (Chapter 4). Making use of these mutants, we investigated which of the four Trp residues within GLA are essential for inducing photoreduction of disulfide bonds and which structural changes occur within the different mutants upon illumination (Chapter 5).

State of the art

1.1 Protein folding and stabilization

1.2 UV irradiation effects

1.3 α -Lactalbumin as a model protein

1.3.1 Primary, secondary and tertiary structure

1.3.2 Location of cation binding sites

1.3.3 Stability of α -lactalbumin

1.4 References

1.1 Protein folding and stabilization

Proteins control and regulate essentially every chemical process on which our life depends. Moreover proteins provide key components of virtually all the structural frameworks within our body. However, to exert these biological functions, newly synthesised proteins have to fold into tightly packed structures. Understanding how a protein adopts its unique native state and how it remains folded has intrigued many scientists for decades. Since the work of Anfinsen (1) in the 1960s and 1970s, it has been clear that the essential information that encodes the structure of proteins is contained within the amino-acid sequence. A remarkable observation is that very different sequences of amino acid residues can generate proteins with a similar fold. This suggests that the way a specific fold is encoded in the sequence is not determined by the character of individual amino acids but by the distribution of the different residues in the amino acid sequence. In particular, patterns of hydrophobic and hydrophilic residues largely determine the structure of a fold (2). In many globular proteins, most of the hydrophobic amino acid chains comprise the inner core and form connections between the different helices, whereas polar and charged amino acids are part of the outer shell (3). In addition to the role of patterns, side chains of individual amino acids are of major importance as they determine the complexity, specificity and stability of individual proteins (2). Studies on the stability of small enzymes which fold reversibly at high temperatures have permitted to determine many characteristics that enhance protein stability (4). Some of these characteristics, e.g. entropic stabilization by introduction of prolines or disulfide bridges, have been successfully used in protein-engineering to increase the stability of industrially important proteins. Other strategies for protein stabilization comprise helix optimization, introduction of salt bridges and the introduction of clusters of aromatic-aromatic interactions. In some cases very large differences in stability can be due to only one or very few point mutations (5). It has also been shown that stability differences between homologous, naturally occurring proteins can be the result of very few variations in amino acid sequence (5,6)

In addition to the question of how the information for the unique folding state is encoded in the amino acid sequence, there has been a second question namely how a protein could find its unique native state within a finite time. Indeed, the complete folding of some proteins, such as small helical bundles, has been observed to occur in less than 50 μ s (7). By contrast, simple calculations suggest that a small protein would take over a billion years to find its native state by

a random search of all possible conformations. To solve this apparent paradox, a logical starting point is to study small proteins with less than about 100 residues. Most of these proteins can be modelled as a simple two-state transition without the significant population of partially folded intermediates. In the unfolded state (U) the protein has a high degree of disorder, whereas in the fully folded, native state (N) it has only one distinct conformation. The native state of a protein is that with the lowest free-energy. To pass between the unfolded and the native low free-energy states, the protein must cross the transition state, a higher free-energy barrier. As the transition state corresponds to the least stable state, it is difficult to determine its structure. The principle experimental method for identifying transition states for folding is the Φ -value analysis introduced by Fersht (8,9). These studies involve the use of site-directed mutagenesis to probe the role of individual residues in the folding process.

Studies of a range of small proteins have suggested that the hydrophobic effect is the major driving force in protein folding. Conformations are formed due to packing of the side chains of hydrophobic amino acids into the interior of the protein. The folding process of a protein generally depends on the strength of this hydrophobic effect and on the stability of local segments of the structure. Within small proteins and pure α -helical proteins, a large number of events occur almost simultaneously. These proteins undergo an enormous reduction in conformational space and hydrodynamic radius, form local segments of structure and immediately gain some tertiary interactions (3).

For larger proteins, the folding process generally involves the population of one or more partially folded intermediates prior to the formation of the completely folded native state. The process from the unfolded state to the intermediate state is rapid, usually occurring within the dead time of stopped-flow measurements (1-30 ms), while the rate-limiting step in the folding reaction is the process from the intermediate to the native state. For instance, in most α/β proteins the hydrophobic cores collapse in the early stages of folding (10) while the formation of β sheets seems to be a rate limiting step. This results in the formation of a stabilized intermediate state, the 'molten globule' which is characterized by its compactness, the presence of most secondary structure elements and the absence of rigid tertiary structure. The molten globule of α -lactalbumine, an α/β protein, is the best characterized folding intermediate of globular proteins and has been studied intensively by various spectroscopic and physicochemical techniques.

There has been considerable debate over the significance of intermediates, whether they serve to help the protein find its correct fold efficiently or whether they are unavoidable traps that slow down folding (11,12). Regardless of the outcome of this debate, the structural properties of intermediates provide important evidence about the folding of large or multi-domain proteins. In particular, they suggest that these proteins generally fold in modules, in other words, folding can take place largely independently in different segments or domains of the protein (9,13). When the native-like fold is established within local regions or domains, the modules interact to form the correct overall structure (14,15). This happens in a final cooperative folding step when all the side chains become locked in their unique close-packed arrangement and water is excluded from the protein core (16).

Within living cells, the folding of larger proteins is often facilitated by a series of auxiliary proteins (17). These proteins include folding catalysts that enhance slow steps in protein folding, such as the formation of disulfide bonds and proline isomerization, and "molecular chaperones" that act to avoid protein misfolding of newly synthesized proteins. Living systems have developed mechanisms of quality control to check, whether proteins are correctly folded, and to destruct all misfolded or damaged polypeptides. The best-understood quality control mechanisms are in the endoplasmic reticulum, the major folding compartment of eukaryotic cells (18). They involve ubiquitination of proteins, followed by their destruction in the cytosol by the proteasome (19).

Because of the key role played by protein folding within the cell, it is inevitable that mistakes in folding will give rise to the malfunctioning of biological processes and hence to disease. A large number of diseases are associated with misfolding and more are being added each year (20). In some disorders, such as cystic fibrosis, the ability of a protein to fold correctly is reduced by familial mutations leading to the loss of an irreplaceable function. Misfolded proteins can be highly toxic, because of their tendency to form intracellular aggregates (21). In addition to misfolding of newly synthesized proteins, misfolded proteins can also arise in cells through postsynthetic denaturation or chemical damage (19). Within cells, proteins are constantly exposed to highly reactive molecules such as reactive oxygen species, reactive sugars, enzymes, fatty acids that can act as detergents and other unfolded proteins that act as nuclei for aggregation.

1.2 UV irradiation effects

For a protein the cell is a hostile environment, especially in warm-blooded species, as many intracellular conditions favour denaturation. In addition, proteins from light-exposed parts of a living organism are prone to damage caused by UV irradiation. The damaging effect of UV light on the structure and function of proteins and other bio-molecules becomes painfully apparent to many individuals who expose themselves for any time to intense sunlight. However, the phenomenon of sunburn is just one of many different biological effects. Other effects include induction of skin cancer, killing and mutation of many types of cells, growth delay, photoprotection and photoreactivation. The interest to describe and better understand what damage near-UV light can induce in the structure and function of proteins not only results from the effects on health. The industrial production and commercialization of recombinant proteins requires an accurate characterization of their respective stability profiles. Besides of the destabilizing influence caused by chemicals, moisture and temperature, the destabilizing influence of near-UV light is of major importance as the exposure of enzymes to near UV irradiation induces structural changes and alters their bio-catalytic function (22).

Proteins are targets for photo-destruction due to absorption of incident light by endogenous chromophores within the protein structure. Endogenous chromophores can be amino acid side chains or bound prosthetic groups such as heme and flavine. For most proteins without prosthetic groups absorption only occurs with light at wavelengths smaller than ca. 320 nm (23). The major chromophoric amino acids present in proteins are tryptophan (Trp), tyrosine (Tyr), phenylalanine (Phe), histidine (His), cysteine (Cys) and cystine. All other major amino acids do not absorb light significantly at wavelengths larger than ca. 230 nm. In addition, peptide bonds only exhibit a weak absorption band at 210-220 nm. Thus, direct absorption of solar UV light (>ca. 290 nm) by the protein backbone is negligible.

Among the major chromophoric amino acids, tryptophan has the strongest absorption in near-UV. The indole ring of Trp has a larger molar absorption coefficient than the other species which makes it the main component in photo-induced destruction of proteins. Based on studies with aqueous tryptophan, a following scheme of the excitation of Trp can be drawn (24). Under UV irradiation, the Trp molecule experiences transition into excited singlet state S₁. The main channels of S₁ decay are fluorescence and intersystem crossing into the triplet state (³Trp). In

absence of quenchers the main channel of triplet decay is transition into the ground state by phosphorescence. Both fluorescence and phosphorescence of tryptophan are widely used probes in studying the structure and dynamic processes in proteins. Unlike the singlet state the triplet state undergoes chemical reactivity as well as energy transfer processes. One of these processes is direct transfer of an electron of ^3Trp to a suitable acceptor (25). Disulfides, such as lipoaat (a cyclic disulfide) and cystine, undergo reduction to give the disulfide radical anion and the tryptophan radical-cation.



Alternatively, photo-ionization of Trp can lead to indirect electron transfer via the formation of a hydrated electron (2) (23). Addition of this hydrated electron can occur at a number of sites, particularly with a cystine to give the disulfide radical anion (3).



The latter radical can readily dissociate to give a thiyl anion and a thiyl radical (4) while the Trp cation radical can react with O_2 to form Trp decomposition products.

Since the disulfide radical anion of cyclic lipoaat is known to break apart, Bent and Hayon in 1975 (26) suggested that quenching of the triplet state of Trp by vicinal disulfide bonds in proteins could be an important process, possibly resulting in the rupture of the disulfide bridge. Despite the huge amount of information available about the impact of UV light on amino acids in solutions, little is known about Trp-mediated photolysis of disulfide bonds in proteins. In the 1960's a large number of studies (27-29), found that disulfide bonds, Trp, Tyr and Phe are effectively destroyed on UV irradiation of the protein. Evidence was provided that the photosensitivity of the disulfide bond depends on its micro-environment (29). Some data suggested that quanta primarily absorbed in the side chains of aromatic amino acid residues contribute to the destruction of the cystine residue (28). UV induced effects were observed recently in human plasma fibronectin (30), cutinase from *Fusarium solani pisi* (31-33) and bovine somatotropin (34). In both fibronectin and cutinase exposure to 280 nm light causes

changes in the fluorescence spectrum of the protein and generates free sulfhydryl groups. Although *Fusarium solani pisi* cutinase contains two disulfide bridges, Prompers et al. (32) could demonstrate that the unusual fluorescence behaviour results from structural changes caused by the breakage of only one disulfide bond. As this disulfide bond is in direct contact with the single Trp residue while the intact cystine is located on the other site of the protein, the authors assumed that the cleavage is mediated by the excited Trp. Possibly, the induced disruption involves electron transfer from the excited-state tryptophan to the disulfide bridge which is known to be a strong quencher (35). Another possible mechanism (proposed by Neves-Petersen(31)) is that the excited-state dipole moment of Trp on UV illumination induces a dipole moment in the adjacent disulfide bond (highly polarizable, a property correlated with good fluorescence quenchers), and energy can be transferred from the Trp to the disulfide bond. This could induce vibrational modes in the disulfide bond that lead to its disruption.

In view of the important impact of UV irradiation on the structure and function of proteins, it is of the utmost importance to further unravel the conditions of Trp-mediated photolysis of disulfide bonds. The most detailed information can be obtained by studying one of the best-understood proteins, namely α -lactalbumin

1.3 α -Lactalbumin as a model protein

α -Lactalbumin (LA) is a small (M_r 14200), acidic (pI 4-5), Ca^{2+} binding milk protein. LA performs an important function in mammary secretory cells: it is one of the two components of lactose synthase, which catalyzes the final step in lactose biosynthesis in the lactating mammary gland (36). The other component of this system is galactosyltransferase (GT), which is involved in the processing of proteins in various secretory cells by transferring galactosyl groups from UDP-galactose to glycoproteins containing *N*-acetylglucosamine. In the lactating mammary gland, the specificity of GT is modulated by interaction with LA, which increases its affinity and specificity for glucose:



Structural studies on GT and lactose synthase have shown that two flexible loops at the substrate-binding site of GT undergo a marked conformational change upon binding with UDP-galactose. This locks the sugar-nucleotide in the binding site and creates (i) the oligosaccharide binding cavity; (ii) a protein-protein interacting site for the enzyme's partner, alpha-lactalbumin (LA); and (iii) a metal ion binding site. LA holds and puts glucose right in the acceptor binding site of GT, which then maximizes the interactions with glucose, thereby making it a preferred acceptor for the lactose synthase reaction. The interaction of LA with GT also stabilizes the sugar-nucleotide-enzyme complex, kinetically enhancing the sugar transfer (37,38).

Besides the role of LA modulating the activity of the lactose synthase, new intriguing properties have been evidenced, such as the apoptotic activity in tumor cells of a partly folded variant of LA bound to oleic acid (39,40), the ability of the protein to bind histones (41,42) and the bactericidal activity of some of its chymotryptic peptides (43).

1.3.1 Primary, secondary and tertiary structure

Most α -lactalbumins (LA), including human, guinea pig, bovine, goat, camel, equine and rabbit proteins, consist of 123 amino acid residues. LA is homologous in sequence to the lysozyme family, but its cell lytic activity exhibits only about 10^{-6} of the specific activity of hen egg white lysozyme (44). X-ray crystallography has shown that the three-dimensional structure of LA is very similar to that of lysozyme (45,46). Native LA consists of two domains: a large α -helical domain and a small β -sheet domain, which are connected by a calcium binding loop (Fig. 1). The α -helical domain is composed of four α -helices (H1:5-11, H2:23-34, H3:86-98 and H4:105-110) and two short 3_{10} helices (h1b: 18-20 and h3c: 115-118). Helix 4, also called 'flexible loop/helix' (residues 105-110), adopts the helical conformation at higher pH values (6.5-8.0) and the 'loop' conformation at low pH (4.6) (47,48). The β -sheet domain is composed of a series of loops, a small three-stranded anti-parallel β -pleated sheet (residues 41-44, 47-50, and 55-56) and a short 3_{10} helix (h2: 77-80). The two domains are divided by a deep cleft between them. At the same time, the two domains are held together by the disulfide bridge between residues Cys73 and Cys91, forming the Ca^{2+} binding loop. Overall, the structure of α -LA is stabilized by four disulfide bridges (Cys6-Cys120, Cys61-Cys77, Cys73-Cys91, and Cys28-Cys111).

There are two hydrophobic cores in the structure of native LA (Fig. 1). One, called aromatic cluster I, is the contact site of β -galactosyltransferase (49). It mainly consists of the residues Phe 31, His 32, Gln 117 and Trp 118 from helix 2 and the 3_{10} helix h3c. The flexible region (105-111) –although not in contact itself- is known to be important for β -galactosyltransferase binding (50). A second hydrophobic core, called aromatic cluster II or the hydrophobic box, comprises the tryptophan residues Trp 26, Trp 60 and Trp104 among other residues from helix 2 and 3 and the β -sheet domain (Phe 53, Gln 54, and Tyr 103).

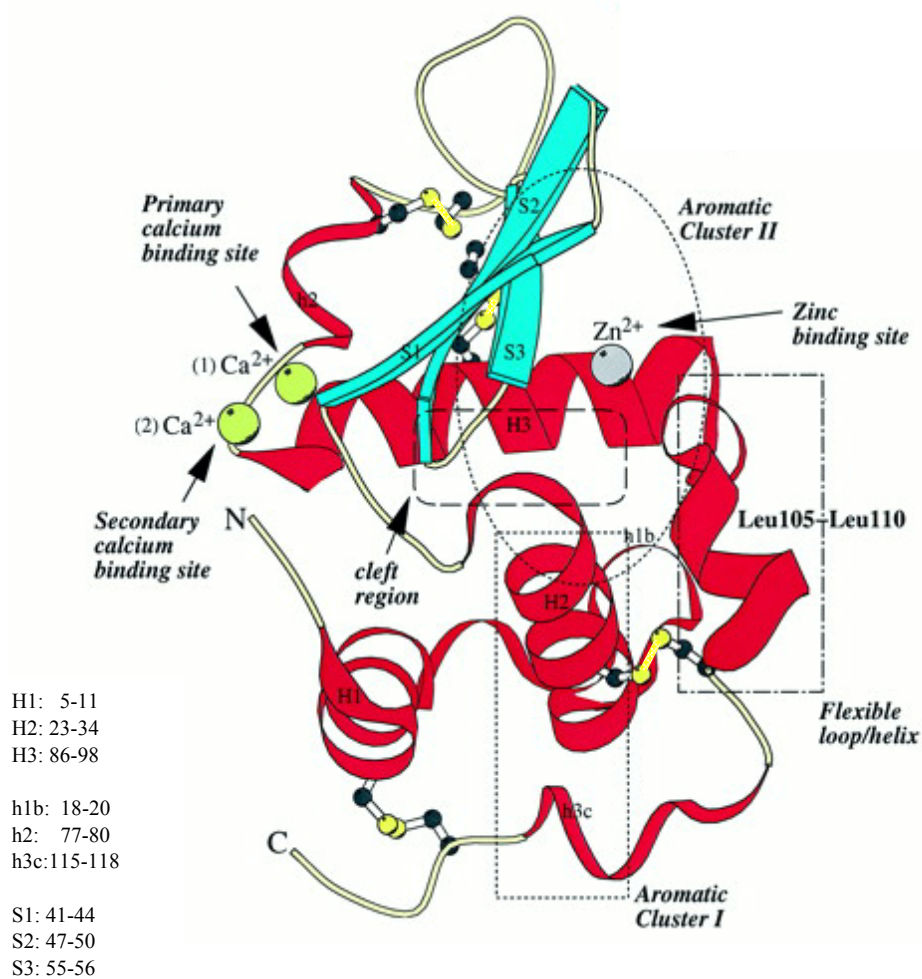


Figure 1: Structure of α -lactalbumin and the functional regions of the molecule showing the location of metal ions identified in α -lactalbumin crystal structures. The structure of bovine α -lactalbumin is schematically represented. The location of the major secondary structural elements (S, β -strand; H, α -helix; h, 3_{10} helix) is highlighted. The four disulfide bridges (yellow) are also shown. (*Chrysina ED et al. JBC 2000, 47, 37021-37029(51)*)

1.3.2 Location of cation binding sites

One of the most interesting features of LA is its ability to bind metal cations. The protein has a single strong calcium binding site, which is formed by oxygen ligands from carboxylic groups of three Asp residues (82, 87 and 88) and two carbonyl groups of the peptide backbone (Lys 79 and Asp 84) in a loop between two helices. In addition, one or two water molecules take part in direct coordinating Ca^{2+} . Overall the oxygen ligands form a distorted pentagonal bipyramidal structure. A secondary calcium binding site has also been identified by X-ray crystallography in human LA 7.9 Å away from the primary strong calcium binding site (52). Four residues are involved in Ca^{2+} coordination at this site in a tetrahedral arrangement (Thr-38, Gln-39, Asp-83 and the carbonyl oxygen of Leu-81). The binding of Ca^{2+} to apo-LA causes pronounced changes in structure and function, mostly in tertiary, but not secondary, structure. Differential scanning and isothermal titration microcalorimetry have been used to study the energetics of structural changes in α -lactalbumin and the transition between native and denatured states induced by binding Ca^{2+} and Na^+ (53-55). Isothermal titration calorimetry (ITC) has been used extensively to study the binding of small molecules to proteins. ITC measures directly the energy associated with a chemical reaction triggered by the mixing of two components. A typical ITC experiment is carried out by the stepwise addition of one of the reactants (~10 μL per injection) into the reaction cell (~1 mL) containing the other reactant. A typical experiment is shown in Chapter 2, Figure 2. The chemical reaction created by each injection either releases or absorbs a certain amount of heat (q_i) proportional to the amount of ligand that binds to the protein in a particular injection ($v \times \Delta L_i$) and the characteristic binding enthalpy (ΔH) for the reaction:

$$q_i = v \times \Delta H \times \Delta L_i \quad (1)$$

where v is the volume of the reaction cell and ΔL_i is the increase in the concentration of bound ligand after the i th injection. As modern ITC instruments operate on the heat compensation principle, the instrumental response (measured signal) is the amount of power (microcalories per second) necessary to maintain constant the temperature difference between the reaction and reference cells (Chapter 2, Fig. 2A). The heat after each injection is therefore obtained by calculating the area under each peak and is plotted against molar ratio of the components (Chapter 2, Fig. 2B). Because the amount of uncomplexed protein available progressively decreases after each successive injection, the magnitude of the peaks becomes progressively

smaller until complete saturation is achieved. The corrected area under each peak is given by equation 1, which is used to analyze the data. The quantity ΔL_i is the difference between the concentration of bound ligand in the i th and $(i-1)$ th injections, and its functional form depends on the specific binding model. For the simplest case, in which the protein has one binding site, equation 1 becomes:

$$q_i = v \times \Delta H \times [P] \times \left(\frac{K_a [L]_i}{1 + K_a [L]_i} - \frac{K_a [L]_{i-1}}{1 + K_a [L]_{i-1}} \right) \quad (2)$$

where K_a is the binding constant, $[P]$ is the concentration of protein, $[L]$ is the concentration of free ligand. Analysis of the data yields ΔH and $\Delta G = -RT \ln K_a$. The entropy change is obtained by using the standard thermodynamic expression $\Delta G = \Delta H - T \Delta S$. By repeating a titration at different temperatures, it is also possible to determine the change in heat capacity (ΔC_p) associated with the binding reaction

$$\left(\Delta C_p = \frac{\partial \Delta H}{\partial T} \right) \quad (3)$$

ΔC_p is a good indicator of changes in hydrophobic interactions with binding, being negative if hydrophobic bounds are formed and positive if they are broken.

By DSC, ITC and circular dichroism, Griko and Remeta (54) have found that removal of Ca^{2+} from the α -lactalbumin enhances its sensitivity to pH and ionic conditions. This is caused by non-compensated negative charge-charge interactions at the cation binding site, which significantly reduces its overall stability. Moreover, the binding of Ca^{2+} shifts the thermal transition to higher temperatures by more than 40°C (53-56). The binding of calcium is an important step in folding by which the two domains of the protein get locked in place to yield the native structure. Vanderheeren et al. (57) found that calcium stabilizes not only the native state but also to a certain degree the partially unfolded one. The latter effect results from the stabilization of secondary structural elements (58).

Besides calcium, LA binds other physiologically significant cations such as Mg^{2+} , Mn^{2+} , Na^+ and K^+ , which can compete with Ca^{2+} for the same primary binding site (59, 60). They induce similar, albeit smaller, structural changes in LA. LA also has several zinc binding sites, one of which is located in the cleft region. The binding of Zn^{2+} ions to Ca^{2+} -loaded LA decreases thermal stability, causes aggregation and increases its susceptibility to protease digestion (61). The Zn-loaded LA precipitates out of solution as amorphous aggregates but does not fibrillate.

Although LA is not associated to any specific disease, bovine LA is able to form amyloid fibrils if the protein is induced to adopt the molten globule (MG) state at low pH under conditions of high ionic strength (62). Fibril formation at pH 2.0 is even more rapid upon partial reduction of the four disulfide bridges or upon protein dissection. Under these circumstances the protein adopts a more open conformation than that of the partly folded state in acid solution. These various observations can be interpreted as indicating that partly folded, but substantially open and dynamic states of proteins are those required for triggering the process of fibrillogenesis (62, 63).

1.3.3 Stability of α -lactalbumin

At acidic pH (A-state) or in the apo-state at elevated temperatures α -lactalbumin forms a classic 'molten globule' (64-66). The molten globule state typically exhibits native-like compactness and the native tertiary fold of the molecule, but does not have specific side-chain packing interactions (67-68). Other characteristics are the compactness of the protein molecule with a radius of gyration 10 to 30 % larger than the native state and the presence of a loosely packed hydrophobic core that increases the hydrophobic surface accessible to solvent. In addition to their role in protein folding, molten globules may have other biological functions. For example, partially structured proteins existing under physiological conditions may serve as a conformational switch or target for gene regulation (69). Molten globules are involved in a number of biological or pathological processes that require the protein to become partially unfolded, such as the interaction with molecular chaperones, translocation across biological membranes, formation of amyloid, and dissociation of supramolecular complexes (70).

The structure of the molten globule state of bovine and human α -lactalbumin has been characterized in great detail by various techniques including circular dichroism (CD), fluorescence, nuclear magnetic resonance (NMR), hydrogen-exchange labeling (71-76) and protein engineering techniques (77-80). These studies have shown that the hydrophobic core in the molten globule state is loosely packed and stabilized by non-specific hydrophobic interactions (67, 81, 82). It has also been shown that the α -lactalbumin molten globule has a heterogeneous (bipartite) structure in which the α -domain is weakly formed and the β -domain is

disordered (66, 78). Results from protein dissection studies provide evidence that the β -domain can be removed from the LA molecule without impairing the capability of the rest of the chain to adopt a molten globule state (83, 84). Peptide studies (85), urea induced unfolding (86) and hydrogen exchange studies (74, 76) have revealed the presence of structured helices in the molten globule state of LA that are important for the stability of the α -domain structure. These studies show that all the secondary structure elements formed in the 'A' state of LA (the H1-, H2-, H3-, and H4-helices and a 3_{10} -helix) are localized in the α -domain. Among different LA species, the same helices are protected from hydrogen-exchange in the A-state. However, the stabilities of the individual helical elements vary with the LA species (71, 73, 74, 79, 87, 88). The urea induced unfolding patterns of the molten globule of bovine and human α -lactalbumin at pH 2 have been followed and compared by Redfield and coworkers (89, 90). These studies indicate that both the α - and β -domains are at least partially collapsed in the molten globules of both bovine and human α -lactalbumin in 0 M urea. In both proteins, resonances appearing at the lowest concentrations of denaturant correspond to the N-terminal residues and to the β -domain of native α -lactalbumin. The residues most resistant to denaturant are clustered together in the α -domain of the native structure of α -lactalbumin, indicating that the molten globule has a highly stable native-like core. The stability of the α -domain core is found to differ between human and bovine α -lactalbumin. In human α -lactalbumin, residues from the H3-helix are found to be less resistant to unfolding than residues from the other helices. Residues located in the H1, H2, H4, and C-terminal 3_{10} helices form a highly stable core in the absence of a folded H3-helix (86). In bovine α -lactalbumin, all four α -helices and the C-terminal 3_{10} helix unfold over a relatively narrow range of urea concentrations indicating that, in contrast to human α -lactalbumin, the C-helix is a required element in the stable molten globule core (91). These differences in behaviour between bovine and human α -lactalbumin appear to arise from amino acid substitutions found in the B- and C-helices that result in more extensive contacts between the B- and C-helix regions in bovine α -lactalbumin. Although the molten globule state of goat α -LA has not been studied in as much detail as the molten globules of the bovine and human proteins, the amino acid sequence of goat α -LA has 94% identity with that of the bovine protein (only 7 of 123 residues in the sequence are different between the two proteins), so that the molten globule of the goat protein must be similar to that of the bovine protein (92).

Information about the native-like tertiary fold of the α -domain in the LA molten globule has also been provided by disulfide exchange studies. Two disulfide bridges, Cys6-Cys120 and Cys28-Cys111, are located in the α -domain. Peng et al. (77) have reported on the structural

specificity of local regions in the α -domain. Their disulfide exchange study showed that, in the molten globule, formation of the Cys28-Cys111 disulfide bond is strongly preferred, while the Cys6-Cys120 disulfide bond is labile. Thus, the local region surrounding the Cys28-Cys111 disulfide bond has a high preference for adopting a native-like structure in the molten globule state. Analogous results were obtained by Moriarty et al. (93) with a set of peptides derived from the region of the Cys28-Cys111 disulfide. Moreover, results with peptides from the vicinity of disulfide bridge Cys6-Cys120 demonstrate that there is very little enhancement of local structure due to the formation of the Cys6-Cys120 disulfide bond. This agrees with the findings of Kuwajima et al. (94) that this disulfide bond is reduced very quickly by agents as dithiothreitol (DTT), as it is 140 times more reactive than normal disulfides in the fully accessible state. The superreactivity arises from the geometric strain imposed on this disulfide bond by the native structure.

Although the α -domain has a native tertiary structure in the molten globule state, this domain itself is not sufficient to form the native state. Peng and Kim (77) have reported that a single-chain recombinant model of the α -domain of human LA, consisting of residues 1–39 and 81–123, forms a molten globule with the same overall tertiary fold as that found in intact LA, but does not form the native structure with specific side-chain interactions. Wu et al. (95) studied two variants of human LA : LA(α) containing only the two disulfide bonds in the α -helical domain, Cys6-Cys120 and Cys28-Cys111, but lacking the β -sheet domain and the interdomain cysteines, which are replaced by alanines. Conversely, LA(β) contains the Cys61-Cys77 disulfide bond in the β -sheet domain and the interdomain Cys73-Cys91 disulfide bond, with the cysteines in the α -helical domain replaced by alanines. They found that only LA(β) binds calcium, leading to the cooperative formation of a substantial number of tertiary interactions. In this case, the β domain acquires a native-like backbone topology. Therefore, not only the α -domain but also the β -domain is necessary for the folding from the molten globule to the native state of human LA. Specific interactions within α -lactalbumin imposed by the β -sheet domain and interdomain disulfide bonds, as opposed to the two α -helical domain disulfides, are necessary for the Ca^{2+} -induced progression from the molten globule toward a more native-like structure. These results suggest that organization of the β domain, coupled with calcium binding, constitutes the locking step in the folding of α -lactalbumin from the molten globule to the native state. It is interesting to note that a LA mutant in which all eight cysteines were mutated to alanine, was nearly as compact as wild type LA at acidic pH (96). Overall the architecture of the

protein fold of LA is determined by the polypeptide sequence itself and not as a result of disulfide bond cross-linking.

1.4 References

1. Anfinsen, C.B. (1973) Principles that govern folding of protein chains. *Science* 181, 223-230.
2. Baker, D. (2000) A surprising simplicity to protein folding. *Nature* 405, 39-42.
3. Schultz, C.P. (2000) Illuminating folding intermediates. *Nat. Struct. Biol.* 7, 7-10.
4. Eijnsink, V.G.H., Bjork, A., Gaseidnes, S., Sirevag, R., Synstad, B., van den Burg, B. and Vriend, G. (2004) Rational engineering of enzyme stability. *J. Biotechnol.* 113, 105-120.
5. Sandgren, M., Gualfetti, P.J., Shaw, A., Gross, L.S., Saldajeno, M., Day, A.G., Jones, T.A. and Mitchinson, C. (2003) Comparison of family 12 glycoside hydrolases and recruited substitutions important for thermal stability. *Protein Sci.* 12, 848-860.
6. Serrano, L., Day, A.G. and Fersht, A.R. (1993) Step-wise mutation of barnase to binase - A procedure for engineering increased stability of proteins and an experimental analysis of the evolution of protein stability. *J. Mol. Biol.* 233, 305-312.
7. Yang, W.Y. and Gruebele, M. (2003) Folding at the speed limit. *Nature* 423, 193-197.
8. Matouschek, A., Kellis, J.T., Serrano, L. and Fersht, A.R. (1989) Mapping the transition-state and pathway of protein folding by protein engineering. *Nature* 340, 122-126.
9. Fersht, A.R. (1999) *Structure and mechanism in protein science: a guide to enzyme catalysis and protein folding*. Freeman, W.H. and Company, New York.
10. Li, R.H. and Woodward, C. (1999) The hydrogen exchange core and protein folding. *Protein Sci.* 8, 1571-1590.
11. Capaldi, A.P., Kleanthous, C. and Radford, S.E. (2002) Im7 folding mechanism: misfolding on a path to the native state. *Nat. Struct. Biol.* 9, 209-216.
12. Roder, H. and Colon, W. (1997) Kinetic role of early intermediates in protein folding. *Curr. Opin. Struct. Biol.* 7, 15-28.
13. Dinner, A.R., Sali, A., Smith, L.J., Dobson, C.M. and Karplus, M. (2000) Understanding protein folding via free-energy surfaces from theory and experiment. *Trends Biochem. Sci.* 25, 331-339.
14. Khan, F., Chuang, J.I., Gianni, S. and Fersht, A.R. (2003) The kinetic pathway of folding of barnase. *J. Mol. Biol.* 333, 169-186.
15. Vendruscolo, M., Paci, E., Karplus, M. and Dobson, C.M. (2003) Structures and relative free energies of partially folded states of proteins. *Proc. Natl. Acad. Sci. USA* 100, 14817-14821.

16. Cheung, M.S., Garcia, A.E. and Onuchic, J.N. (2002) Protein folding mediated by solvation: water expulsion and formation of the hydrophobic core occur after the structural collapse. *Proc. Natl. Acad. Sci. USA* 99, 685-690.
17. Gething, M.J. & Sambrook, J. (1992) Protein folding in the cell. *Nature* 355, 33-45.
18. Sitia, R. and Braakman, I. (2003) Quality control in the endoplasmic reticulum protein factory. *Nature* 426, 891-894.
19. Goldberg, A.L. (2003) Protein degradation and protection against misfolded or damaged proteins. *Nature* 426, 895-899.
20. Dobson, C.M. (2004) Experimental investigation of protein folding and misfolding. *Methods* 34, 4-14.
21. Selkoe, D.J. (2003) Folding proteins in fatal ways. *Nature* 426, 900-904.
22. Bhattacharya, D., Basu, S. and Mandal, P.C. (2000) UV radiation effects on flavocytochrome b(2) in dilute aqueous solution. *J. Photoch. Photobio. B* 59, 54-63.
23. Davies, M.J. and Truscott, R.J.W. (2001) Photo-oxidation of proteins and its role in cataractogenesis. *J. Photoch. Photobio. B* 63, 114-125.
24. Tsentalovich, Y.P., Snytnikova, O.A. and Sagdeev, R.Z. (2004) Properties of excited states of aqueous tryptophan. *J. Photoch. Photobio. A* 162, 371-379.
25. Creed, D. (1984) The photophysics and photochemistry of the near-UV absorbing amino-acids .1. Tryptophan and Its Simple Derivatives. *Photochem. Photobiol.* 39, 537-562.
26. Bent, D.V. and Hayon, E. (1975) Excited-state chemistry of aromatic amino-acids and related peptides .3. Tryptophan. *J. Am. Chem. Soc.* 97, 2612-2619.
27. Augenstein, L.G. and Ghiron, C.A. (1961) The inactivation of trypsin by ultraviolet light, I: The correlation of inactivation with the disruption of constituent cystine. *Proc. Natl. Acad. Sci. USA* 47, 1530-1547.
28. Dose, K. (1968) The photolysis of free cystine in the presence of aromatic amino acids. *Photochem. Photobiol.* 8, 331-335.
29. Augenstein, L.G. and Riley, P. (1964) The inactivation of enzymes by ultraviolet light, IV: The nature and involvement of cystine disruption. *Photochem. Photobiol.* 3, 353-367.
30. Miles, A.M., Brew, S.A., Ingham, K.C. and Smith, R.L. (1995) Photoinduced Structural-Changes in the Collagen Gelatin-Binding Domain of Fibronectin. *Biochemistry* 34, 6941-6946.
31. Neves-Petersen, M.T., Gryczynski, Z., Lakowicz, J., Fojan, P., Pedersen, S., Petersen, E. and Petersen, S.B. (2002) High probability of disrupting a disulfide bridge mediated by an endogenous excited tryptophan residue. *Protein Sci.* 11, 588-600.
32. Prompers, J.J., Hilbers, C.W. and Pepermans, H.A.M. (1999) Tryptophan mediated photoreduction of disulfide bond causes unusual fluorescence behaviour of *Fusarium solani* pisi cutinase. *FEBS Lett.* 456, 409-416.

33. Weisenborn, P.C.M., Meder, H., Egmond, M.R., Visser, T.J.W.G. and van Hoek, A. (1996) Photophysics of the single tryptophan residue in *Fusarium solani* cutinase: evidence for the occurrence of conformational substates with unusual fluorescence behaviour. *Biophys. Chem.* 58, 281-288.
34. Miller, B.L., Hageman, M.J., Thamann, T.J., Barron, L.B. and Schoneich, C. (2003) Solid-state photodegradation of bovine somatotropin (bovine growth hormone): evidence for tryptophan-mediated photooxidation of disulfide bonds. *J. Pharm. Sci. US* 92, 1698-1709.
35. Chen, Y. and Barkley, M.D. (1998) Toward understanding tryptophan fluorescence in proteins. *Biochemistry* 37, 9976-9982.
36. Hill, R.L. and Brew, K. (1975) Lactose Synthetase. *Advances in Enzymology and Related Areas of Molecular Biology* 43, 411-490.
37. Ramakrishnan, B., Boeggeman, E. and Qasba, P. K. (2002). beta-1,4-galactosyltransferase and lactose synthase: Molecular mechanical devices. *Biochem. Biophys. Res. Comm.* 291, 1113-1118.
38. Qasba, P. K., Ramakrishnan, B. and Boeggeman, E. (2005). Substrate-induced conformational changes in glycosyltransferases. *Trends in Biochemical Sciences* 30, 53-62.
39. Häkansson, A., Zhivotovsky, B., Orrenius, S., Sabharwal, H. and Svanborg, C. (1995) Apoptosis induced by a human milk protein. *Proc. Natl. Acad. Sci. USA* 92, 8064-8068.
40. Svensson, M., Sabharwal, H., Hakansson, A., Mossberg, A.K., Lipniunas, P., Leffler, H., Svanborg, C. and E. Linse, S. (1999) Molecular characterization of alpha-lactalbumin folding variants that induce apoptosis in tumor cells. *J. Biol. Chem.* 274, 6388-6396.
41. Düringer, C., Hamiche, A., Gustafsson, L., Rimura, H. and Svanborg, C. (2003) HAMLET interacts with histones and chromatin in tumor cell nuclei. *J. Biol. Chem.* 278, 42131-42135.
42. Permyakov, S.E., Pershikova, I.V., Khokhlova, T.I., Uversky, V.N. and Permyakov, E.A. (2004) No need to be HAMLET or BAMLET to interact with histones: Binding of monomeric alpha-lactalbumin to histones and basic poly-amino acids. *Biochemistry* 43, 5575-5582.
43. Pellegrini, A., Thomas, U., Bramaz, N., Hunziker, P. and von Fellenberg, R. (1999) Isolation and identification of three bactericidal domains in the bovine alpha-lactalbumin molecule. *Biochim. Biophys. Acta* 1426, 439-448.
44. McKenzie, H.A. (1996) Alpha-lactalbumins and lysozymes. In: *Lysozymes: Model Enzymes in Biochemistry and Biology*. Jollès, P., editor. Birkhäuser, Basel. 365-409.
45. Acharya, K.R., Ren, J.S., Stuart, D.I., Phillips, D.C. and Fenna, R.E. (1991) Crystal-structure of human alpha-lactalbumin at 1.7-Å resolution. *J. Mol. Biol.* 221, 571-581.
46. Acharya, K.R., Stuart, D.I., Phillips, D.C., McKenzie, H.A. and Teahan, C.G. (1994) Models of the 3-dimensional structures of echidna, horse, and pigeon lysozymes - Calcium-binding lysozymes and their relationship with alpha-lactalbumins. *J. Prot. Chem.* 13, 569-584.
47. Harata, K. and Muraki, M. (1992) X-ray structural evidence for a local helix-loop transition in alpha-lactalbumin. *J. Biol. Chem.* 267, 1419-1421.

48. Pike, A.C.W., Brew, K. and Acharya, K.R. (1996) Crystal structures of guinea-pig, goat and bovine alpha-lactalbumin highlight the enhanced conformational flexibility of regions that are significant for its action in lactose synthase. *Structure* 4, 691-703.
49. Ramakrishnan, B. and Qasba, P.K. (2001) Crystal structure of lactose synthase reveals a large conformational change in its catalytic component, the beta 1,4-galactosyltransferase-1. *J. Mol. Biol.* 310, 205-218.
50. Malinovskii, V.A., Tian, J., Grobler, J.A. and Brew, K. (1996) Functional site in alpha-lactalbumin encompasses a region corresponding to a subsite in lysozyme and parts of two adjacent flexible substructures. *Biochemistry* 35, 9710-9715.
51. Chrysina, E.D., Brew, K. and Acharya, K.R. (2000) Crystal structures of apo- and holo-bovine alpha-lactalbumin at 2.2-A resolution reveal an effect of calcium on inter-lobe interactions. *J. Biol. Chem.* 275, 37021-37029.
52. Chandra, N., Brew, K. and Acharya, K.R. (1998) Structural evidence for the presence of a secondary calcium binding site in human alpha-lactalbumin. *Biochemistry* 37, 4767-4772.
53. Griko, Y.V., Freire, E. and Privalov, P.L. (1994) Energetics of the alpha-lactalbumin states - A calorimetric and statistical thermodynamic study. *Biochemistry* 33, 1889-1899.
54. Griko, Y.V. and Remeta, D.P. (1999). Energetics of solvent and ligand-induced conformational changes in alpha-lactalbumin. *Protein Sc.* 8, 554-561.
55. Hendrix, T., Griko, Y.V. and Privalov, P.L. (2000). A calorimetric study of the influence of calcium on the stability of bovine alpha-lactalbumin. *Biophys. Chem.* 84, 27-34.
56. Veprintsev, D.B., Permyakov, S.E., Permyakov, E.A., Rogov, V.V., Cawild typehern, K.M. and Berliner, L.J. (1997) Cooperative thermal transitions of bovine and human apo-alpha-lactalbumins: evidence for a new intermediate state. *FEBS Lett.* 412, 625-628.
57. Vanderheeren, G., Hanssens, I., Meijberg, W. and Vanaerschot, A. (1996) Thermodynamic characterization of the partially unfolded state of Ca²⁺-loaded bovine alpha-lactalbumin: evidence that partial unfolding can precede Ca²⁺ release. *Biochemistry* 35, 16753-16759.
58. Vanderheeren, G. and Hanssens, I. (1994) Thermal unfolding of bovine alpha-lactalbumin - Comparison of circular-dichroism with hydrophobicity measurements. *J. Biol. Chem.* 269, 7090-7094.
59. Permyakov, E.A., Morozova, L.A. and Burstein, E.A. (1985) Cation Binding Effects on the Ph, Thermal and Urea Denaturation Transitions in Alpha-Lactalbumin. *Biophys. Chem.* 21, 21-31.
60. Permyakov, E.A., Kalinichenko, L.P., Morozova, L.A., Yarmolenko, V.V. and Burstein, E.A. (1981) Alpha-lactalbumin binds magnesium-ions - Study by means of intrinsic fluorescence technique. *Biochem. Biophys. Res. Commun.* 102, 1-7.
61. Permyakov, E.A. and Berliner, L.J. (2000) alpha-Lactalbumin: structure and function. *FEBS Lett.* 473, 269-274.

62. Goers, J., Permyakov, S.E., Permyakov, E.A., Uversky, V.N. and Fink, A.L. (2002). Conformational prerequisites for alpha-lactalbumin fibrillation. *Biochemistry* 41, 12546-12551.
63. de Laureto, P. P., Frare, E., Battaglia, F., Mossuto, M.F., Uversky, V.N. and Fontana, A. (2005). Protein dissection enhances the amyloidogenic properties of alpha-lactalbumin. *FEBS J.* 272, 2176-2188.
64. Permyakov, E.A., Yarmolenko, V.V., Kalinichenko, L.P., Morozova, L.A. and Burstein, E.A. (1981) Calcium-binding to alpha-lactalbumin - Structural rearrangement and association constant evaluation by means of intrinsic protein fluorescence changes. *Biochem. Biophys. Res. Commun.* 100, 191-197.
65. Dolgikh, D.A., Gilmanshin, R.I., Brazhnikov, E.V., Bychkova, V.E., Semisotnov, G.V., Venyaminov, S.Y. and Ptitsyn, O.B. (1981) Alpha-lactalbumin - Compact state with fluctuating tertiary structure. *FEBS Lett.* 136, 311-315.
66. Kuwajima, K. (1996) The molten globule state of alpha-lactalbumin. *FASEB J.* 10, 102-109.
67. Arai, M. and Kuwajima, K. (2000) Role of the molten globule state in protein folding. *Adv. Prot. Chem.*, 53, 209-282.
68. Arai, M., Ito, K., Inobe, T., Nakao, M., Maki, K., Kamagata, K., Kihara, H., Amemiya, Y. and Kuwajima, K. (2002) Fast compaction of alpha-lactalbumin during folding studied by stopped-flow X-ray scattering. *J. Mol. Biol.* 321, 121-132.
69. Wright, P.E. and Dyson, H.J. (1999) Intrinsically unstructured proteins: re-assessing the protein structure-function paradigm. *J. Mol. Biol.* 293, 321-331.
70. Chakraborty, S., Ittah, V., Bai, P., Luo, L., Haas, E. and Peng, Z.Y. (2001) Structure and dynamics of the alpha-lactalbumin molten globule: fluorescence studies using proteins containing a single tryptophan residue. *Biochemistry* 40, 7228-7238.
71. Baum, J., Dobson, C.M., Evans, P.A. and Hanley, C. (1989) Characterization of a partly folded protein by NMR methods - studies on the molten globule state of guinea-pig alpha-lactalbumin. *Biochemistry* 28, 7-13.
72. Alexandrescu, A.T., Evans, P.A., Pitkeathly, M., Baum, J. and Dobson, C.M. (1993) Structure and dynamics of the acid-denatured molten globule state of alpha-lactalbumin - A 2-dimensional NMR-study. *Biochemistry* 32, 1707-1718.
73. Chyan, C.L., Wormald, C., Dobson, C.M., Evans, P.A. and Baum, J. (1993) Structure and stability of the molten globule state of guinea-pig alpha-lactalbumin - A hydrogen-exchange study. *Biochemistry* 32, 5681-5691.
74. Schulman, B.A., Redfield, C., Peng, Z.Y., Dobson, C.M. and Kim, P.S. (1995) Different subdomains are most protected from hydrogen-exchange in the molten globule and native states of human alpha-lactalbumin. *J. Mol. Biol.* 253, 651-657.

75. Balbach, J., Forge, V., Lau, W.S., Jones, J.A., Van Nuland, N.A.J. and Dobson, C.M. (1997) Detection of residue contacts in a protein folding intermediate. *Proc. Natl. Acad. Sci. USA* 94, 7182-7185.
76. Forge, V., Wijesinha, R.T., Balbach, J., Brew, K., Robinson, C.V., Redfield, C. and Dobson, C.M. (1999) Rapid collapse and slow structural reorganisation during the refolding of bovine alpha-lactalbumin. *J. Mol. Biol.* 288, 673-688.
77. Peng, Z.Y. and Kim, P.S. (1994) A protein dissection study of a molten globule. *Biochemistry* 33, 2136-2141.
78. Wu, L.C., Peng, Z.Y. and Kim, P.S. (1995) Bipartite structure of the alpha-lactalbumin molten globule. *Nat. Struct. Biol.* 2, 281-286.
79. Schulman, B.A. and Kim, P.S. (1996) Proline scanning mutagenesis of a molten globule reveals non-cooperative formation of a protein's overall topology. *Nat. Struct. Biol.* 3, 682-687.
80. Pardon, E., Haezebrouck, P., Debaetselier, A., Hooke, S.D., Fancourt, K.T., Desmet, J., Dobson, C.M., Van Dael, H. and Joniau, M. (1995) A Ca²⁺-binding chimera of human lysozyme and bovine alpha-lactalbumin that can form a molten globule. *J. Biol. Chem.* 270, 10514-10524.
81. Kuwajima, K. (1989) The molten globule state as a clue for understanding the folding and cooperativity of globular-protein structure. *Proteins* 6, 87-103.
82. Uchiyama, H., PerezPrat, E.M., Watanabe, K., Kumagai, I. and Kuwajima, K. (1995) Effects of amino acid substitutions in the hydrophobic core of alpha-lactalbumin on the stability of the molten globule state. *Protein Eng.* 8, 1153-1161.
83. de Laureto, P.P., Vinante, D., Scaramella, E., Frare, E., & Fontana, A. (2001). Stepwise proteolytic removal of the beta subdomain in alpha-lactalbumin - The protein remains folded and can form the molten globule in acid solution. *European Journal of Biochemistry* 268, 4324-4333.
84. Wu, L. C. and Kim, P. S. (1998). A specific hydrophobic core in the alpha-lactalbumin molten globule. *J.Mol. Biol.* 280, 175-182
85. Demarest, S.J., Boice, J.A., Fairman, R. and Raleigh, D.P. (1999) Defining the core structure of the alpha-lactalbumin molten globule state. *J. Mol. Biol.* 294, 213-221.
86. Schulman, B.A., Kim, P.S., Dobson, C.M. and Redfield, C. (1997) A residue-specific NMR view of the non-cooperative unfolding of a molten globule. *Nat. Struct. Biol.* 4, 630-634.
87. Alexandrescu, A.T., Evans, P.A., Pitkeathly, M., Baum, J. and Dobson, C.M. (1993). Structure and dynamics of the acid-denatured molten globule state of alpha-lactalbumin - A 2-dimensional NMR-study. *Biochemistry* 32, 1707-1718
88. Demarest, S.J., Fairman, R. and Raleigh, D.P. (1998). Peptide models of local and long-range interactions in the molten globule state of human alpha-lactalbumin. *J. Mol. Biol.* 283, 279-291.
89. Quezada, C.M., Schulman, B.A., Froggatt, J.J., Dobson, C.M., & Redfield, C. (2004). Local and global cooperativity in the human alpha-lactalbumin molten globule. *J. Mol. Biol.* 338, 149-158.

90. Redfield, C. (2004). Using nuclear magnetic resonance spectroscopy to study molten globule states of proteins. *Methods* 34, 121-132.
91. Wijesinha-Bettoni, R., Dobson, C. M. and Redfield, C. (2001). Comparison of the denaturant-induced unfolding of the bovine and human alpha-lactalbumin molten globules. *J. Mol. Biol.* 312, 261-273.
92. Saeki, K., Arai, M., Yoda, T., Nakao, M. and Kuwajima, K. (2004) Localized nature of the transition-state structure in goat alpha-lactalbumin folding. *J. Mol. Biol.* 341, 589-604.
93. Moriarty, D.F., Demarest, S.J., Robblee, J., Fairman, R. and Raleigh, D.P. (2000) Local interactions and the role of the 6-120 disulfide bond in alpha-lactalbumin: implications for formation of the molten globule state. *Biochim. Biophys. Acta-Protein Structure and Molecular Enzymology* 1476, 9-19.
94. Kuwajima, K., Ikeguchi, M., Sugawara, T., Hiraoka, Y. and Sugai, S. (1990) Kinetics of disulfide bond reduction in alpha-lactalbumin by dithiothreitol and molecular basis of superreactivity of the Cys6-Cys120 disulfide bond. *Biochemistry* 29, 8240-8249.
95. Wu, L.C., Schulman, B.A., Peng, Z.Y. and Kim, P.S. (1996) Disulfide determinants of calcium-induced packing in alpha-lactalbumin. *Biochemistry* 35, 859-863.
96. Redfield, C., Schulman, B.A., Milhollen, M.A., Kim, P.S. and Dobson, C.M. (1999) alpha-Lactalbumin forms a compact molten globule in the absence of disulfide bonds. *Nat. Struct. Biol.* 6, 948-952.

**Structural basis for difference in heat capacity
increments for Ca²⁺ binding to two α -lactalbumins**

A. Vanhooren, K. Vanhee, K. Noyelle, Z. Majer¹, M. Joniau and I. Hanssens

*Interdisciplinary Research Center, Katholieke Universiteit Leuven Campus
Kortrijk, Kortrijk, Belgium*

*¹Department of Organic Chemistry, Eötvös Loránd University, Budapest,
Hungary*

Based on Biophysical Journal, 2002, 82, 407-417

2.1 Abstract

Thermodynamic parameters for the unfolding of, as well as for the binding of Ca^{2+} to, goat α -lactalbumin (GLA) and bovine α -lactalbumin (BLA) are deduced from isothermal titration calorimetry (ITC) in a buffer containing 10 mM Tris-HCl, pH 7.5 near 25°C. Among the different parameters available, the heat capacity increments (ΔC_p) offer the most direct information for the associated conformational changes of the protein variants. The ΔC_p values for the transition from the native to the molten globule state are rather similar for both proteins, indicating that the extent of the corresponding conformational change is nearly identical. However, the respective ΔC_p values for the binding of Ca^{2+} are clearly different. The data suggest that a distinct protein region is more sensitive to a Ca^{2+} -dependent conformational change in BLA than is the case in GLA. By analysis of the tertiary structure we observed an extensive accumulation of negatively charged amino acids near the Ca^{2+} -binding site of BLA. In GLA, the cluster of negative charges is reduced by the substitution of Glu11 by Lys. The observed difference in ΔC_p values for the binding of Ca^{2+} is presumably in part related to this difference in charge distribution.

2.2 Introduction

α -Lactalbumin (LA) is a small globular protein. Its shape resembles that of a prolate ellipsoid. A deep cleft divides the molecule roughly into two lobes. One lobe, the α -domain, contains four α -helices, the other is characterized by the presence of a β -sheet (1-3). A loop of 10 amino acids that spans the cleft is strongly Ca^{2+} binding (1, 2, 4) and is assumed to play a role in the mutual positioning of the two domains. In the absence of Ca^{2+} and under mild denaturing conditions, a number of specific tertiary interactions dissolve cooperatively during a process which behaves as a two-state transition (5, 6). As a result, the protein adopts a slightly expanded molten globule state. In this state of LA, the β -domain is significantly unfolded while the α -domain retains its native helices as well as a native-like tertiary fold (7-10). The further unfolding of these secondary structures under stronger denaturing conditions occurs non-cooperatively (11-13).

Molten globule states are universal stable intermediates in folding processes of globular proteins (14-16) and much attention is being devoted to elucidate the characteristics that determine their structure and stability. The careful study of mutant proteins with a directed substitution offers an excellent approach to this problem. However, comparative studies of the unfolding behavior of closely related natural proteins can offer additional solutions.

Bovine α -lactalbumin (BLA) is known to be less stable than goat α -lactalbumin (GLA).¹⁷ The observation that the amino acid sequences of GLA and BLA differ by only 7 amino acids invited us to analyze the different thermodynamic parameters for the unfolding of both proteins under identical conditions of pH and low ionic strength. In a neutral to slightly basic medium and near room temperature the apo-forms of both LAs convert from the native to the molten globule state while the Ca²⁺-bound proteins are in their native conformation. Therefore, the analysis of the heat exchange (ΔH_{exp} -values) from isothermal titration calorimetry (ITC) measurements with Ca²⁺ at different temperatures yields the thermodynamic parameters (ΔH , ΔS , ΔG , ΔC_p) for the binding of the Ca²⁺ ion in addition to those for the conformational transition of the apo-proteins. Several authors have shown that even monovalent cations bind in a specific way to LAs (18-20), the ability of cations to interact with LA being optimal when the ionic radius equals that of Ca²⁺ (21). To avoid small monovalent cations we performed our measurements in a Tris-HCl buffer. However, Tris-H⁺ possesses a large deprotonation enthalpy. Upon possible protonation or deprotonation of the protein that might occur during conformational changes and Ca²⁺ binding, the measured heat exchange (ΔH_{exp} -values) also includes a contribution for the transfer of those protons from or to the components of the Tris-HCl buffer. Therefore, the impact of the deprotonation or protonation of the buffer components is measured to eventually correct the observed heat exchange (ΔH_{exp}). Of the resulting thermodynamic parameters (ΔH , ΔS , ΔG , ΔC_p), derived for the conformational transition and for the Ca²⁺ binding of the LAs, especially the heat capacity increments (ΔC_p values) are closely related to changes in the exposure of hydrophobic surface (22-25). Therefore, the ΔC_p values offer direct information on the extent of the conformational changes of LAs (26, 27).

Our analysis indicates that the heat capacity increments for the transition from the native state of apo-GLA and -BLA to their respective intermediary molten globule state ($\Delta C_{p \text{ NI}}$) have about half the value of those for the complete unfolding of a LA and are rather similar for both protein species. The $\Delta C_{p \text{ NI}}$ values agree with the observation that the molten globule state of a LA is

characterized by a highly unfolded β -domain and a well conserved native-like fold of the α -domain (7-10). In contrast, the heat capacity increments for the binding of Ca^{2+} ($\Delta C_{p, \text{Ca}^{2+}}$) are larger for BLA than for GLA. These differences in $\Delta C_{p, \text{Ca}^{2+}}$ occur as well for Ca^{2+} binding to the apo-LAs in their molten globule states as for binding to the native states. Therefore, a distinct region within BLA is clearly more sensitive to a Ca^{2+} -dependent exposure to solvent than is the corresponding region in GLA. By careful analysis of the respective tertiary structures of the native proteins we observed an increased accumulation of negatively charged amino acids near the Ca^{2+} -binding site of BLA. In GLA the cluster of negative charges is less pronounced as Glu-11, which participates in the negative cluster in BLA, is mutated to a positively charged Lys. Obviously, this different distribution of charged amino acids near the Ca^{2+} binding site contributes to the observed difference in $\Delta C_{p, \text{Ca}^{2+}}$ -values between apo-GLA and -BLA.

2.3 Materials and Methods

2.3.1 Materials

BLA was purchased from Sigma, St. Louis, Missouri. The protein was decalcified by applying a sample in 10 mM EDTA and 10 mM $(\text{NH}_4)_2\text{CO}_3$, pH 8.5, to a Sephacryl-HR-100 column. Elution was done with 5 mM $(\text{NH}_4)_2\text{CO}_3$, pH 8.5. The protein fraction was checked for its Ca^{2+} and Na^+ content by atomic absorption spectroscopy; typically it contained less than 0.05 and 0.08 mol of the respective cation/mol of protein. Preparations meeting these requirements were lyophilized and stored at -20°C until use. As $(\text{NH}_4)_2\text{CO}_3$ desintegrates upon lyophilization, salt free protein samples were obtained.

GLA was prepared from fresh milk whey. After addition of Tris and EDTA to final concentrations of 50 and 1 mM, respectively, and adjustment of the pH to 7.5 with HCl, the whey was applied to a Phenyl-Sepharose column (Pharmacia, Uppsala, Sweden). Apo-GLA was bound hydrophobically to the column (28, 29), while the other whey proteins were eluted with the Tris-EDTA buffer, pH 7.5. α -Lactalbumin was eluted by changing the eluting buffer to 50 mM Tris, 1 mM Ca^{2+} , pH 7.5. The Ca^{2+} -GLA was then demetallized as described above.

Lyophilized GLA and BLA samples were also checked for EDTA content, using a method based on the formation of a fluorescent terbium-EDTA-salicylic acid complex (30). Samples containing 500 μ l of a mixture of terbium nitrate and sodium salicylate (1 mM each), 1 ml of protein solution (15-80 μ M) and 500 μ l of Capso buffer (0.1 M, pH 11) were shaken for 15 minutes and transferred into a 10 \times 10 mm cuvette. The resultant fluorescence was measured with an Aminco-Bowman Series 2 spectrofluorimeter (excitation 340 nm, emission 545 nm) and compared with a calibration curve of samples containing EDTA (0-50 μ M). The residual EDTA-content for both BLA and GLA was below the detection limit, indicating that the molar ratio EDTA/protein was less than 0.02.

DE-MALDI-TOF mass spectroscopy revealed that each purified protein consists of a single component with a molecular mass of 14186 and 14178 for GLA and of BLA, respectively. The analysis was performed by M-Scan Ltd (Ascot, UK) using a Voyager STR Biospectrometry Research Station laser-desorption mass spectrometer coupled with Delayed Extraction.

Tris was a product of Merck, Darmstadt, Germany. HEPES and MOPS were purchased from Boehringer, Mannheim, Germany. Tris-HCl buffer was obtained by direct titration of Tris with HCl. Any back titration is avoided to exclude Na⁺ and other small cations from the buffer solution. These cations are suspected to bind competitively to the specific Ca²⁺ site (19-20). Buffer solutions of HEPES and MOPS were obtained by titration of the above sulfonic acids with either KOH or NaOH in order to distinguish the impact of K⁺ and/or Na⁺ cations.

BLA and GLA concentrations were determined by UV-spectrophotometry using the value $\epsilon_{280} = 28500$ (mol/l)⁻¹ cm⁻¹ for both proteins. This value has been determined for BLA (31). An identical molar extinction coefficient is applicable to both proteins as GLA and BLA contain Trp, Tyr and Cys groups at identical locations (32).

2.3.2 Circular Dichroism

Circular dichroism measurements were made on a Jasco J-600 spectropolarimeter (Jasco, Tokyo, Japan), using 5 mm cuvettes and a protein concentration of about 25 μ M. At each temperature of the transition curve, measurements were started 5 min after temperature equilibration of the sample. Evidence that an equilibrium state had been obtained was provided by the fact that the

ellipticity values were identical in heating and cooling runs, provided that the samples had not been exposed to high temperatures (>345 K) for more than 15 min.

2.3.3 Isothermal Titration Calorimetry

Microcalorimetric titration measurements were made in a MicroCal MCS isothermal titration calorimeter (MicroCal Inc., Northampton, MA). In a typical experiment, 1.3 ml of approximately $35 \mu\text{M}$ α -lactalbumin in 10 mM Tris-HCl, pH 7.5 near 25°C , was titrated in twenty steps with $40 \mu\text{l}$ of 3.5 mM CaCl_2 . The Ca^{2+} concentration of the titrant was determined using a Perkin-Elmer 3300 absorption spectrometer. During titration, the injection syringe was rotated at 200 rpm. The values of the molar enthalpy changes were determined from the titration curves after subtraction of a baseline measured in the absence of protein. To allow for a valid comparison of the results, special attention is given to titrate all the samples with Ca^{2+} from the same stock solution. In this way possible errors resulting from an inaccurate ion content are neutralized when comparing the resulting thermodynamic parameters.

2.4 Results

2.4.1 Near-UV ellipticity changes of GLA and BLA as a function of temperature

Several authors have shown that even monovalent cations bind in a specific way to LAs (18-20), the ability of the cations to interact with LA being optimal when the ionic radius equals that of Ca^{2+} (21). To avoid small monovalent cations we preferred a buffer of Tris/Tris- H^+ in this comparative study of Ca^{2+} -binding to apo-GLA and -BLA.

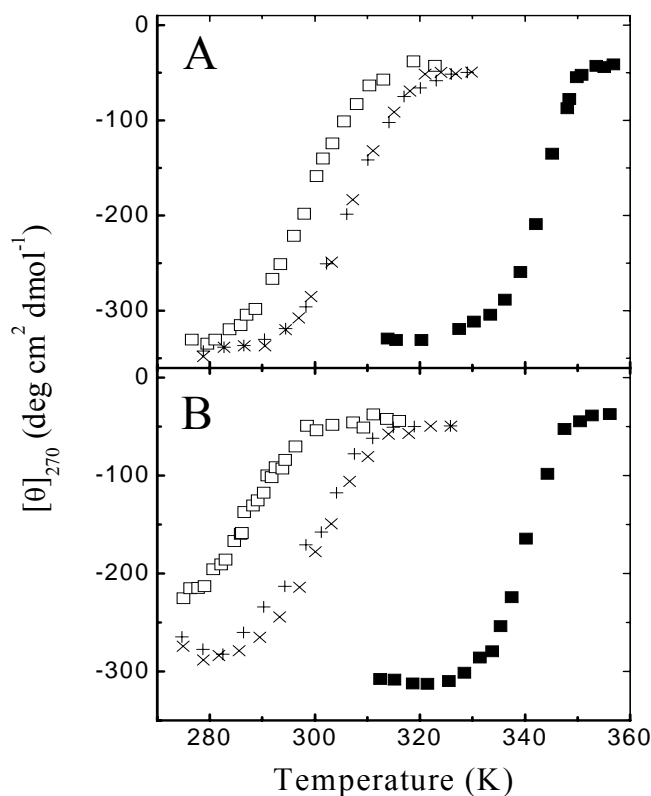


Figure 1: Ellipticity at 270 nm as a function of temperature for GLA (A) and BLA (B). The solvent conditions are 25 μM GLA in 10 mM Tris-HCl, pH 7.5 and 2 mM Ca²⁺ (■), in 10 mM Tris-HCl, 2 mM EGTA, pH 7.5 without further additions (□) or with 10 mM NaCl (×) and in 10mM MOPS-NaOH, 2 mM EGTA, pH 7.5 (+).

Before starting the calorimetric titrations we first verified the unfolding of the apo- and Ca²⁺-bound proteins under the solvent conditions of the subsequent calorimetric titrations. The unfolding of tertiary structure of LAs is monitored by the change of their near-UV ellipticity. Because of the immobilization of aromatic side chains by specific contacts, native LA shows a pronounced negative ellipticity near 270 nm. In the molten globule state, the interactions of the aromatic residues are randomized and the near-UV ellipticity approaches zero. The open and filled squares of Figures 1A and 1B represent the mean residue ellipticity at 270 nm of apo- and Ca²⁺-bound GLA and BLA, respectively, in 10 mM Tris-HCl as a function of temperature.

At 276 K (3 °C) the ellipticity values of apo-GLA and Ca²⁺-GLA in 10 mM Tris-HCl are nearly the same (Fig. 1A, open and filled squares), indicating that in both conditions GLA reaches a quasi-identical native state. In contrast, at 276 K and in the mentioned buffer conditions, the ellipticity value of apo-BLA is less negative than that of Ca²⁺-BLA (Fig. 1B, open and filled squares). This observation suggests that in the buffer of 10 mM Tris-HCl only a fraction of apo-BLA is folded into the native state at 276 K.

Furthermore, the near-UV CD curves indicate that the transition from the unfolded to the native conformation for apo-GLA as well as that for apo-BLA (Fig. 1, A and B, open squares) is mainly completed at 320 K (47 °C). The Ca^{2+} -bound proteins stay native up to the latter temperature (Fig. 1, A and B, filled squares). This increased thermal stability resulting from Ca^{2+} binding, which is a general property of all α -lactalbumins (4), is useful for the analysis of the ITC measurements.

2.4.2 Isothermal Titration Calorimetry of apo-GLA and -BLA with Ca^{2+}

Fig. 2, A and B, represents a typical example of an isothermal titration experiment. In panel 2A the heat exchange is shown at subsequent injections of Ca^{2+} into an apo-BLA solution at 313.6 K (40.5 °C).

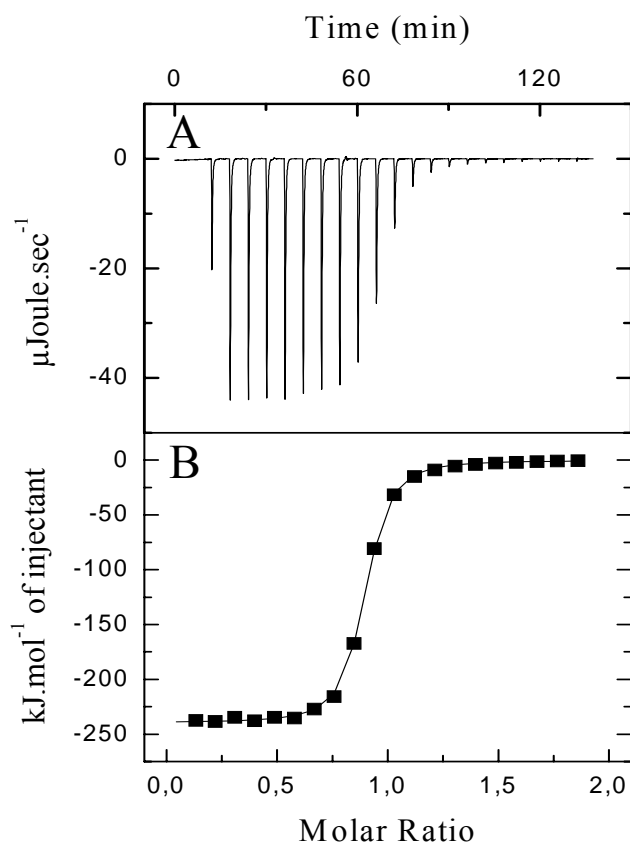


Figure 2: (A) Profile of the heat exchange measurement for a calorimetric titration of apo-BLA in 10mM Tris-HCl with Ca^{2+} . The sample solution (1.3 ml of 35 μM BLA at 313.7 K) was titrated with 2 μL injections of 3.5 mM Ca^{2+} . (B) Profile of the heat exchange per mol of injected Ca^{2+} as a function of the molar ratio of the injectant to BLA for the above titration. The line through the experimental points represents the optimal fit for a mono-ligand binding. From the curve fitting $\Delta H_{\text{Ca}^{2+},\text{exp}}$ and $K_{\text{Ca}^{2+},\text{app}}$ are obtained.

By deconvolution of the subsequent titration curve (Fig. 2B), the molar heat exchange for Ca²⁺ binding ($\Delta H_{Ca^{2+},exp(T)}$) is calculated. In case sufficient data points are gathered to reproduce accurately the drop of the heat release near the equivalence point, also a reliable value for the Ca²⁺-binding constant ($K_{Ca^{2+},app(T)}$) can be deduced. The further treatment of both series of data is described in the following sections.

Influence of possible proton exchange on the $\Delta H_{Ca^{2+},exp(T)}$ -values

The experimental values for molar release of heat upon Ca²⁺ binding ($-\Delta H_{Ca^{2+},exp(T)}$) to GLA and BLA in a buffer of 10 mM Tris-HCl, pH 7.5 near 298 K, are plotted as a function of temperature in Fig. 3, A and B, respectively. A number of distinct differences between both sigmoid curves are observed: (1) the transition domain, characterized by the steepest part of the curve, is situated at a higher temperature for GLA than for BLA; (2) in the center of the transition domain, the slope is larger for GLA than for BLA; (3) at the extremities of the respective transition domains, the slope is smaller for GLA than for BLA.

Before starting the analysis of the temperature dependence of the $\Delta H_{Ca^{2+},exp(T)}$ -values we looked for the possible contribution resulting from protonation of Tris or deprotonation of Tris-H⁺. Indeed, if LA would loose or acquire a proton upon Ca²⁺ binding and/or changing conformation these protons should be transferred to or withdrawn from the buffer components. In this case the $\Delta H_{Ca^{2+},exp(T)}$ -values would have to be corrected for the possible deprotonation enthalpy of the buffer ($\Delta H_{deprot(T)}$). The evaluation of this contribution is realized by measuring the binding of Ca²⁺ to the LAs in buffers with different deprotonation enthalpies. The real Ca²⁺-binding enthalpy can then be calculated according to:

$$\Delta H_{Ca^{2+},real(T)} = \Delta H_{Ca^{2+},exp(T)} - n_{H^+} \cdot \Delta H_{deprot(T)} \quad (1)$$

where n_{H^+} designates the number of protons that are released ($n_{H^+}>0$) or taken up ($n_{H^+}<0$) by the buffer.

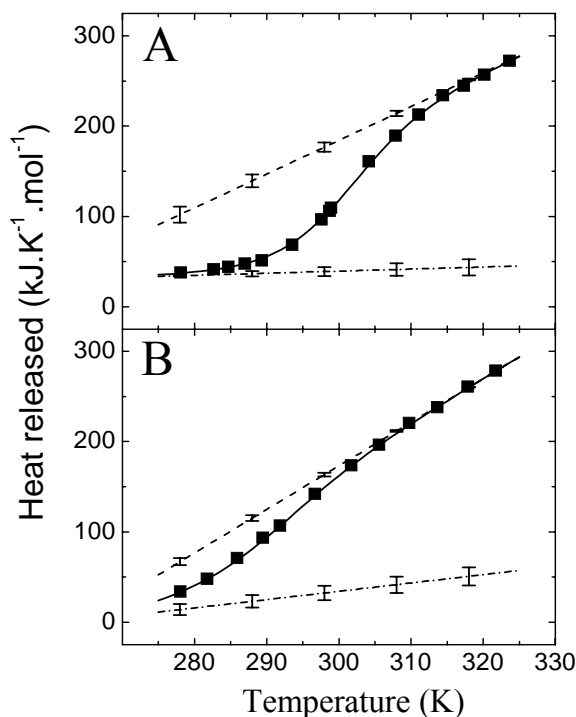


Figure 3: Molar heat release ($-\Delta H_{\text{Ca}^{2+},\text{exp}}$) for Ca^{2+} binding to GLA (A) and BLA (B). The black squares (■) represent experimental values. The full lines represent the curves fitted according to the combined Eq. 1-7. The dashed lines represent the temperature dependence of $-\Delta H_{\text{Ca}^{2+},\text{IN}}$. The dash-dot lines represent the temperature dependence of $-\Delta H_{\text{Ca}^{2+},\text{N}}$. The error bars represent standard deviation.

Table 1: Experimental enthalpy values for the binding of Ca^{2+} to GLA and BLA in different buffer conditions

Buffers	$\Delta H_{\text{deprot}}^*$ (kJ.mol ⁻¹)	GLA		BLA	
		T_{exp} (°C)	$\Delta H_{\text{Ca}^{2+},\text{exp}}^{\#}$ (kJ.mol ⁻¹)	T_{exp} (°C)	$\Delta H_{\text{Ca}^{2+},\text{exp}}^{\#}$ (kJ.mol ⁻¹)
pH 7.95 at 9.5 °C					
Tris-HCl 10 mM	48.1	9.7	-41.3	9.3	-50.3
Tris HCl 20 mM	48.1	9.1	-38.9	9.9	-42.7
Tris-HCl 10 mM, KCl 10mM	48.1	9.3	-30.4	9.5	-28.9
HEPES-KOH 10 mM	20.3	9.0	-29.4	9.0	-32.3
MOPS-KOH 10 mM	21.2	10.3	-31.3	9.0	-29.9
Tris-HCl 10 mM, NaCl 10 mM	48.1	9.2	-18.5	9.2	-9.5
HEPES-NaOH 10 mM	20.3	9.2	-17.1	8.6	-9.5
MOPS-NaOH 10 mM	21.2	9.3	-18.0	9.1	-10.4
pH 6.95 at 45 °C					
Tris-HCl 10 mM	46.5	45.1	-256.0	45.1	-260.9
Tris-HCl 10 mM, NaCl 10 mM	46.5	45.1	-249.7	45.1	-257.8
MOPS-NaOH 10 mM	22.6	45.1	-246.8	45.1	-256.1

* Values for ΔH_{deprot} for MOPS and HEPES were obtained from Fukada et al. (50); the ΔH_{deprot} -values for Tris were obtained from Samland et al. (51).

[#] Standard deviations of multiple experiments were typically ± 1.5 kJ/mol.

We measured the $\Delta H_{Ca^{2+},exp(T)}$ -values for the binding of Ca²⁺ to GLA and BLA in 10 mM MOPS, HEPES and Tris-HCl, respectively, at the low and high temperature extremes of the transition curve. As the equilibrium $Tris + H^+ \leftrightarrow Tris-H^+$ is sensitive to temperature, a Tris-HCl buffer of pH 7.5 near 25 °C (298.1 K) shifts from pH 7.95 near 9.5 °C (282.6 K) to pH 6.95 near 45 °C (318.1 K). We accounted for this pH shift by adjusting the pH of the MOPS and HEPES buffer to pH 7.95 near 9.5 °C and to pH 6.95 near 45 °C, respectively. This large difference in pH by no means invalidates our comparative study.

The $\Delta H_{Ca^{2+},exp(T)}$ -values determined at pH 7.95 near 9.5 °C are summarized in Table 1. Interestingly, the values vary as to whether the sulfonic acids, MOPS and HEPES, have been titrated with KOH or NaOH in order to attain pH 7.95 near 9.5 °C. However, the respective Ca²⁺ binding enthalpies in MOPS and HEPES buffer are, within the experimental error, identical with the $\Delta H_{Ca^{2+},exp(T)}$ values that are obtained in Tris-HCl buffer to which 10 mM KCl or NaCl is added. In the presence of 10 mM K⁺ and Na⁺, respectively, the $\Delta H_{Ca^{2+},exp(T)}$ -values of GLA and BLA are identical in the different buffer systems and are not influenced by the deprotonation enthalpy of the buffer. This observation allows concluding that neither GLA nor BLA exchange an appreciable amount of protons upon Ca²⁺ binding at the lower temperature limit of the transition curves.

Concerning the observation that the $\Delta H_{Ca^{2+},exp(T)}$ -values of GLA and BLA are dependent on the nature of the dissolved monovalent cation, the near UV ellipticity curves presented by the right(+) and diagonal(\times) crosses in Fig. 1, A and B, show that the transition of both apo-proteins is shifted to higher temperatures by the addition of 10 mM Na⁺. Therefore the $\Delta H_{Ca^{2+},exp(T)}$ -values at 9.5°C in the absence and presence of Na⁺ (and presumably also of K⁺) are influenced by small differences in protein conformation depending on whether Na⁺ (or K⁺) is added to the solution or not. Nevertheless, the fact that the $\Delta H_{Ca^{2+},exp(T)}$ -values in the presence of equal concentrations of Tris-H⁺, K⁺ or Na⁺ ions are different (Table 1A) indicates that the ion effect is not a pure question of ionic strength. It affirms the idea that Na⁺ and even that K⁺ bind in a specific way to LAs (18-20).

The results of Table 1 show that also near 45°C (318.1K) at pH 6.95 and in the presence of 10 mM Na⁺ (10 mM MOPS-NaOH and 10 mM Tris-HCl with 10 mM NaCl), the $\Delta H_{Ca^{2+},exp(T)}$ -

values of GLA and of BLA are identical within experimental error. The values are not dependent on the deprotonation enthalpy of the buffer. As a consequence, also under the experimental conditions of the high temperature extreme of the transition curves, no noticeable amount of protons is exchanged.

The fact that the Ca^{2+} binding enthalpies of GLA and BLA are not influenced by the buffer deprotonation enthalpy, neither before nor after the transition domain, strongly suggests that the $\Delta H_{\text{Ca}^{2+},\text{exp}(T)}$ -values do not require corrections for protonation or deprotonation of the buffer within the whole temperature region investigated.

Analysis of the temperature dependence of the $\Delta H_{\text{Ca}^{2+},\text{exp}(T)}$ -values

From the above results we have learned that the experimental enthalpy values for Ca^{2+} binding to apo-GLA and -BLA (Fig. 3, A and B) do not contain noticeable contributions from proton exchange with the buffer substances. For the further analysis of the $\Delta H_{\text{Ca}^{2+},\text{exp}(T)}$ -values we assumed that, in the considered temperature range (276-320 K), native apo-LA equilibrates with the intermediary unfolded molten globule state and that all Ca^{2+} -bound LA is native. The latter assumption is in agreement with the constant near-UV CD signal of Ca^{2+} -LA below 320 K (Fig. 1). Under the conditions of the above assumptions $\Delta H_{\text{Ca}^{2+},\text{exp}(T)}$ consists of only two contributions, one for Ca^{2+} binding to the fraction of native apo-LA ($\alpha_{\text{N}(T)}$) and another for Ca^{2+} binding to the fraction of molten globule ($1 - \alpha_{\text{N}(T)}$). The respective molar enthalpies are represented by $\Delta H_{\text{Ca}^{2+},\text{N}(T)}$ and $\Delta H_{\text{Ca}^{2+},\text{IN}(T)}$. The subscript N refers to Ca^{2+} binding to native apo-LA, the subscript IN emphasizes that Ca^{2+} binding to intermediary unfolded apo-LA also includes a transition to the native state of the protein. Hence,

$$\Delta H_{\text{Ca}^{2+},\text{exp}(T)} = \alpha_{\text{N}(T)} \times \Delta H_{\text{Ca}^{2+},\text{N}(T)} + (1 - \alpha_{\text{N}(T)}) \times \Delta H_{\text{Ca}^{2+},\text{IN}(T)} \quad (2)$$

The values of the enthalpy change in the above equation are temperature-dependent. They can be related to the respective values at the standard temperature (298 K) by the heat capacity increments $\Delta C_{\text{p Ca}^{2+},\text{N}}$ and $\Delta C_{\text{p Ca}^{2+},\text{IN}}$. Assuming that the respective heat capacity increments do not depend significantly on temperature, we write

$$\Delta H_{\text{Ca}^{2+},\text{N}(T)} = \Delta H_{\text{Ca}^{2+},\text{N}(298)} + \Delta C_{\text{p Ca}^{2+},\text{N}} \times (T - 298) \quad (3)$$

and

$$\Delta H_{Ca^{2+},IN(T)} = \Delta H_{Ca^{2+},IN(298)} + \Delta C_{p\ Ca^{2+},IN} \times (T - 298) \quad (4)$$

$\alpha_{N(T)}$ in Eq. 2 is further expressed as a function of $K_{NI(T)}$, the equilibrium constant for the unfolding from the native to the intermediary unfolded state of the apo-protein

$$\alpha_{N(T)} = 1 / (1 + K_{NI(T)}) \quad (5)$$

The equilibrium constant in its turn is expressed as a function of the characteristic thermodynamic parameters

$$K_{NI(T)} = \exp \left(-(\Delta H_{NI(298)} - T\Delta S_{NI(298)} + \Delta C_{p\ NI} (T - 298 - T \ln T/298)) / RT \right) \quad (6)$$

$\Delta H_{NI(298)}$ and $\Delta S_{NI(298)}$ are the transition enthalpy and entropy at 298 K, respectively.

Finally, as $\Delta H_{Ca^{2+},N(T)}$ is the enthalpy exchange for Ca²⁺ binding to native apo-LA whereas $\Delta H_{Ca^{2+},IN(T)}$ combines the value for Ca²⁺ binding with that for a conformational change from an intermediary unfolded to a native Ca²⁺ protein, the enthalpy change for the unfolding of apo-LA ($\Delta H_{NI(298)}$) is substituted in Eq. 6 by ($\Delta H_{Ca^{2+},N(298)} - \Delta H_{Ca^{2+},IN(298)}$). The related heat capacity change ($\Delta C_{p\ NI}$) is also substituted by ($\Delta C_{p\ Ca^{2+},N} - \Delta C_{p\ Ca^{2+},IN}$).

$$\Delta H_{NI(298)} = \Delta H_{Ca^{2+},N(298)} - \Delta H_{Ca^{2+},IN(298)} \quad (7)$$

$$\Delta C_{p\ NI} = \Delta C_{p\ Ca^{2+},N} - \Delta C_{p\ Ca^{2+},IN} \quad (8)$$

The results of the curve fittings according to the combined Eqs 2-8 are shown in Fig. 3, A and B. The full line in each of these figures, represents the best fit of the $-\Delta H_{exp(T)}$ values as a function of temperature. The fitting offers the numeric values of five independent parameters: $\Delta H_{Ca^{2+},IN(298)}$, $\Delta C_{p\ Ca^{2+},IN}$, $\Delta H_{Ca^{2+},N(298)}$, $\Delta C_{p\ Ca^{2+},N}$ and $\Delta S_{NI(298)}$. These values are collected in Table 2. To enable a direct comparison of the complementary thermodynamic parameters, the resulting values of $\Delta H_{NI(298)}$, of $\Delta C_{p\ NI}$, of the product $T_{(298)} \times \Delta S_{NI(298)}$ and of $\Delta G_{NI(298)}$ are also added to Table 2. In Fig. 3, A and B, the temperature dependence of the respective $\Delta H_{Ca^{2+},IN(T)}$ (Eq. 4) and $\Delta H_{Ca^{2+},N(T)}$ values (Eq. 3) is also represented. The $\Delta H_{Ca^{2+},IN(T)}$ values are represented by the dashed lines. These lines are tangent to the experimental enthalpy values in the high temperature region and their slopes equal the respective $\Delta C_{p\ Ca^{2+},IN}$ values. The $\Delta H_{Ca^{2+},N(T)}$ values are presented by the dash-and-dot lines. These lines are supposed to touch the experimental curve at sufficiently low temperatures. Their slopes equal $\Delta C_{p\ Ca^{2+},N}$.

Table 2: Summary of the thermodynamic parameters obtained from isothermal titration of GLA and BLA with Ca^{2+} at different temperatures

Parameter		GLA	BLA
$\Delta H_{\text{Ca}^{2+},\text{IN}(298)}$	(kJ mol ⁻¹)	- 177.4 ± 5	- 164.3 ± 2
$\Delta H_{\text{Ca}^{2+},\text{N}(298)}$	(kJ mol ⁻¹)	- 38.9 ± 5	- 32.4 ± 8
$\Delta H_{\text{NI}(298)}$	(kJ mol ⁻¹)	138.5 ± 10	131.9 ± 10
$\Delta S_{\text{NI}(298)}$	(kJ K ⁻¹ mol ⁻¹)	463 ± 32	460 ± 35
$T_{(298)} \times \Delta S_{\text{NI}(298)}$	(kJ mol ⁻¹)	138.0 ± 10	137.1 ± 10
$\Delta G_{\text{NI}(298)}$	(kJ mol ⁻¹)	+ 0.5 ± 0.2	- 5.2 ± 0.5
$\Delta C_{\text{p Ca}^{2+},\text{IN}}$	(kJ K ⁻¹ mol ⁻¹)	- 3.74 ± 0.2	- 4.83 ± 0.1
$\Delta C_{\text{p Ca}^{2+},\text{N}}$	(kJ K ⁻¹ mol ⁻¹)	- 0.23 ± 0.2	- 0.92 ± 0.1
$\Delta C_{\text{p NI}}$	(kJ K ⁻¹ mol ⁻¹)	3.51 ± 0.3	3.91 ± 0.2

The parameters $\Delta H_{\text{Ca}^{2+},\text{IN}(298)}$, $\Delta H_{\text{Ca}^{2+},\text{N}(298)}$, $\Delta S_{\text{NI}(298)}$, $\Delta C_{\text{p Ca}^{2+},\text{IN}}$ and $\Delta C_{\text{p Ca}^{2+},\text{N}}$ are obtained directly from the fittings in Figure 3A and 3B. The other parameters are deduced as complementary from classical thermodynamic equations.

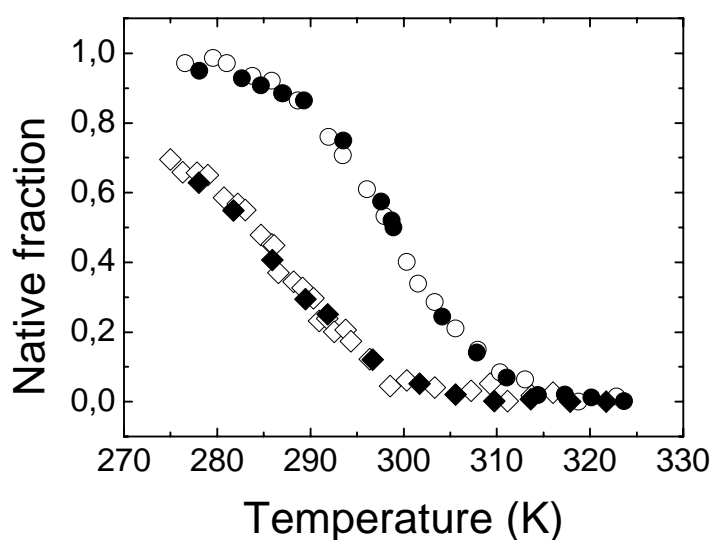


Figure 4: Thermal transition curves for apo-GLA (circles) and apo-BLA (diamonds) calculated from the ellipticity change at 270 nm (open symbols) and from the molar enthalpy change upon Ca^{2+} binding (black symbols), respectively. For the calculation of the fractions of native BLA from the ellipticity change it has been assumed that the compact native state of apo-BLA has the same ellipticity value as native Ca^{2+} -loaded BLA.

It is a prerequisite of a two-state equilibrium that different physico-chemical characteristics register the same transition. As a verification of this requirement we compared the thermal transitions resulting from the ellipticity changes (Fig. 1, A and B) with those obtained from the titration calorimetry (Fig. 3, A and B). The fractions of native apo-GLA, deduced from ellipticity changes, are easily calculated as the limit values at both extremes of the transition curve are clearly obtained (Fig. 1A). For the calculation of the fractions of native apo-BLA from the ellipticity changes, we supposed that the near-UV CD signal of native apo-BLA equals the value of native Ca²⁺-BLA (Fig. 1B). The native fractions, deduced from titration calorimetry, are calculated for both apo-LAs according to Eq. 2. The results are plotted in Fig. 4. The agreement of both series of fractional changes for GLA as well as for BLA, is a confirmation that near-UV CD changes and heat exchanges register the same unfolding equilibrium and that the assumption of a two-state transition, made to deduce the fitting procedure, is reliable.

The Ca²⁺ binding constants

At each temperature an apparent constant for the binding of Ca²⁺ to LA is obtained by simulation of the ITC titration curve (Fig. 2B). However in the lower temperature region, Ca²⁺ binding to LA is very strong resulting in very steep ITC titration curves near the equivalence points. In this case, the simulation procedure offers an inaccurate, mostly underestimated value of the binding constant. This is the case whenever the product of the binding constant times the concentration of the dissolved macromolecule exceeds a value of 1000 (Users Manual of MicroCal Inc.). In our titration experiments, using a protein concentration of 35 μ M, apparent binding constants of 2.8×10^7 and larger are obtained below 310 K. Therefore, no account is taken of these values. Above 310 K, the experimental decrease of the heat exchange near the equivalence point becomes spread over several injections of the Ca²⁺ solution (Fig. 2B) and the apparent Ca²⁺-binding constants ($K_{Ca^{2+},app(T)}$) are smaller than 2.8×10^7 . These values are gathered in Table 3.

The term apparent binding constant ($K_{Ca^{2+},app(T)}$) refers to the fact that in our ITC measurements Ca²⁺ binds to an equilibrium mixture of native and expanded apo-LA. However, in the conditions of our experiments and below 320 K, Ca²⁺-bound LA is compactly folded (Fig. 1). $K_{Ca^{2+},app(T)}$ defined in this way can be related with $K_{Ca^{2+},N(T)}$, the constant for Ca²⁺ binding to

native apo-LA, and with $K_{NE(T)}$, the constant for the equilibrium between native and intermediary unfolded apo-LA, by the following equation

$$K_{Ca^{2+},app(T)} = \frac{[Ca^{2+}\text{-}LA_N]}{([LA_N] + [LA_I]) \times [Ca^{2+}]} = \frac{K_{Ca^{2+},N(T)}}{(1 + K_{NI(T)})} \quad (9)$$

The thermodynamic parameters in Table 2 allow us to calculate $K_{NI(T)}$ -values at different temperatures. From the available $K_{Ca^{2+},app(T)}$ and calculated $K_{NI(T)}$ values, constants for Ca^{2+} binding to native LA ($K_{Ca^{2+},N(T)}$) are obtained. These values are added in Table 3. They are also introduced, together with $\Delta H_{Ca^{2+},N(298)}$ and $\Delta C_{p,Ca^{2+},N}$ -values (from Table 2), in a van 't Hoff-equation equivalent to Eq. 6 in order to calculate $\Delta S_{Ca^{2+},N(298)}$ and subsequently $K_{Ca^{2+},N(298)}$. The latter values equal $1.1 (\pm 0.2) \times 10^9$ and $3.9 (\pm 0.8) \times 10^9$ for GLA and BLA, respectively. These binding constants and the corresponding thermodynamic parameters are collected in Table 4. Taking into account the partial unfolding of both apo-LAs at 298 K, the apparent constants for the binding of Ca^{2+} to the mixed population of native and intermediary unfolded apo-GLA or -BLA (estimated $K_{Ca^{2+},app(298)}$) are $5.7 (\pm 1) \times 10^8$ and $4.3 (\pm 0.8) \times 10^8$, respectively.

Table 3: Summary of $K_{Ca^{2+},app}$, $K_{NI,apoLA}$ and $K_{Ca^{2+},N}$ values for GLA and BLA

Temperature (K)	$K_{Ca^{2+},app}$ ($\text{mol}^{-1} \cdot \text{L}$)	$K_{NI,apoLA}$	$K_{Ca^{2+},N}$ ($\text{mol}^{-1} \text{L}$)
GLA			
314.7	$(15.0 \pm 0.3) \times 10^6$	28 ± 1.1	$(4.4 \pm 0.4) \times 10^8$
317.3	$(3.4 \pm 0.2) \times 10^6$	54 ± 2.9	$(1.8 \pm 0.2) \times 10^8$
320.1	$(1.4 \pm 0.1) \times 10^6$	108 ± 5.9	$(1.5 \pm 0.2) \times 10^8$
BLA			
313.7	$(8.3 \pm 0.4) \times 10^6$	210 ± 7.6	$(17.6 \pm 1.2) \times 10^8$
317.8	$(3.1 \pm 0.1) \times 10^6$	570 ± 14	$(17.7 \pm 0.9) \times 10^8$
321.7	$(0.9 \pm 0.1) \times 10^6$	1542 ± 43	$(14.0 \pm 1.5) \times 10^8$

Below 310 K apparent binding constants of 2.8×10^7 and larger are obtained. No account is taken of these values as the product of $K_{Ca^{2+},app}$ times the concentration of the dissolved macromolecule ($35 \mu\text{M}$) exceeds 1000 in these conditions, which prohibits the definition of valuable data (ITC Users Manual of MicroCal Inc.).

Table 4: Thermodynamic parameters for the binding of Ca²⁺ to native apo-LA at 298 K

Parameter		GLA	BLA
$\Delta H_{Ca^{2+},N(298)}$	(kJ mol ⁻¹)	- 38.9 ± 5	- 32.4 ± 8
$\Delta S_{Ca^{2+},N(298)}$	(J K ⁻¹ mol)	+ 42 ± 15	+ 75 ± 25
$T_{(298)} \times \Delta S_{Ca^{2+},N(298)}$	(kJ mol ⁻¹)	+12.6 ± 5	+ 22.3 ± 8
$\Delta G_{Ca^{2+},N(298)}$	(kJ mol ⁻¹)	51.5 ± 0.4	- 54.7 ± 0.5
$K_{Ca^{2+},N(298)}$	(mol ⁻¹ L)	1.1 (±0.2) × 10 ⁹	3.9 (±0.4) × 10 ⁹
$\Delta C_{p, Ca^{2+},N}$	(kJ K ⁻¹ mol ⁻¹)	- 0.23 ± 0.2	- 0.92 ± 0.1

2.5 Discussion

The final goal of this isothermal titration calorimetry (ITC) study is the mutual comparison of the thermodynamic properties for the thermal unfolding and for the Ca²⁺ binding of apo-GLA and apo-BLA. To avoid small monovalent cations we performed our measurements in a Tris-HCl buffer (10 mM Tris-HCl, pH 7.5 near 25 °C).

The thermodynamic parameters for the thermal unfolding of a LA are frequently deduced from differential scanning calorimetry (DSC) data (33-36). A plot of a DSC scan represents the heat capacity as a function of temperature. The excess heat absorption upon unfolding of the protein offers a bell-shaped heat capacity peak; under the peak an ‘S-shaped’ baseline shift occurs as a consequence of the different specific heat capacities of the protein states before and after the transition. In the case of an apo-LA this offers a specific inconvenience. Indeed, at neutral pH and low ionic strength (10 mM Tris-HCl, pH 7.5 near 25 °C) apo-LA already starts to denature at temperatures below 0° C. This results in an incomplete DSC transition peak (13, 37, 38) and in a lack of reference values needed to draw the ‘S-shaped’ baseline. As a consequence the calculation of fractional changes of the protein states as a function of temperature, as well as the computation of the transition enthalpy is compromised. Nevertheless, to enable the analysis of the data, it has been postulated that any native Ca²⁺-LA has the same heat capacity as the native apo-LA variant (13, 26, 27). Our results, however, indicate that this hypothesis does not hold for every type of LA.

In our study we derived the thermodynamic parameters for the unfolding of apo-GLA and -BLA in 10 mM Tris-HCl from ITC measurements with Ca²⁺. The analysis of ITC-data is enabled by the fact that the temperature intervals for the thermal unfolding of the apo- and the Ca²⁺-LAs are

clearly separated from each other (open and filled squares in Fig. 1, A and B). The ITC-data offer at each temperature an absolute value of the heat exchange on Ca^{2+} binding (Fig. 3, A and B). Under the conditions of our experiments (pH 7-8) the $\Delta H_{\text{b Ca}^{2+}, \text{exp}}$ -values are free from contributions due to protonation or deprotonation of buffer substances. The data are analyzed assuming that the transition between the native and the molten globule state of LA is in a two-state equilibrium and that, within the considered temperature range, constant heat capacity increments can be assigned to the transition. To verify the reliability of the above assumptions we compared the thermal transitions resulting from our ITC analysis with those obtained from the near-UV ellipticity changes. The good overlap of the fractional changes derived by both methods (Fig. 4) points out that after all the combined assumption of a global two-state equilibrium and a constant heat capacity increment for the transition, holds within the conditions of our study. Moreover, our thermal analyses are based on the agreement of the calorimetric enthalpy values (Fig. 3, A and B) and of the van 't Hoff enthalpies for two-state transition (Eq. 2-8). The ability to fit a curve of experimental enthalpy values as a function of temperature to the combined equations is in a complementary way confirmatory for the applicability of the assumptions.

In agreement with observations of Segawa and Sugai (17), our near-UV CD transition curves (Fig. 1, A and B) indicate that native apo-GLA is more thermostable than apo-BLA. This statement is further evidenced by the transition curves resulting from the calorimetric titrations (Fig. 3, A and B). The free energy values for the transition (ΔG_{NI}) of both LAs result from positive ΔH_{NI} - and positive ΔS_{NI} -values (Table 2), therefore the thermal unfolding of both apo-LAs is entropy driven. However the larger free energy change for the transition of apo-GLA than for apo-BLA (+ 0.5 kJ/mol and - 5.2 kJ/mol, respectively, at 298 K) results from a larger melting enthalpy for the former than for the latter apo-protein (138.5 and 131.9 kJ mol⁻¹, respectively, at 298K). In the transition region the ΔS_{NI} -values are very similar for both proteins (463 J K⁻¹ mol⁻¹ and 460 J K⁻¹ mol⁻¹, respectively, at 298 K). Comparable results are obtained by Desmet (21).

The most important contribution of the present study comes from the observed differences in heat capacity increment. The heat capacity change between two protein states (ΔC_p) is the thermodynamic property that can be connected most directly to the exposure of surface area (39). Several research groups have developed algorithms relating the ΔC_p values to the area of hydrophobic and hydrophilic surfaces that become exposed and hydrated during the unfolding of the protein (22-25). In those equations, the contributions from the exposure of hydrophobic

surface are dominant. In BLA a clear correlation has been found between the $\Delta C_{p,NI}$ value and the amount of residual secondary structure of the denatured protein (26, 27). At room temperature the ΔC_p value between completely unfolded and native LA is estimated at 7.5 - 8.0 kJ K⁻¹ mol⁻¹ (15, 26), whereas that between the molten globule and the native state of LA's is 3.5 - 4.0 kJ K⁻¹ mol⁻¹ (25, 26). Our ITC study offers $\Delta C_{p,NI}$ values of 3.51 and 3.91 kJ K⁻¹ mol⁻¹ for the thermal transition of apo-GLA and -BLA, respectively. It has been pointed out that, in the molten globule state of LA, the β -sheet domain is significantly unfolded while the α -helix domain retains its native helices as well as its tertiary fold (7-10). The fact that the ΔC_p values for the expansion of native apo-GLA and -BLA to the molten globule state are nearly half of those for complete unfolding, is in good correspondence with the above statement. Furthermore, the mutual resemblance of both $\Delta C_{p,NI}$ values suggests that the extent of the temperature-induced conformational change is nearly identical for both apo-LAs.

In contrast to the good resemblance of the $\Delta C_{p,NI}$ values, clear differences are revealed between the respective $\Delta C_{p,Ca^{2+},N}$ and $\Delta C_{p,Ca^{2+},IN}$ values (Table 2). The values of $\Delta C_{p,Ca^{2+},N}$ amount to -0.23 for GLA and -0.92 kJ K⁻¹ mol⁻¹ for BLA. By several authors (13, 40-42) Ca²⁺ binding to native apo-LA is supposed not to affect the conformation of the protein and the heat capacity change for Ca²⁺ binding to this state is estimated to approach zero. The small value of $\Delta C_{p,Ca^{2+},N}$ for GLA (-0.23 kJ K⁻¹ mol⁻¹) is in fair agreement with this point of view. However this statement does not apply to BLA. The relatively important $\Delta C_{p,Ca^{2+},N}$ -value for BLA (-0.92 kJ K⁻¹ mol⁻¹) indicates that Ca²⁺-BLA is more compactly folded than native apo-BLA. A recent x-ray diffraction study reveals that on removal of Ca²⁺ from crystallized BLA, a minor expansion of the metal binding site triggers a more important separation of the helical and the β -sheet domain at the opposite face of the protein molecule (43). Such conformational differences between native apo- and Ca²⁺-conformers undoubtedly contribute to the observed $\Delta C_{p,Ca^{2+},N}$ value for BLA. However, the poor $\Delta C_{p,Ca^{2+},N}$ value for GLA suggests that the latter protein variant, in its native state, is less susceptible for the above as well as for eventual other events due to Ca²⁺-induced access of solvent into its hydrophobic regions. This different influence of Ca²⁺ is unexpected as the Ca²⁺-binding site is very much conserved among the different LAs (1). Indeed, all 10 amino acids of the Ca²⁺ binding loop are identical in GLA and BLA (Fig. 5, Lys79-Asp88). In order to investigate possible origins for different $\Delta C_{p,Ca^{2+},N}$ -values in GLA and BLA we have inspected the location of the differing amino acids within the spatial structure of those proteins. In BLA, 7 amino acids differ from GLA (Fig. 5).

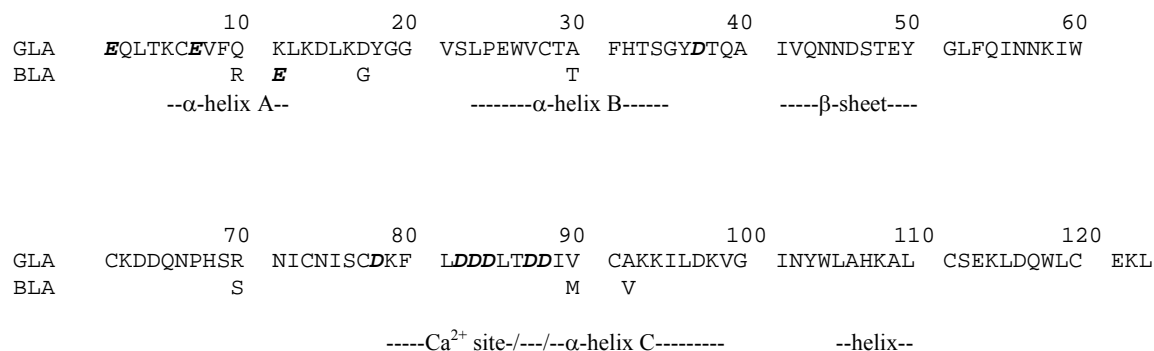


Figure 5: Amino acid sequences of GLA and BLA. The complete sequence of GLA is given; the sequence of BLA only highlights the positions that differ from GLA. The amino acids that approach each other in the tertiary structure creating a negatively charged cluster around the Ca²⁺-binding site, are printed boldly. The location of the principal secondary structural elements is also marked.

Three neutral residues are conservatively replaced by other neutral ones (Ala30Thr, Val90Met and Ala92Val). One neutral amino acid in GLA is replaced by a positively charged one in BLA (Gln10Arg). Two charged amino acids become neutral (Asp17Gly and Arg70Ser) and one positively charged residue in GLA is replaced by a negatively charged one in BLA (Lys11Glu). Strikingly, Glu-11 in BLA contributes to a large cluster of negative charges (see Fig. 6). The cluster is composed of Asp78, -82, -83, -84, -87 and -88 which are located on the Ca²⁺-binding loop, of Asp37 which is located in a loop between helix B and the β-sheet, of Glu7 and Glu11 on helix A near the NH₂-terminus and of the terminal Glu1. As a consequence, quite different subparts of the molecule encounter each other in the negatively charged cluster. Undoubtedly, in a medium of low ionic strength and in the absence of a metal ion, the realization of a close approach between the Ca²⁺-binding loop and the NH₂-terminal region within this protein is hindered by the strong repulsion of charges from both substructures. Upon binding, Ca²⁺ accommodates the carboxyl groups of Asp82, -87 and -88 (4) thereby considerably reducing the repulsion between the above substructures. In contrast, the repulsion between the above substructures in apo-GLA is already counteracted by the presence of a positive Lys in position 11 (Fig. 6A) and the binding of Ca²⁺ is in this case hardly able to effect a closer mutual approach of the mentioned substructures. Additional evidence for the suggestion that in 10 mM Tris-HCl the compact state of native apo-BLA suffers more from repulsive charges than the equivalent apo-GLA comes from the larger temperature shift when 10 mM NaCl is added (compare the curves marked by open squares and diagonal crosses in Fig. 1, A and B). Indeed, the larger temperature shift indicates that apo-BLA is stabilized more than apo-GLA by a reduction of the repulsive forces.

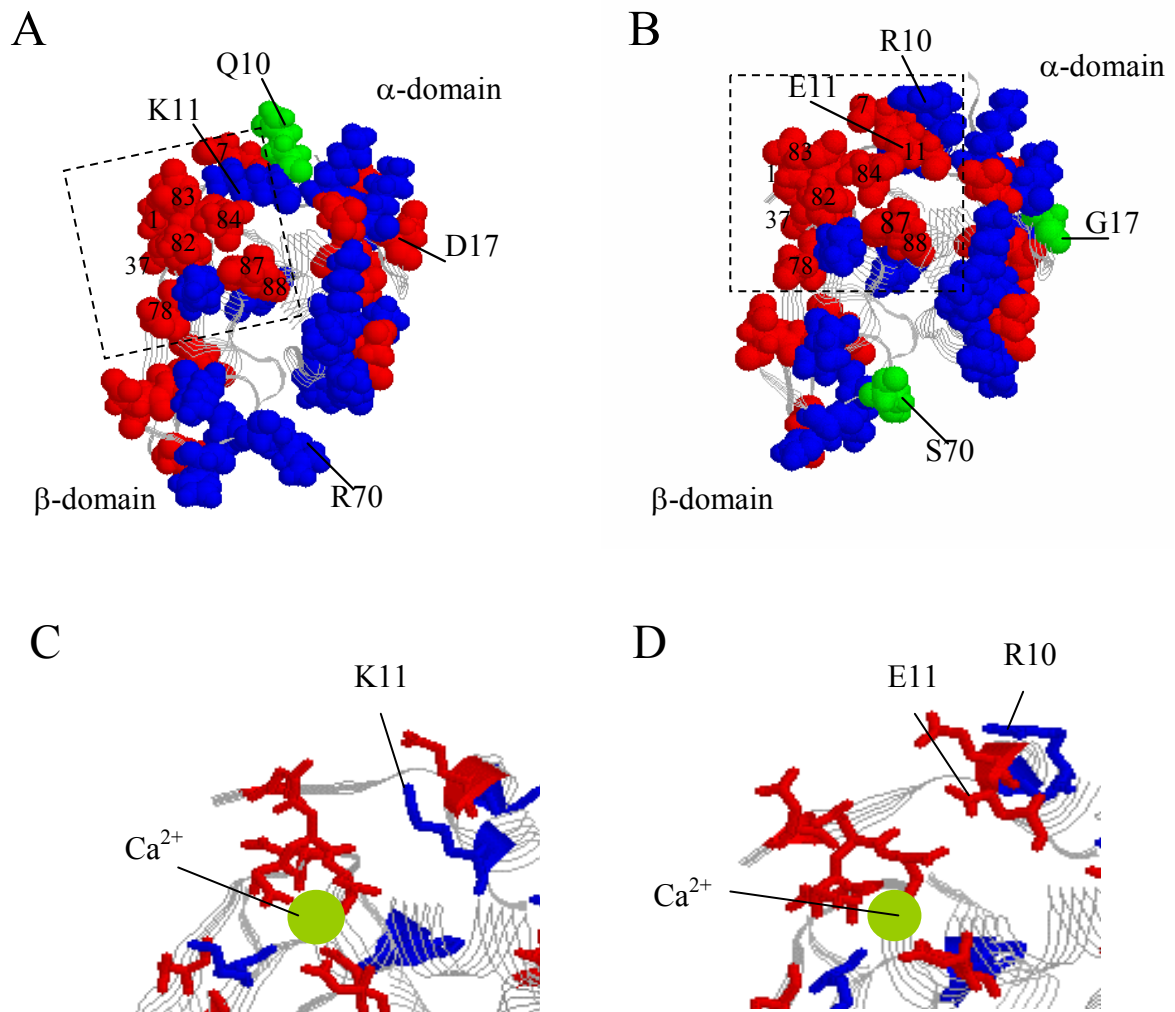


Figure 6: Space distribution of charges in LA at pH 7.5. The crystal structures of GLA (A) and BLA (B) are generated from the coordinates deposited under the codes 1HFYa and 1HFZa, respectively, in the Brookhaven Protein Data Bank (52). The negatively charged Asp and Glu residues are presented in red. The positively charged Lys, Arg and His residues are in blue. The amino acids that are differently charged in GLA and BLA are also explicitly marked. Only those neutral amino acids that meet the above requirement are drawn space filled in green. The negatively charged amino acids within the Ca²⁺-binding loop as well as those immediately surrounding this loop ($< 10 \text{ \AA}$), are numbered according to their sequence in the peptide chain. The positions of the COOH-terminal residues 121-123 are not clearly defined from the electron density maps. Therefore none of those amino acids is drawn. Details of the Ca²⁺ binding site of GLA (C) and BLA (D) are shown, corresponding with the dashed lines of A and B, respectively

Finally, in our study we determined Ca²⁺ binding constants for GLA and BLA. Since it has been found that α -LAs bind Ca²⁺ with high specificity (5) the binding constant for Ca²⁺ at a neutral pH and near 25°C has been determined by different authors. Most published values concern apparent constants for the binding of Ca²⁺ to apo-BLA that is partially in a molten globule state. Although there is no full agreement, most authors found evidence for a binding constant between

10^8 and 10^9 (6, 41, 44-47). Our estimated $K_{Ca^{2+},app}$ values at 298 K (5.7×10^8 and 4.3×10^8 for apo-GLA and -BLA, respectively) are in good agreement with these data. Furthermore, our study makes clear that larger values must be considered for the binding constant of Ca^{2+} to native apo-LA ($K_{Ca^{2+},N(T)}$); at 298 K these values are 1.05×10^9 and 3.95×10^9 for GLA and BLA, respectively. As well the negative $\Delta H_{Ca^{2+},NI}$ as the positive $\Delta S_{Ca^{2+},NI}$ values contribute favorably to the large binding constants. Interestingly, the larger $K_{Ca^{2+},N(298)}$ value for BLA results from a more favorable entropy contribution for Ca^{2+} binding to native apo-BLA than to -GLA (Table 4). This can be interpreted by the fact that the large cluster of exclusively negative groups near the Ca^{2+} -binding site of BLA offers a better probability that Ca^{2+} will be trapped than is offered by the corresponding surroundings in GLA.

By application of standard thermodynamic equations we calculated $K_{Ca^{2+},N(T)}$ at 338 K ($65^\circ C$), a temperature at which native Ca^{2+} -LA is destabilized (results not tabulated). The respective values for the binding to GLA and BLA are 1.3×10^8 and 3.9×10^8 . The latter value is close to $K_{Ca^{2+},N(T)} = 2.9 \times 10^8$, obtained from Ca^{2+} exchange between BLA and EDTA at 338 K (42). This indicates that even at that high temperature, native Ca^{2+} -LA does not tend to dissociate in a direct way. In an earlier paper we deduced that the Ca^{2+} release at that temperature is mediated by a partial unfolding of Ca^{2+} -bound LA (41). In agreement with this finding it has been shown that derivatives of LA with a reduced number of disulfide bonds are able to bind Ca^{2+} and to keep the β -domain folded, even in the absence of the native structure of the α -domain (48, 49). Furthermore, the lack of specific side-chain packing within the α -domain results in a significant thermal destabilization of the Ca^{2+} -bound β -domain (48, 49). This pattern of destabilization, with a preliminary disturbance of the α -domain and subsequent Ca^{2+} release and unfolding of the β -domain, presumably also accounts for the pattern of the temperature-induced destabilization of Ca^{2+} -LA with four intact disulfide bridges (41). In contrast to this, by forced decalcification of LA the β -domain region destabilizes and unfolds at low temperatures. In a complementary way of what has been described above, the significant interdomain interaction effects that the unfolding of the β -domain results in a reduction of the side-chain packing in the α -domain (7-10). The contribution of the extended accumulation of negative charges near the Ca^{2+} -binding site to this ability for interdomain interaction has to be investigated more thoroughly.

2.6 Acknowledgement

We thank Wim Noppe for the purification and decalcification of the α -lactalbumins. This research was supported by grant G-0253-97 from the Flemish Fund for Scientific Research.

2.7 References

1. Acharya, K.R., Ren, J., Stuart, D.I., Phillips, D.C. and Fenna, R.E. (1991) Crystal structure of human α -lactalbumin at 1.7 Å resolution. *J. Mol. Biol.* 221, 571-581.
2. Acharya, K.R., Stuart, D.I., Walker, N.P.C., Lewis, M. and Phillips D.C. (1989) Refined structure of baboon α -lactalbumin at 1.7 Å resolution. *J. Mol. Biol.* 208, 99-127.
3. Pike, A.C.W., Brew, K. and Acharya, K.R. (1996) Crystal structures of guinea-pig, goat and bovine α -lactalbumin highlight enhanced conformational flexibility of regions that are significant for its action in lactose synthase. *Structure* 4, 691-703.
4. Stuart, D.I., Acharya, K.R., Walker, N.P.C., Smith, S.G., Lewis, M. and Phillips, D.C. (1986) α -Lactalbumin possesses a novel calcium binding loop. *Nature* 324, 84-87.
5. Hiraoka, Y., Segawa, T., Kuwajima, K., Sugai, S. and Moroi, N. (1980) α -Lactalbumin: a calcium metalloprotein. *Biochem. Biophys. Res. Commun.* 95, 1098-1104.
6. Kuwajima, K., Harushima, Y., and Sugai, S. (1986) Influence of Ca(II) binding on the structure and stability of bovine α -lactalbumin studied by circular dichroism and magnetic resonance spectra. *Int. J. Peptide Protein Res.* 27, 18-27.
7. Baum, J., Dobson, C.M., Evans, P.A., and Hanley, C. (1989) Characterization of a partly folded protein by NMR methods: Studies on the molten globule state of guinea pig α -lactalbumin. *Biochemistry* 28, 7-13.
8. Alexandrescu, A.T., Evans, P.A., Pitkeathly, M., Baum, J., and Dobson, C.M. (1993) Structure and dynamics of the acid-denatured molten globule state of α -lactalbumin. *Biochemistry* 32, 1707-1718.
9. Peng, Z., and Kim, P.S. (1994) A protein dissection study of a molten globule. *Biochemistry* 33, 2136-2141.
10. Wu, L.C., Peng, Z. and Kim, P.S. (1995) Bipartite structure of the α -lactalbumin molten globule. *Nat. Struct. Biol.* 2, 281-286.
11. Vanderheeren, G., and Hanssens, I. (1994) Thermal unfolding of bovine α -lactalbumin. *J. Biol. Chem.* 269, 7090-7094.
12. Vanderheeren, G., Hanssens, I., Meijberg, W. and Van Aerschot, A. (1996) Thermodynamic

- characterization of the partially unfolded state of Ca^{2+} -loaded α -lactalbumin: evidence that partial unfolding can precede Ca^{2+} release. *Biochemistry* 35, 16753-16759.
13. Griko, Y.V., Freire, E. and Privalov, P.L. (1994) Energetics of the alpha-lactalbumin states. A calorimetric and statistical thermodynamic study. *Biochemistry* 33, 1889-1899.
 14. Arai, M. and Kuwajima, K. (2000) Role of the molten globule state in protein folding. *Adv. Prot. Chem.* 53, 209-282.
 15. Haynie, D.T. and Freire, E. (1993) Structural energetics of the molten globule state. *Proteins* 16, 115-140.
 16. Ptitsyn, O.B. (1994) Kinetic and equilibrium intermediates in protein folding. *Protein Eng.* 7, 593-596.
 17. Segawa, T. and Sugai, S. (1983) Interactions of divalent metal ions with bovine, human and goat α -lactalbumin. *J. Biochem. (Tokyo)* 93, 1321-1328.
 18. Permyakov, E.A., Yarmolenko, U.V., Kalinichenko, L.P., Morozova, L.A. and Burstein E.A. (1981) Calcium binding of α -lactalbumin. Structural rearrangement and association constant evaluation by means of intrinsic protein fluorescence changes. *J. Biol. Chem.* 256, 8582-8586.
 19. Hiraoka, Y. and Sugai, S. (1985) Equilibrium and kinetic study of sodium- and potassium-induced conformational changes of apo- α -lactalbumin. *Int. J. Peptide Protein Res.* 26, 252-261.
 20. Desmet, J. and Van Cauwelaert, F. (1988) Calorimetric experiments of Mn^{2+} -binding to α -lactalbumin. *Biochim. Biophys. Acta* 957, 411-419.
 21. Desmet, J., Hanssens, I. and Van Cauwelaert, F. (1987) Comparison of the binding of Na^+ and Ca^{2+} to bovine α -lactalbumin. *Biochim. Biophys. Acta* 912, 211-219.
 22. Livingstone, J.R., Spolar, R.S. and Record, M.T. (1991) The contribution to the thermodynamics of protein folding from reduction in water-accessible nonpolar surface area. *Biochemistry* 30, 4237-4244.
 23. Privalov, P.L. and Makhatadze, G.I. (1992) Contribution of hydration and noncovalent interactions to the heat-capacity effect on protein unfolding. *J. Mol. Biol.* 224, 715-723.
 24. Oobataka, M. and Ooi, T. (1993) Hydration and heat-stability effects on protein unfolding. *Prog. Biophys. Mol. Biol.* 59, 237-284.
 25. Freire, E. (1995) Thermodynamics of partly folded intermediates in proteins. *Annu. Rev. Biomol. Struct.* 24, 141-165.
 26. Griko, Y.V. (1999) Denaturation versus unfolding: energetic aspects of residual structure in denaturated α -lactalbumin. *J. Prot. Chem.* 18, 361-369.
 27. Griko, Y.V. (2000) Energetic basis of structural stability in the molten globule state: α -lactalbumin. *J. Mol. Biol.* 297, 1259-1268.
 28. Lindahl, L. and Vogel, H.J. (1984) Metal-ion dependent hydrophobic interaction chromatography of α -lactalbumins. *Anal. Biochem.* 140, 394-402.

29. Noppe, W., Haezebrouck, P., Hanssens, I. and De Cuyper, M. (1998) A simplified purification procedure of alpha-lactalbumin from milk using Ca²⁺-dependent adsorption in hydrophobic expanded bed chromatography. *Bioseparation* 8, 153-158.
30. Lee Y.C. (2001) Fluorimetric determination of EDTA and EGTA using terbium-salicylate complex. *Anal. Biochem.* 293, 394-402.
31. Kronman, M.J. and Andreotti, R.E. (1964) Inter- and intramolecular interactions of α -lactalbumin. I. The apparent heterogeneity at acid pH. *Biochemistry* 3, 1145-1151.
32. Gill, S.C. and von Hippel, P.H. (1989) Calculation of protein extinction coefficients from amino acid sequence data. *Anal. Biochem.* 182, 319-326.
33. Dolgikh, D.A., Abaturon, L.V., Bolotina, I.A., Brazhnikov, E.V., Bychkova, V.E., Gilmanshin, R.I., Lebedev, Y.O., Semisotnov, G.V., Tiktopulo, E.I. and Ptitsyn, O.B. (1985) Compact state of a protein molecule with pronounced small-scale mobility: bovine α -lactalbumin. *Eur. Biophys. J.* 13, 109-121.
34. Pfeil, W. and Sadowski, M.L. (1985) A scanning calorimetric study of bovine and human apo- α -lactalbumin. *Stud. Biophys.* 109, 163-170.
35. Xie, D., V. Bhakuni, and E. Freire. (1993) Are the molten globule and the unfolded states of apo- α -lactalbumin enthalpically equivalent? *J. Mol. Biol.* 232, 5-8.
36. Ptitsyn, O.B., and Uversky, V.N. (1994) The molten globule is a third thermodynamic state of protein molecules. *FEBS Lett.* 341, 15-18.
37. Yutani, K., Ogasahara, K. and Kuwajima, K. (1992) Absence of the thermal transition in apo- α -lactalbumin in the molten globule state. *J. Mol. Biol.* 228, 347-350.
38. Veprintsev, D.B., Permyakov, S.E., Permyakov, E.A., Rogov, V.V., Cawild typehern, K.M. and Berliner, L.J. (1997) Cooperative thermal transitions of bovine and human apo- α -lactalbumins: evidence for a new intermediate state. *FEBS Lett.* 412, 625-628.
39. Ladbury, J.E. and Chowdry, B.Z. (1996) Sensing the heat: the application of isothermal titration calorimetry to thermodynamic studies of biomolecular interactions. *Chem. Biol.* 3, 791-801.
40. Kuroki, R., Nitta, K. and Yutani, K. (1992) Thermodynamic changes in the binding of Ca²⁺ to a mutant human lysozyme (D86/92). Enthalpy-entropy compensation observed upon Ca²⁺ binding to proteins. *J. Biol. Chem.* 267, 24297-24301.
41. Vanderheeren, G., and Hanssens, I. (1999) Spectroscopic study of the thermal unfolding of α -lactalbumin. *Recent Res. Dev. Biochem.* 1, 45-61.
42. Hendrix, T.M., Griko, Y. and Privalov, P. (2000) A calorimetric study of the influence of calcium on the stability of bovine α -lactalbumin. *Biophys. Chem.* 84, 27-34.
43. Chrysinina, E.A., Brew, K. and Acharya, K.R. (2000) Crystal structures of apo- and holo-bovine α -lactalbumin at 2.2 Å resolution reveal an effect of calcium on inter-lobe interactions. *J. Biol. Chem.* 275, 37021-37029.

44. Permyakov, E.A., Morozova, L.A. and Burstein, E.A. (1985) Cation binding effects on the pH, thermal and urea denaturation transitions in α -lactalbumin. *Biophys.Chem.* 21, 21-31.
45. Bryant, D.T.W. and Andrews, D. (1984) High affinity binding of Ca(II) to bovine α -lactalbumin in the absence and presence of EGTA. *Biochem. J.* 220, 617-620.
46. Desmet, J. (1992) The effect of metal ion binding on protein stability: a thermodynamic analysis of the binding to α -lactalbumin. Ph.D. Thesis. Katholieke Universiteit Leuven (Belgium).
47. Berliner, L.C. and Johnson, J.D. (1988) α -Lactalbumin and calmodulin. In: *Calcium-binding proteins. Volume II: Biological Functions*. Thompson, M.V., editor. CRC Press, Florida. 79-116.
48. Hendrix, T.M., Griko, Y. and Privalov, P. (1996) Energetics of structural domains in α -lactalbumin. *Protein Sci.* 5, 923-931.
49. Wu, L.C., Schulman, B., Peng, Z. and Kim P.S. (1996) Disulfide determinants of calcium-induced packing in α -lactalbumin. *Biochemistry* 35, 859-863.
50. Fukuda, H. and Takahashi, K. (1998) Enthalpy and heat capacity changes for the proton dissociation of various buffer components in 0.1 M potassium chloride. *Proteins* 33, 159-166.
51. Samland, A.K., Jelesarov, I., Kuhn, R., Amrhein, N. and Macheroux, P. (2001) Thermodynamic characterization of ligand-induced conformational changes in UDP-N-acetylglucosamine enolpyruvyl transferase. *Biochemistry* 40, 9950-9956.

**Photo-excitation of tryptophan groups induces reduction
of two disulfide bonds in goat α -lactalbumin**

A. Vanhooren, B. Devreese¹, K. Vanhee, J. Van Beeumen¹, I. Hanssens

*Interdisciplinary Research Center, Katholieke Universiteit Leuven Campus
Kortrijk, Kortrijk, Belgium*

*¹Laboratory for Protein Biochemistry and Protein Engineering, University of
Ghent, Belgium*

Based on Biochemistry 2002, 41, 11035-11043

3.1 Abstract

During the former physico-chemical studies of α -lactalbumin (Chapter 2), we observed an unusual increase and red shift of the fluorescence spectra due to the exposure to near-UV light. In this study we present evidence that these fluorescence changes are caused by cleavage of disulfide bonds and by the related conformational changes. Illumination of goat α -lactalbumin (GLA) with light of 280 or 295 nm results in tryptophan-mediated photolysis of disulfide bonds within the protein. The photolysis is not dependent on the absence or presence of Ca^{2+} and is observed on illumination of both native and of partially unfolded GLA. However, photolysis of native GLA results in a partial unfolding of the protein. The latter phenomenon is most clearly observed on fluorescence measurements at low temperature (near 3°C). The photolysis induces some dimerization and oligomerization, but most GLA molecules remain monomeric.

To obtain more information on the reaction products, the illuminated protein is treated with iodoacetamide to label the free thiol groups, next it is fragmented with trypsin and the fragments are analyzed through mass spectrometry. By this approach we observe that the cleavage of disulfide bonds is restricted to Cys6-Cys120 and Cys73-Cys91. The photolytic cleavage of either of these disulfide bonds results in the formation of a single free thiol, a phenomenon restricted to Cys120 and to Cys91, respectively. We also found indications that a thioether linkage is formed between Cys73 and Trp60. The alkylsulfenylation of Trp60 presumably results from a combination of primary thiyl and tryptyl radicals.

3.2 Introduction

Exposure of enzymes to near-UV radiation induces structural changes and alters their biocatalytic function (1). The damage is initiated through photon absorption of the chromophoric amino acids. The indole nucleus is the most strongly near-UV absorbing group in proteins. Therefore, tryptophan residues are primary components in the activation of protein photodegradation. The nature of these degradation reactions depends on the microenvironment within the protein (2). Some decades ago it has been suggested that absorption of near-UV light by the

aromatic amino acid residues contributes to reductive splitting of disulfides in proteins (3). In spite of the important impact that this phenomenon may have on the inactivation of enzymes and hormones, only recently a clearly certified example of tryptophan-mediated photoreduction of a disulfide bond within a protein (cutinase) has been registered (4). For a better understanding of the phenomenon it is important that more examples of this kind of photolysis are described and that the concomitant structural changes are being characterized. Indeed, up to now very little is known about the resulting photo-products.

In the past years we have studied the conformational changes of α -lactalbumins (LAs). LAs are small globular proteins. The variant from goat milk (GLA) consists of 123 amino acids. Its three-dimensional X-ray structure determined by Pike et al. (5), is presented in Figure 1. A deep cleft divides the molecule into two lobes. One lobe comprises the residues 1-39 and 85-123. That lobe contains four helices.

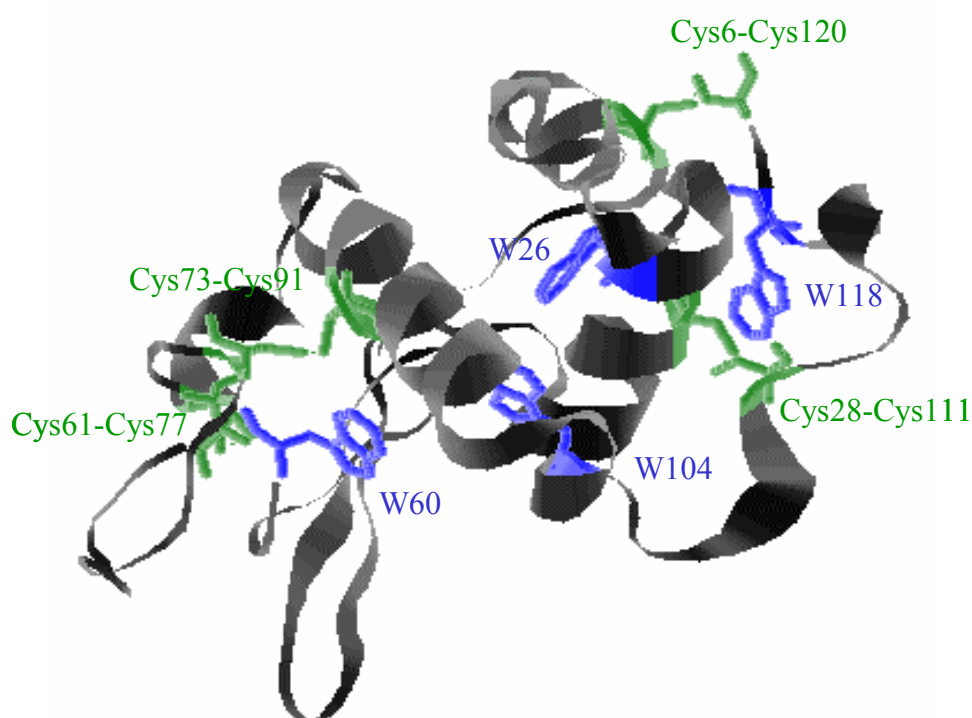


Figure 1: SWISS-MODEL diagram (31) of the X-ray structure of GLA (PDB entry 1HFY) showing the four disulfide bridges (green) and the four Trp side chains (blue).

The second, consisting of residues 40-84, is characterized by the presence of a 3-stranded β -sheet. The unfolding of LAs has been studied intensively because the molecule adopts a ‘molten globule’ state under mild denaturing conditions. In this situation the protein is still compact but lacks well-defined tertiary interactions, and the hydrophobic interior is readily accessible for solvent molecules (6, 7). Near-UV circular dichroism and fluorescence spectroscopy have been widely used for the characterization of the molten globule state (8 - 14). Both spectroscopic properties mainly reflect the nature of the interactions of the tryptophan residues with their surroundings. GLA contains four Trp residues, located at positions 26, 60, 104 and 118. The protein also contains four disulfide bridges between residues 6-120, 28-111, 61-77, and 73-91. In the native state, the fluorescence signal of Trp60 and Trp118 is significantly quenched by the disulfide bridges in their vicinity (15). These structural characteristics make of LA a suitable protein for a more thorough investigation of disulfide disruption under the influence of photo-excited Trp residues.

In this work we describe an unusual increase and red shift of the fluorescence of GLA by irradiation of the protein at 280 or 295 nm. We provide evidence that these fluorescence changes are accompanied by cleavage of disulfide bonds. Mass spectrometry of the tryptic fragments of the carbamidomethylated protein has been used as an effective method for the analysis of the free thiol groups within partly reduced LA (16). On applying this method to illuminated GLA we find that out of the four S-S bonds in intact GLA only Cys6-Cys120 and Cys73-Cys91 become disrupted. This observation makes clear that not all the disulfide bonds in GLA are in a favorable environment for Trp-mediated photolysis. The ability for an excited Trp to initiate cleavage of a disulfide bond seems to be enhanced both by direct Van der Waals contact (Trp60 with Cys73-Cys91) and by the weakness of the bond (Cys6-Cys120 is more distant from Trp118 than Cys28-Cys111, but the former bond is weaker than the latter). Concerning the resulting products, our results indicate that Trp-mediated photolysis only results in a partial reduction of the involved disulfide bond and that only a single free Cys is created in each case. We find indications that the second Cys can form a thioether linkage with the indole group of the Trp residue involved.

3.3 Materials and Methods

3.3.1 Materials

Goat α -lactalbumin (GLA) was prepared from fresh milk whey. After addition of Tris and EDTA to final concentrations of 50 and 1 mM, respectively, and adjustment of the pH to 7.5 with HCl, the whey was applied to a Streamline-Phenyl column (Pharmacia, Uppsala, Sweden). Apo-GLA was bound hydrophobically to the column, while the other whey proteins were eluted with the Tris-EDTA buffer, pH 7.5 (17). GLA was eluted by changing the eluting buffer to 50 mM Tris, 25 mM Ca^{2+} , pH 7.5, and Ca^{2+} -GLA was then demetallized as described previously (18). All experiments were performed in 10 mM Tris-HCl buffer, pH 7.5, containing either 2 mM Ca^{2+} or 2 mM EGTA. The GLA concentration was determined by spectrophotometry using $\epsilon_{280} = 28500 \text{ (mol/l)}^{-1} \text{ cm}^{-1}$. 5,5'-Dithiobis(2-nitrobenzoic acid) (DTNB, Ellman's reagent) used for the analysis of free thiol groups, is a product from Eastman (Rochester, N.Y.).

3.3.2 Preparation of illuminated GLA

Two and a half ml of a degassed solution containing 27 μM GLA or 3SS-CAM-GLA (see further) at pH 7.5, was illuminated in a 10 x 10 mm cuvette within an Aminco-Bowman Series 2 spectrofluorimeter (Rochester, N.Y.). The excitation wavelength was centered at 280 nm. In order to ensure an important photon flux, a broad bandpass of 16 nm was applied. Ferrioxalate actinometry showed that under these conditions, the incident flux was $6.10^{14} \text{ photons}\cdot\text{sec}^{-1}$. During illumination the solutions were stirred at 120 rpm. Spectroscopic studies were carried out immediately after illumination. The concentration of free thiol groups was determined with DNTB using a molar extinction coefficient of $13600 \text{ (mol/l)}^{-1} \text{ cm}^{-1}$ for TNB^- (19, 20).

3.3.3 Preparation of 3SS-GLA

GLA in which the disulfide bridge Cys6-Cys120 is selectively reduced (3SS-GLA) was prepared according to the method of Kuwajima et al.(21) with the following modifications. Starting from 5 mg/ml GLA and after reduction of the disulfide bridge, 3SS-GLA was immediately separated from dithiothreitol by passing the reaction mixture through a Sephadex G-25 column equilibrated with 10 mM Tris-HCl buffer at pH 7.5 containing 2 mM EDTA. The number of free thiol groups was checked with DNTB as described above.

3.3.4 Labeling of the free thiol groups

The thiol groups in 3SS-GLA or in illuminated GLA were carbamidomethylated by adding an equal volume of 10 mM iodoacetamide in 0.9 M Tris-HCl buffer at pH 8 containing 1 mM CaCl₂, allowing the reaction to proceed for 30 min in the dark at room temperature (16). The proteins were separated from excess reagent by gel filtration through a Sephadex G-25 column equilibrated with 10 mM ammonium bicarbonate, pH 7.5, and lyophilized. 3SS-GLA that has been carbamidomethylated and purified in this way is called 3SS-CAM-GLA.

3.3.5 Peptide mapping

The proteins were resuspended in 25 mM ammonium bicarbonate, pH 8 at a concentration of approximately 100 pmol/μl. Trypsin (Promega) was added in a 1:40 ratio (w:w), and the mixture was incubated for 4 h at 37°C. 1 μl of the resulting peptide mixture was subjected to Matrix-assisted laser desorption/ionization mass spectrometry (MALDI-TOF) on a Micromass (Manchester, UK) M@ldi instrument using α-cyano hydroxycinnamic acid as matrix. Alternatively, electrospray ionization mass spectrometry (ESI-MS) on a Q-TOF mass spectrometer (Micromass) was used, especially for MS/MS experiments. Also the intact proteins were analysed on the Q-TOF mass spectrometer.

3.3.6 Fluorescence measurements

Steady state fluorescence was measured with an Aminco-Bowman Series 2 spectrofluorimeter (Rochester, N.Y.) provided with a 150 Watt xenon lamp for continuous radiation. The GLA concentration used was approximately 5 μ M and 27 μ M for intact and illuminated GLA respectively. Amounts of 2.5 ml of the degassed protein solutions were transferred into a 10 x 10 mm cuvette for fluorescence spectroscopy. Except when explicitly mentioned, the excitation wavelength was 280 nm. The bandpass for the excitation and emission slits were 4 nm and 1 nm, respectively, with 345 nm as the emission wavelength. The cuvette holder was thermostated by circulating water from an external water bath. The fluorimeter was equipped with a magnetic stirrer mounted under the cuvette holder. A small magnetic stirring bar (length 5 mm, diameter 2 mm) at the bottom of the cuvette was rotated at the speed of an external field (120 rpm).

3.3.7 Circular dichroism spectroscopy

The CD measurements were performed on a Jasco J-600 spectropolarimeter (Tokyo, Japan). Cuvettes of 10 mm and 1 mm were used for the near-UV and far-UV region, respectively. During the 5 minutes equilibration at 4 °C, the illuminated samples were shielded from the light beam. In the near-UV region (250-350 nm), the ellipticity monitored at 270 nm is mainly due to aromatic residues and reflects the tertiary conformation of the protein.

3.3.8 High performance gel filtration

Analysis of LA-oligomers was carried out using a HPLC apparatus equipped with a gel filtration column (Superose 12 HR 10/30, Pharmacia, Uppsala, Sweden). Equilibration, calibration and elution were run at room temperature with a 0.5 ml min⁻¹ flow rate of 50 mM NaH₂PO₄.H₂O, 0.15 M NaCl, pH 7. The eluting protein was monitored by its absorbance at 230 nm. Calibration with standard proteins (IgG, BSA, β -lactoglobulin, cytochrome C and vitamin B12) allowed an estimation of the molecular weight of the LA components.

3.3.9 Absorption measurements

The absorption measurements were performed on an Uvikon 933 double beam UV/VIS spectrophotometer (Kontron Instruments, Milano, Italy) at room temperature.

3.4 Results

3.4.1 Unusual fluorescence behavior of native GLA

The first indication that irradiation at 280 nm affects GLA, came from the changes of the emission spectra at 3°C. Figure 2 represents spectra of non-irradiated and irradiated GLA in different conditions of pH and Ca²⁺ content. The full line spectra were obtained when the GLA solutions were carefully kept in the dark until scanning. The dotted spectra were obtained when the same, non-stirred solutions were irradiated, for a 20 minutes period, by the excitation beam within the fluorimeter (excitation wavelength 280 nm, bandpass 4 nm). Upon smooth stirring, the fluorescence spectra rapidly regained the initial value, but started to evolve to the dotted scans after stirring was stopped. The most plausible explanation for the above observations is obtained by accepting that the measured changes in fluorescence result from the combined effects of a radiation-dependent structural transformation of GLA and a diffusion of these molecules. Under conditions of limited diffusion and absence of perturbation, an excess of transformed GLA molecules remains accumulated in the light path of the excitation beam. The rapid return to the original fluorescence upon smooth stirring results from the homogenization of the solution.

To study the effect of dissolved oxygen on the fluorescence change, the GLA solution was saturated with pure nitrogen. As the photo-induced effects did not change, oxygen from the dissolved air did not affect the results. It is also worth noting that, upon excitation at 295 nm, where absorption by any other chromophore except Trp is excluded, identical observations are made as at 280 nm. However, due to the decreased absorption at 295 nm, the intensity of the fluorescence change is less pronounced than upon excitation at 280 nm.

The fluorescence spectra in Figure 2 provide information on the nature of the irradiation-induced fluorescence changes. The full lines in Figures 2A and 2B represent spectra of non-irradiated apo- and Ca^{2+} -GLA solutions, respectively, at 3°C and pH 7.5. These spectra are characteristic for non-transformed GLA, in the quasi native (Figure 2A) and in the native state (Figure 2B). The full line in Figure 2C represents the spectrum of non-irradiated GLA at 3°C and pH 2. This acid medium is commonly accepted to provide the mild denaturing conditions necessary to obtain the molten globule state of LA (7). The full line spectrum of Figure 2C is characteristic of LA in such a partially unfolded conformation. The relatively high emission maximum wavelength is indicative of the good solvent accessibility to the hydrophobic clusters that contain the fluorescent Trp-groups within LA. The relatively high fluorescence intensity is indicative for the reduction of fluorescence quenching that has been observed in this slightly expanded conformation. Indeed, according to Sommers and Kronman (8) fluorescence quenching of native LA (full lines of Figures 2A and 2B) is promoted by transfer of excitation energy from Trp26 and Trp104 to Trp60 and, further on to two vicinal disulfide bridges. This postulated model of energy transfer and contact quenching is supported experimentally by the phosphorescence decay observed at low temperatures (22). In a recent study, Chakraborty et al. (15) observed that the adjacent disulfide bonds also significantly quench Trp118.

The dashed lines of Figures 2A and 2B represent the spectra of the non-stirred GLA solutions irradiated at 280 nm for 28 minutes at neutral pH and 3°C. At this pH, either in the absence or in the presence of Ca^{2+} , the irradiation of the native protein provokes a red shift and an increase of the yield of fluorescence. The latter phenomenon is evidenced by the surfaces under the spectra. The red shift refers to an increased polarity due to an improved access of solvent to the fluorophores. The increase of yield results from loss of quenching due to loosening of the protein structure (8). The dashed line of Figure 2C is the spectrum for the non-stirred, irradiated GLA solution at pH 2 and 3°C. At this pH the fluorescence intensity of GLA decreases by prolonged irradiation without perceptible shift in wavelength. The emission maximum of 340 nm is a characteristic property of molten globule LA. The loss of yield could be due either to the photo-destruction of the fluorophore or to an increase of quenching by new neighboring residues in the altered conformation. The lack of wavelength shift supports the idea that the potential irradiation products do not fluoresce.

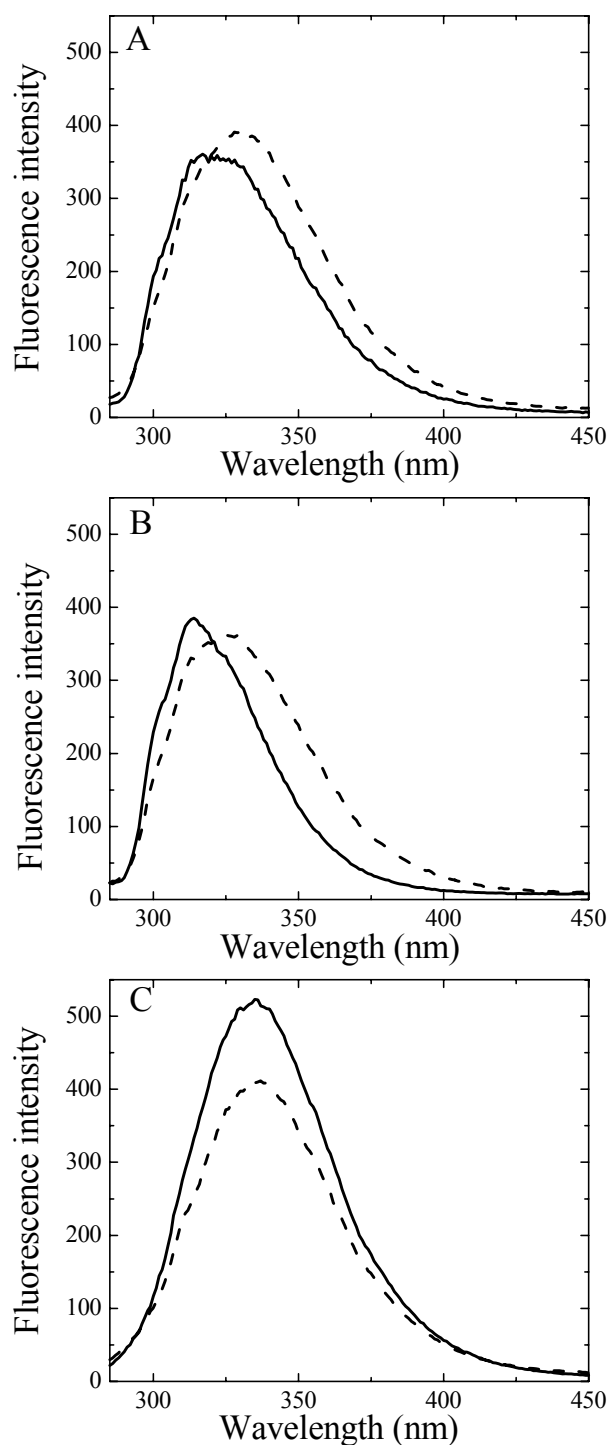


Figure 2: Fluorescence spectra at 3°C and pH 7.5 of 5 μ M apo-GLA (A), Ca²⁺-loaded GLA (B), and GLA at pH 2 in 10 mM HCl (C). Degassed solutions of 2.5 ml, containing 5 μ M apo- or Ca²⁺- loaded GLA, were illuminated in a 10mm \times 10mm cuvette. The fluorescence of the center of the cuvette was observed at a right angle. Excitation was carried out at 280 nm with a band-pass of 4 nm; emission was measured with a bandpass of 1 nm. The solid lines represent the spectra of GLA at the start of irradiation. To ensure homogeneity, the solutions were smoothly stirred during the registration of the spectra. The dashed lines are the spectra of non-stirred GLA after irradiation for 28 min at 280 nm.

3.4.2 Photo-induced cleavage of disulfide bridges

The fluorescence changes upon irradiation of native GLA at 280 or 295 nm are thought to refer to a photo-induced loss of tertiary structure. Indeed, it has been shown recently that illumination of a particular Trp residue mediates photoreduction of an adjacent disulfide bond in the enzyme 'cutinase' (4). To investigate whether the abovementioned fluorescence changes can be linked to photoreduction of disulfide bonds in LA, we have set up a series of illumination experiments at higher protein concentrations (27.3 μ M GLA). The solutions were illuminated using a broad bandpass of wavelengths ranging from 272 to 288 nm in order to increase the incident photon flux. In this way the concentration of free thiol groups generated becomes accessible for chemical analysis. During irradiation the homogeneity in the sample solution was maintained by smooth magnetic stirring. The number of free thiol groups and the fluorescence changes were followed at different temperatures, in the presence and absence of Ca^{2+} . The creation of free thiol groups upon illumination was followed by their reaction with DTNB. To ascertain that the reduction of DTNB results from free thiol groups and not from other potential reducing agents, a sample of illuminated GLA was treated with 2-iodoacetamide prior to addition of DTNB, a treatment which selectively carbamidomethylates the free thiol groups. Since no TNB^- was formed in this case only free thiol groups were responsible for the reduction of DTNB.

In Figure 3 the number of free thiol groups generated per protein molecule (F_{th}) is presented as a function of the irradiation time at pH 7.5 and at 3 $^{\circ}\text{C}$ in 2 mM EGTA. F_{th} increases according to the equation:

$$F_{\text{th}} = F_{\text{th,max}} (1 - e^{-t/\tau}) \quad (1)$$

Under the experimental conditions, the relaxation time (τ) resulting from the curve fit was 152 ± 20 min. Undoubtedly, τ depends on a number of factors related to the instrument settings such as the intensity of the incident light, the surface illuminated, the total volume and the concentration of the protein. The limiting number of free thiol groups ($F_{\text{th,max}}$) was 1.83 ± 0.02 in this case. From this analysis, we calculated that within the first minute of illumination 2.7×10^{14} free thiol groups were formed while 290×10^{14} photons were absorbed. Therefore, under the above conditions, the quantum yield of free thiol groups in intact native apo-GLA was 0.009. Illumination in the presence or absence of Ca^{2+} was done at different temperatures. The $F_{\text{th,max}}$ - values obtained in these different experimental conditions were always below 2.

Near 280 nm the Tyr-groups participate for about a fifth in the absorption of GLA (23). The question arose whether or not these chromophoric groups importantly contribute to the reduction of disulfide bonds. In answer to that question we compared the ratio of created free thiol groups to the absorbed light quanta when a GLA solution was excited by a light beam of 272-288 nm with the ratio obtained upon excitation with a 292-308 nm beam. Tyr residues do not absorb at the latter wavelengths. The resulting yield on excitation at 272-288 nm was smaller by 10-13 % than on excitation at 292-308 nm, indicating that the yield by which an excited Tyr residue might reduce a disulfide bridge is much smaller than the yield by which an excited Trp residue may do so. From the above results we conclude that when illuminated near 280 nm the Tyr residues do not effectively participate to the photo-reduction of disulfide bonds, first because they absorb less photons than the Trp residues, and second because their excited state is considerably less apt to reduce disulfide bonds in GLA than the excited state of Trp.

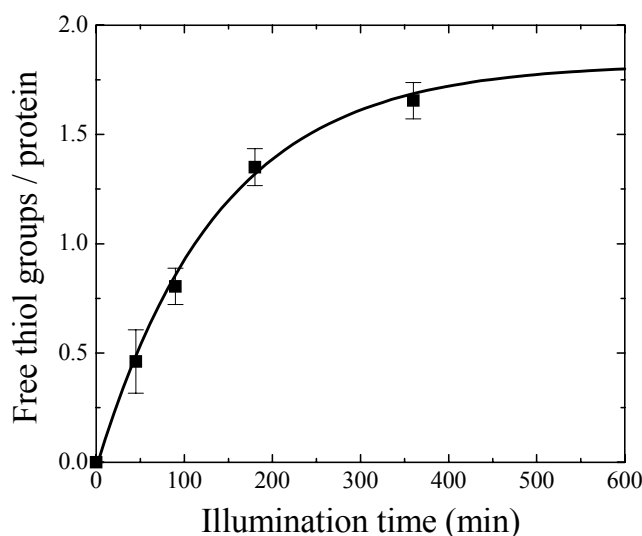


Figure 3: Number of free thiol groups per GLA as a function of illumination time measured with Ellman's reagent. A sample of 2 ml of a degassed apo-GLA solution in 2 mM EGTA at pH 7.5 was illuminated in the cuvette holder of an Aminco-Bowman Series 2 spectrofluorimeter. The excitation wavelength was 280 nm with a band-pass of 16 nm, a temperature 3 °C, and a protein concentration of 28.1 μ M. During illumination, the solution was stirred with a magnetic stirring bar at 120 rpm. The error bars represent experimental divergences (SEM).

The formation of free thiol groups in the above experiments of intensive irradiation and combined stirring was always accompanied with changes in the fluorescence emission spectra. As shown in Figure 4, the illumination of apo-GLA at pH 7.5 and at 3 °C provoked a gradual red shift of the emission maximum. At first the fluorescence yield increased, but upon prolonged

illumination it decreased again. These results agree with the observations on non-stirred solutions upon illumination with a narrow excitation slit (Figure 2A). Also in these common conditions of illumination a decrease of the fluorescence intensity was observed when apo-GLA was already partially unfolded (Figure 2C).

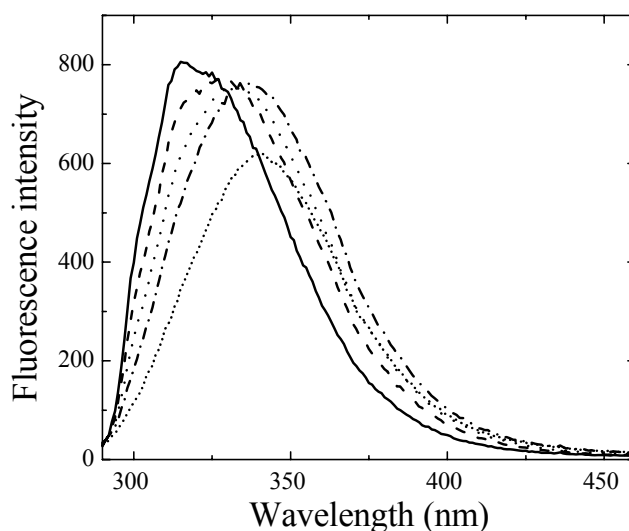


Figure 4: Fluorescence spectra of apo-GLA after different periods of illumination at 280 nm: 0 min (—), 45 min (---), 90 min (.....), 180 min (-.-) and 360 min (-----). The sample and illumination conditions are as described in Figure 3. Despite the strong absorption, the fluorescence spectra were not corrected for inner filter effects.

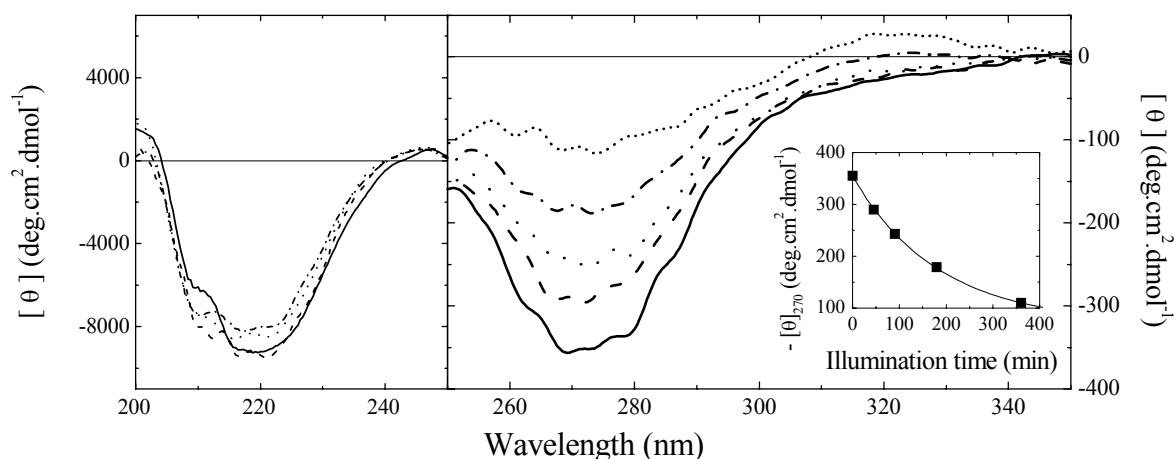


Figure 5: Circular dichroism spectra of apo-GLA in the far- and near-UV regions at different illumination times. The illumination periods are 0 min (—), 45 min (---), 90 min (.....), 180 min (-.-) and 360 min (-----). The sample and illumination conditions are as described in Figure 3. The inset shows the ellipticity at 270 nm as a function of illumination time. The line through the experimental points represents the curve fitted according to a mono-exponential function.

The extent of the near-UV ellipticity of native GLA (Figure 5) drastically decreased on intensive illumination at 280 nm. Interestingly, the decrease of the near-UV ellipticity was found to fit a mono-exponential function, the relaxation time (τ) of which is 183 ± 6 min (see insert in Figure 5). The fairly good correspondence of this value with the relaxation time for the creation of free thiol groups strengthens the idea that both events are related to each other. In contrast to the near-UV, the far-UV CD spectrum of GLA changes only slightly on irradiation. Therefore, we conclude that the tertiary structure of the protein, but not its secondary structure is loosened by prolonged illumination.

3.4.3 Photo-induced dimerization

In our search for an explanation of the relatively low thiol yield (1.83) upon prolonged illumination, we have found evidence that photolysis is accompanied by polymerization reactions. The existence of dimers, trimers and of some polymers was demonstrated by SDS-PAGE (not shown) and by gel filtration (Figure 6). Their relative amounts have been estimated from the surface of the elution peaks. After 6 hours of illumination the fractions are 0.66, 0.18, 0.07 and 0.09 for monomers, dimers, trimers and polymers, respectively. The existence of oligomers suggests that some intermediately formed thiyl radicals from different GLA molecules combine to form intermolecular disulfide bonds.

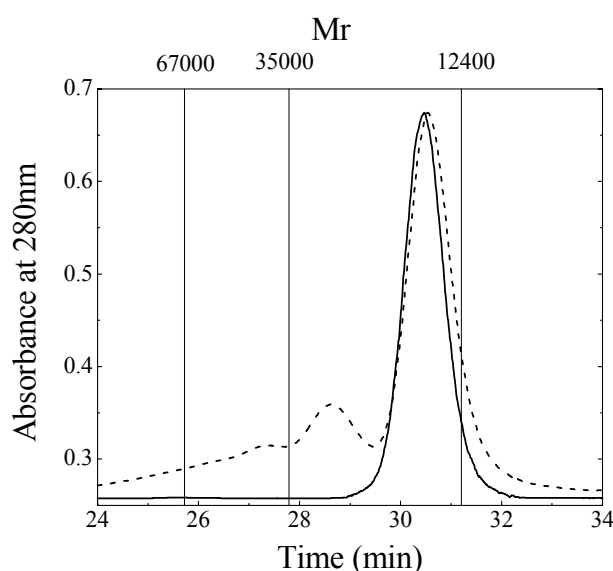


Figure 6: Analysis of LA-oligomers by high performance gel filtration of native (—) and illuminated GLA (---). The illuminated sample was irradiated for 6 hours under the conditions described in Figure 3. The vertical lines represent the elution times of BSA ($M_r = 67.0$ kDa), β -lactoglobulin ($M_r = 35.0$ kDa) and cytochrome c ($M_r = 12.4$ kDa), used as molecular weight markers.

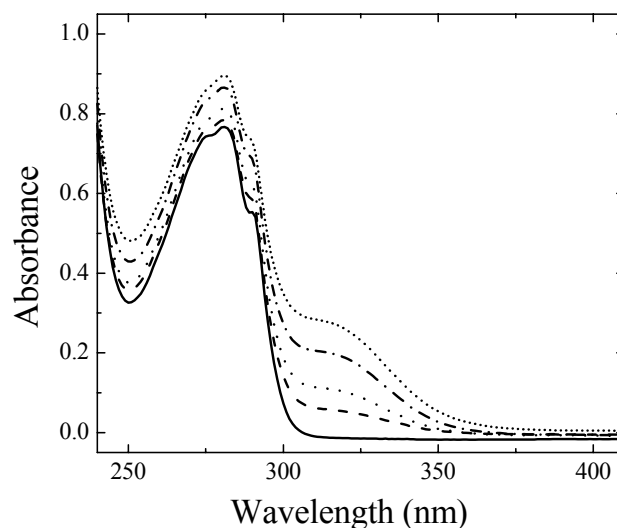


Figure 7: Absorption spectra of apo-GLA as a function of the illumination time: 0 min (—), 45 min (---), 90 min (.....), 180 min (- · - ·) and 360 min (-----). The sample and illumination conditions were as described in the legend of Figure 3.

3.4.4 Photo-induced bleaching of tryptophan

After an initial increase and red shift, the yield of fluorescence of native LA diminishes upon prolonged illumination (Figure 4). It has been suggested that the fluorescence increase and red shift are related to a loss of the native structure (8). In order to obtain more information about the origin of the reduction of fluorescence, we inspected the changes of the absorption spectrum during illumination. The absorption spectra of irradiated GLA (Figure 7, dashed lines) conserve the typical feature of tryptophan as in the original protein (Figure 6, full line) but, gradually, a shoulder is formed on the red wavelength side of the absorption peak. Also, the baseline under the absorption peak becomes apparently elevated. The irradiated protein does not fluoresce upon excitation at wavelengths in the range of the newly formed shoulder (310-325 nm), and the excitation spectrum of the irradiated protein does not exhibit a similar shoulder. The latter observations assure that only intact Trp groups are responsible for the observed fluorescence.

3.4.5 Mass spectrometry

After 3 hours of irradiation and subsequent treatment with iodoacetamide, the mass spectrum of GLA shows three peaks (data not shown). An unchanged GLA peak corresponding

approximately to 50 % of the total amount of protein is observed at 14187 Da. The second and third peak had a mass of 14243 Da and 14300 Da respectively, both accounting for approximately 25 % of the total amount of protein. These two peaks correspond to the mass of GLA with respectively one and two carbamidomethylated thiols. Although quantitation using ESI-MS is not always reliable, we consider the estimation of relative amounts as valid, assuming that the ionization efficiency is only moderately affected by these modifications. MALDI-analysis of the tryptic digests of the proteins revealed the origin of these free cysteines. Comparing the MALDI spectra of the digestion mixture obtained from intact GLA with the one obtained from irradiated and carbamidomethylated GLA revealed two significant differences (Figure 8).

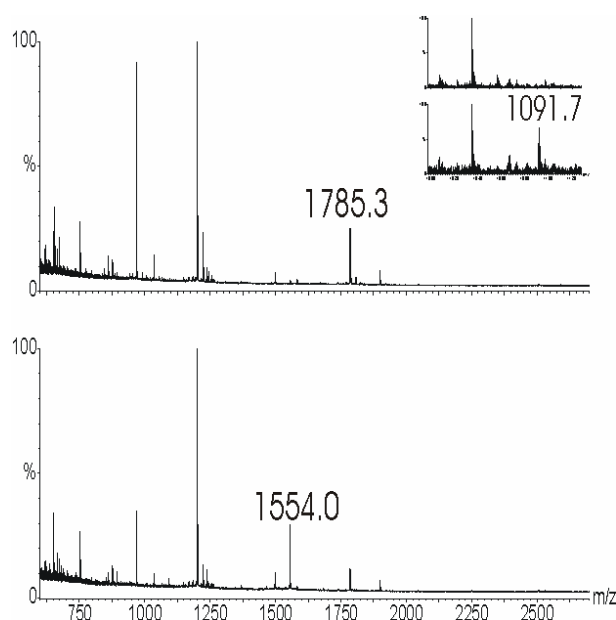


Figure 8: MALDI-TOF mass spectrum of the tryptic digest of apo-GLA (top) and of irradiated apo-GLA (bottom) followed by carbamidomethylation. The spectrum clearly shows a reduction of the magnitude of the peak corresponding to the disulfide-based heterofragment containing Cys6-Cys120 (1785.3 Da). A new peak corresponding to a carbamidomethylated peptide containing Cys6 appears at 1091.7 Da (see the inset). Another new peak at 1554.0 Da appears that corresponds to the heterofragment containing the Cys61-Cys77 disulfide bond.

A new peak with a mass of 1091.7 Da appears which corresponds with a peptide containing the carbamidomethylated Cys 120 (see Table 1). Although the corresponding peptide with Cys 6 (810 Da) was not found, we conclude that it was the disulfide bridge Cys6-Cys120 that had been broken during illumination. The second difference when comparing the MALDI spectra from the digestions of intact GLA with irradiated and carbamidomethylated GLA, was the appearance of

a new peak with a mass of 1554.0 Da for the protonated peptide. This mass approximately accounts for a heterofragment containing two peptides with the cysteines 73, 61 and 77 being linked with the disulfide bridge Cys61-Cys77 (see Table 1). Clearly, this heterofragment results from a triple peptide that has lost a fragment through cleavage of the disulfide bond Cys73-Cys91. In contrast to Cys73-Cys91, the bond Cys61-Cys77 is conserved during illumination.

Table 1: Masses of Peptides Derived from GLA after Digestion with Trypsin^a

mass (Da)	positions	peptide sequence	disulfide bridge
4681.13	17-58	DYGGVSLPEWVCTAFHTSGYD-TQAIVQNNDSTEYGLFQINNK	28-111
1581.73	80-93	FLDDDLTDDIVCAK	73-91
1199.65	99-108	VGINYWLAHK	
1033.49	115-122	LDQWLCEK	6-120
1008.44	71-79	NICNISC DK	73-91, 61-77
967.41	63-70	DDQNPHSR	
752.35	6-11	CEVFQK	6-120
649.31	109-114	ALCSEK	28-111
617.34	1-5	EQLTK	
548.28	59-62	IWCK	61-77

^a The masses of peptides with a carbamidomethylated thiol can be calculated by adding 57.5 Da.

Evidence of the cleavage of Cys73-Cys91 was also found in another sample. Before irradiation, the disulfide bridge Cys6-Cys120 of this GLA sample was cleaved by means of mild reduction with DTT (Kuwajima et al., 1990) and the free thiol groups were carbamidomethylated. This so-called 3SS-CAM-GLA was irradiated for 5 hours and treated again with iodoacetamide. The mass spectrum of irradiated 3SS-CAM-GLA resulted in three peaks of equivalent height at 14300, 14358 and 14415 Da (not shown). The first mass corresponds with that of intact 3SS-CAM-GLA, the latter two correspond with the masses of the protein with one or two additional carbamidomethylated thiols. ESI-MS analysis of the trypsin digests of irradiated 3SS-CAM-GLA shows the appearance of two new masses (Figure 9). As in the prior model, these masses correspond with the products of the breaking of a triple peptide into a double peptide in which Cys61-Cys77 is conserved and Cys73 is not carbamidomethylated (1553.0 Da) and into a single peptide with carbamidomethylated Cys91 (1639.0 Da). The formation of non-carbamidomethylated Cys73 and carbamidomethylated Cys91 was affirmed by ESI MS/MS of the fragmented peptides.

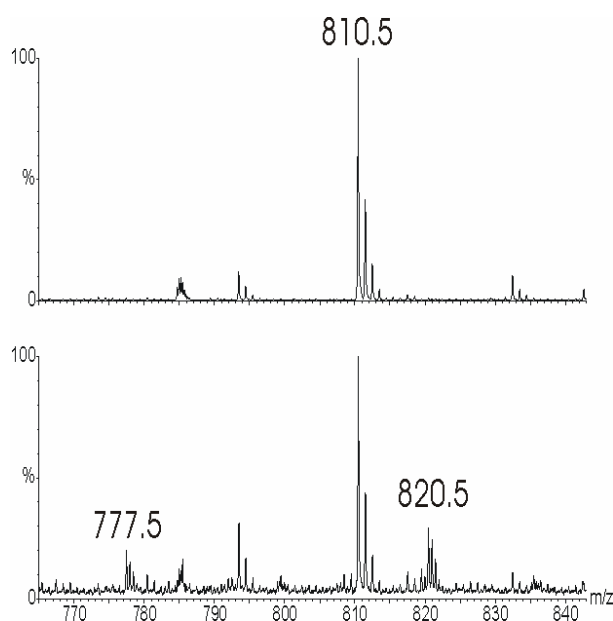


Figure 9: Electrospray mass spectrum of the tryptic digestion of 3-SS-CAM-GLA (top) and of irradiated 3-SS CAM-GLA (bottom) showing two new peaks for doubly charged ions. The peaks correspond to masses of 1555.0 and 1641.0 Da, respectively, for the charged peptides, i.e. 1553.0 and 1639.0 Da, respectively, for the non-charged peptides.

3.5 Discussion

The fluorescence changes offer a first indication that GLA is modified by irradiation at 280 or 295 nm. Under conditions of limited diffusion and absence of perturbation the registered fluorescence spectra are not representative for the bulk of the solution (Figure 2). With stirring, identical changes are observed (Figure 4), although a longer and more intense illumination is required to observe the phenomenon. The illumination of native GLA is also accompanied by the appearance of free thiol groups (Figure 3). The rate at which free thiol groups are formed apparently decreases in an exponential way. The disulfide-thiol conversion within the protein is visibly related to the change of the tertiary conformation of native GLA (Figure 5, insert). Breakage of disulfide bonds does not directly disturb the elements of secondary structure (Figure 5) but allows that these formerly linked elements can migrate away from each other. α -Lactalbumins possess the characteristic that the partially folded state, with loosened tertiary structure and native secondary structural elements, is relatively stable in non-denaturing conditions (24). The quantum yield for the creation of free thiol groups is smaller upon illumination with light of 272-288 nm than upon illumination at 292-308 nm. This indicates that

also within the former wavelength range the photo-reduction of disulfide bonds is predominantly mediated by Trp residues.

Upon prolonged irradiation of GLA, up to 1.84 free thiol groups are detected (Figure 3). The mass spectrum of a GLA sample that was irradiated for 3 hours and subsequently treated with iodoacetamide, consists of three components: a non-carbamidomethylated, a single and a double carbamidomethylated component (not shown). In agreement with the chemical analysis of the number of free thiol groups, the mass spectrum indicates that up to two free thiol groups are formed. It could be expected that the two free thiol groups refer to the cleavage of a single disulfide bond. Therefore, the presence of a large fraction of singly carbamidomethylated protein in the mass spectrum is surprising. The occurrence of this species either suggests that the cleavage of a disulfide bond by photolysis not necessarily results in the formation of 2 free thiol groups or that steric hindrance excludes interaction with an external reagent. A comparison of the mass spectra of the tryptic digests from GLA that was labeled either after photolysis or after chemical reduction (3SS-CAM-GLA) excludes the latter possibility. Indeed, the peak with mass 1091.7 Da in the mass spectrum of photolysed GLA (Figure 8, insert) correlates with a protonated peptide containing carbamidomethylated Cys120, clearly proving the cleavage of disulfide bond 6-120. However, no peak with a mass of 810 Da is found, which would be correlated to a GLA-peptide with carbamidomethylated Cys6. In contrast to these findings, the fragments referring to free thiols at both Cys6 and Cys120 are clearly detected in the spectrum of proteolyzed 3SS-CAM-GLA (not shown).

The formation of only a single free thiol group is also evidenced within the peptide fragments derived from the photolytic cleavage of the Cys73-Cys91 bond. The fragment of photolysed, blocked and digested GLA with a molecular mass of 1639.0 Da, correlates to a peptide of which the free thiol of Cys91 has reacted with iodoacetamide (Figure 9). In the same digest the fragment with the mass of 1553.0 Da correlates to a peptide that contains a non-carbamidomethylated Cys73. No fragment is found that points to the existence of a carbamidomethylated Cys73. In an analogous experiment, Prompers et al. (4) treated irradiated cutinase with DTNB. The mass spectrum of the reaction mixture showed a peak corresponding to the mass of this enzyme having only one derivatized thiol group, but lacked the peak that refers to two complexed thiol groups. Here again, the cleavage of a disulfide bridge induced by photo-excitation of a Trp residue resulted in a single free thiol. Although a lack of accessibility of one of the thiol groups can not be excluded, it is striking that each analysis of thiol groups

from a Trp-mediated, photo-induced cleavage of a disulfide bridge yields only one reactive thiol group. The formation of only one free thiol group, therefore, appears to be an inherent property of Trp-mediated photolysis.

According to Bent and Hayon (24) the rupture of a disulfide bridge upon UV illumination of Trp results in the formation of a thiolate ion and a thiyl radical according to the following scheme:



The presence of a free thiol within the protoproducts provides evidence that proton transfer from the tryptophan cation radical to the thiolate ion is enabled:

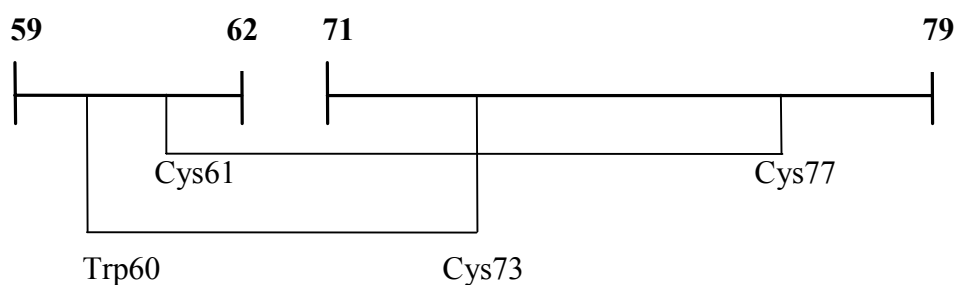


Some intermolecular radical coupling results in dimerization and even trimerization of GLA molecules (Figure 6). Intramolecular radical coupling presumably can result in the sulfenylation of the Trp concerned:



The formation of a shoulder at the red wavelength side of the absorption peak of Trp (Figure 7) is in agreement with the existence of such modified Trp residues. The red-shifted shoulder refers to an increased delocalization of electrons of the aromatic indole nucleus (26). The substitution of a hydrogen of the indole ring by an alkylsulfenyl group enables such extra delocalization.

A more thorough inspection of the mass spectra of the tryptic fragments from irradiated and carbamidomethylated GLA further supports the idea that products are formed according to that scheme. Indeed, the mass peak of 1553.0 Da (Figures 9 and 10), is readily ascribed to a heterofragment containing two peptides linked with the disulfide bridge Cys61-Cys77 and including Cys73.



The mass further indicates that after cleavage of the disulfide bridge Cys73-Cys91, Cys73 is not reactive to iodoacetamide. Interestingly, Trp60 also belongs to the above-mentioned heterofragment (Table 1) enabling the possibility of a radical-induced formation of a thioether linkage between Cys73 and Trp60 within the heterofragment. On further refinement we learn that the mass of the heterofragment is about 4 Da smaller than the result obtained by adding the masses of the individual peptides (1008.4 and 548.3 Da; see Table 1). Clearly, the disulfide bond linking of Cys61 with Cys77 is responsible for a loss of 2 H-atoms, representing 2 Da. The remaining 2 Da refer to the loss of another couple of H-atoms. The data available so far lead to the hypothesis that Trp60 is linked to Cys73.

Finally, it is of interest to remark that such intramolecular sulfenylation of Trp can explain why, in general, only a single reactive thiol group is generated upon the photolysis of a disulfide bond through the absorption of near-UV light by a nearby Trp residue.

Table 2: Shortest Distances (\AA) between the Indol Rings and the Different Disulfide bridges in GLA^a

	Cys6-Cys120	Cys28-Cys111	Cys61-Cys77	Cys73-Cys91
Trp26	14.5	8.9	15.9	10.9
Trp60	28.6	18.2	6.4	3.9
Trp104	20.7	9.0	11.7	7.7
Trp118	9.8	3.4	24.5	22.0

^a A distance shorter than 5 \AA refers to a close van der Waals contact.

Up to now we have been discussing the nature of the Trp-mediated photolysis of disulfide bonds. Next, we want to focus on the specific disulfide bonds that are being attacked. GLA contains four Trp groups and four disulfide bridges. Near-UV irradiation of intact GLA results in the photolysis of only two of these bonds: Cys73-Cys91 and Cys6-Cys120. An inspection of the crystal structure of GLA (5, PDB code 1HFYa) indicates that the disulfide Cys73-Cys91 is in

direct contact with the indole ring of Trp60. This readily explains the transfer of an electron from Trp60 to Cys73-Cys91 and the preference for cleavage of that bond. Within the crystal the positions 4 of the indole ring of Trp60 is oriented towards the S atom of Cys73. Therefore it seems likely that the photochemical reactions (eq 2-6) are initiated by the resonance structures with high electron density at the indolyl C4 atom. As a consequence, also the hydrogen at that position may preferentially be substituted for the sulfenyl-radical resulting from Cys73. Interestingly, the recent structure analysis of 'quinohemoprotein amine dehydrogenase' revealed the existence a thioether bond between the S γ atom of a Cys residue and the indolyl C4 of a modified Trp (27, 28).

Concerning Cys6-Cys120, in crystallized GLA the shortest inter-residue distance between the disulfide group 6-120 and the nearest Trp (Trp118) is at 9.8 Å (see Table 2). Also, the crystal structure shows a direct Van der Waals contact between the indole of Trp118 and the disulfide group 28-111 (shortest inter-residue distance of 3.4 Å, see Table 2). Therefore, the Trp-mediated photolysis of the Cys6-Cys120 bond is not expected. Presumably, moments of direct contact, suited for electron transfer between excited Trp118 and Cys6-Cys120, are enabled by enhanced mobility of the structural elements within a protein in solution. Moreover, the cleavage of the Cys6-Cys120 disulfide bond upon excitation of Trp118 is promoted by the weak strength of this disulfide bond. From high-resolution X-ray data of crystallized baboon LA, it has been deduced that the poor strength of Cys6-Cys120 mainly results from torsion created on the five successive covalent bonds of the Cys-Cys side chain (21, 29). The resolution of the available X-ray data for GLA and for most other LAs exceeds 1.8 Å and, therefore, is not sufficient for an accurate calculation of the torsion energy of the Cys6-Cys120 side chain (21). However, the weakness of that disulfide bond in GLA is obvious from its extraordinarily fast reduction when the protein is treated with chemical reducing agents.

Besides of the weakness of that Cys6-Cys120, also the orientation of Trp118 may be important for the preference for photo-reduction. Indeed, within the crystal structure Trp118 although relatively distant, is oriented in such a way that the indolyl C4 atom is directed towards the S γ atoms of Cys6. As stated above, this may be the optimal orientation for an electron transfer from excited Trp and for the formation of a thioether linkage.

In conclusion, the results of this study suggest that Trp-mediated photo-reduction of a disulfide bond within proteins is more generally enabled and is not restricted to the specific

microenvironment met in cutinase (4, 30). A direct contact between the excited Trp and the considered disulfide bond seems to be favorable for the induction of photolysis. However, the mutual comparison of the reactivity of Cys6-Cys120 and Cys28-Cys111 and of their relative position with respect to Trp118 indicates that other factors are also important. The Trp-mediated photo-reduction of a disulfide bond preferentially results in the formation of a single free cysteine. We have indications that the second Cys residue could form a thioether linkage with the indole group of the mediating Trp residue, however further proof has to be provided.

In order to reveal the impact of individual Trp residues on photolysis of disulfide bridges, recombinant proteins, with a Trp residue replaced by a phenylalanine, were produced. First of all, the influence of the mutations on the structural characteristics is defined and described in the next Chapter. Making use of these mutants, we investigated which of the four Trp residues within GLA are essential for inducing photoreduction of disulfide bonds and which structural changes occur within the different mutants upon illumination (Chapter 5).

3.6 Acknowledgment

We thank Mark Devenijn for providing us with whey from fresh goat milk. The expert assistance of Wim Noppe with the purification and decalcification of goat α -lactalbumin is gratefully acknowledged. We thank prof. Dr. Marcel Joniau for helpful suggestions about redacting this paper.

3.7 References

1. Bhattacharya, D., Basu, S., and Mandal, P. C. (2000) UV radiation effects on flavocytochrome b2 in dilute aqueous solution. *J. Photochem. Photobiol. B* 59, 54-63.
2. Creed, D. (1984) The photophysics and photochemistry of the near-UV absorbing amino acids-I. Tryptophan and its simple derivatives. *Photochem. Photobiol.* 39, 537-562.
3. Dose, K. (1968) The photolysis of free cystine in the presence of aromatic amino acids. *Photochem. Photobiol.* 8, 331-335.
4. Prompers, J.J., Hilbers, C.W. and Pepermans, H.A.M. (1999) Tryptophan mediated photoreduction

- of disulfide bond causes unusual fluorescence behaviour of *Fusarium solani pisi* cutinase. *FEBS Letters* 456, 409-416.
5. Pike, A.C.W., Brew, K. and Acharya, K.R. (1996) Crystal structure of guinea pig, goat and bovine α -lactalbumin highlight the enhanced conformational flexibility of regions that are significant for its action in lactose synthase. *Structure* 4, 691-703.
 6. Ptitsyn, O.B. (1995) Structures of folding intermediates. *Adv. Protein Chem.* 47, 83-229.
 7. Kuwajima, K. (1996) The molten globule state of α -lactalbumin. *FASEB J.* 10, 102-109.
 8. Sommers, P.B. and Kronman, M.J. (1980) Comparative fluorescence properties of bovine, goat, human and guinea pig α -lactalbumin. Characterization of the environments of individual tryptophan residues in partial folding conformers. *Biophys. Chem.* 11, 217-232.
 9. Hanssens, I., Pottel, H., Herreman, W. and Van Cauwelaert, F. (1984) pH-Dependence of the α -lactalbumin structure: a fluorescence study. *Biochem. Biophys. Res. Comm.* 119, 509-515.
 10. Lala, A.K. and Kaul, P. (1992) Increased exposure of hydrophobic surface in molten globule state of α -lactalbumin. Fluorescence and hydrophobic photolabeling studies. *J. Biol. Chem.* 267, 19914-19918.
 11. Veprintsev, D.B., Permyakov, S.E., Permyakov, E.A., Rogov, V.V., Cawild typehern, K.M. and Berliner, L.J. (1997) Cooperative thermal transitions of bovine and human apo- α -lactalbumins: evidence for a new intermediate state. *FEBS Lett.* 412, 625-628.
 12. Grinberg, V.Y., Grinberg, N.V., Burova, T.V., Dagalarondo, M. and Haertlé, T. (1998) Ethanol-induced conformational transitions in holo- α -lactalbumin: spectral and calorimetric studies. *Biopolymers* 46, 253- 265.
 13. Vanderheeren, G., Hanssens, I., Noyelle, K., Van Dael, H. and Joniau M. (1998) The perturbations of goat α -lactalbumin induced by 1,1'-bis(4-anilino-5-naphthalene sulfonate) are Ca^{2+} -dependent. *Biophys. J.* 75, 2195-2204.
 14. Vanhooren, A., Vanhee, K., Noyelle, K., Majer, Z., Joniau, M. and Hanssens I. (2002) Structural basis for difference in heat capacity increments for Ca^{2+} binding to two α -lactalbumins. *Biophys. J.* 82, 407-417.
 15. Chakraborty, S., Ittah, V., Bai, P., Luo, L., Haas, E. and Peng Z. (2001) Structure and dynamics of the α -lactalbumin molten globule: Fluorescence studies using proteins containing a single tryptophan residue. *Biochemistry* 40, 7228-7238.
 16. Ewbank, J.J. and Creighton, T.E. (1993) Structural characterization of the disulfide folding intermediates of bovine α -lactalbumin. *Biochemistry* 32, 3694-3707.
 17. Noppe, W., Haezebrouck, P., Hanssens, I. and De Cuyper, M. (1999) A simplified purification procedure of α -lactalbumin from milk using Ca^{2+} -dependent adsorption in hydrophobic expanded bed chromatography. *Bioseparation* 8, 153-158.
 18. Vanderheeren, G., Hanssens, I., Meijberg, W. and Van Aerschot, A. (1996) Thermodynamic

- characterization of the partially unfolded state of Ca^{2+} -loaded α -lactalbumin: evidence that partial unfolding can precede Ca^{2+} release. *Biochemistry* 35, 16753-16759.
19. Ellman, G. L. (1959) Tissue sulfhydryl group, *Arch. Biochem. Biophys.* 82 , 70-77
 20. Parker, A. and Engel, P.C. (1999) 5,5'-Dithiobis-(2-nitrobenzoic acid) as a probe for a non-essential cysteine residue at the medium chain acyl-coenzyme A dehydrogenase binding site of human 'electron transferring flavoprotein'. *J. Enzym. Inhib.* 14, 381-390.
 21. Kuwajima, K., Ikeguchi, M., Sugawara, T., Hiraoka, Y. and Sugai, S. (1990) Kinetics of disulfide bond reduction in α -lactalbumin by dithiothreitol and molecular basis of superreactivity of Cys6-Cys120 disulfide bond. *Biochemistry* 29, 8240-8249.
 22. Smith, C.A. and Maki, A.H. (1993). Temperature dependence of the phosphorescence quantum yield of various α -lactalbumins and of hen egg-white lysozyme. *Biophys. J.* 64, 1885-1895.
 23. Mach, H., Middaugh, C.R. and Lewis, R.V. (1992) Statistical determination of the average values of extinction coefficients of tryptophan and tyrosine in native proteins. *Anal. Biochem.* 200, 74-80.
 24. Arai, M. and Kuwajima, K. (2000) Role of the molten globule state in protein folding. *Adv. Prot. Chem.* 53, 209-282.
 25. Bent, D.V. and Hayon, E. (1975) Excited state chemistry of aromatic amino acids and related peptides. III Tryptophan. *J. Am. Chem. Soc.* 97, 2612-2619.
 26. Alberty, R.A. and Silby R.J. (1992) Electronic spectroscopy of molecules. *In: Physical Chemistry.* John Wiley & Sons, New York. Chapter 15.
 27. Datta, S., Mori, Y., Takagi, K., Kawaguchi, K., Chen, Z.W., Okajima, T., Kuroda, S., Ikeda, T., Kano, K., Tanizawa, K. and Mathews, F.S. (2001) Structure of a quinoxinoprotein amine dehydrogenase with an uncommon redox cofactor and highly unusual crosslinking. *Proc. Natl. Ac. Sc. U.S.A.* 98, 14268-14273.
 28. Satoh, A., Kim, J. K., Miyahara, I., Devreese, B., Vandenberghe, I., Hacisalihoglu, A., Okajima, T., Kuroda, S., Adachi, O., Duine, J. A., Van Beeumen, J., Tanizawa, K. and Hirotsu, K. (2002) Crystal structure of quinoxinoprotein amine dehydrogenase from *Pseudomonas putida* - Identification of a novel quinone cofactor engaged by multiple thioether cross-bridges. *J. Biol. Chem.* 277, 2830-2834.
 29. Acharya, K.R., Stuart, D.I., Philips, D.C. and Scheraga, H.A. (1990) A critical evaluation of the predicted and X-ray structure of α -lactalbumin. *J. Prot. Chem.* 9, 549-563.
 30. Neves-Petersen, M.T., Gryczynski, Z., Lakowicz, J., Fojan, P., Pedersen, S., Petersen E. and Petersen S. B. (2002) High probability of disrupting a disulfide bridge mediated by an endogenous excited tryptophan residue. *Protein Sci.* 11, 588-600.
 31. Guex, N. and Peitsch MC. (1997) Swiss-model and the Swiss-PDB viewer: an environment for comparative protein modeling. *Electrophoresis* 18, 2714-2723.

**Tryptophan to phenylalanine substitutions allow
differentiation of short and long range conformational
changes during denaturation of goat α -lactalbumin**

*A. Vanhooren, A. Chedad, V. Farkas¹, Z. Majer¹, H. Van Dael, M. Joniau and I.
Hanssens*

*Interdisciplinary Research Center, Katholieke Universiteit Leuven Campus
Kortrijk, Kortrijk, Belgium*

*¹Department of Organic Chemistry, Eötvös Loránd University, Budapest,
Hungary.*

Based on Proteins, 2005, 60, 118-130

With Addendum

4.1 Abstract

UV illumination of LA induces the reduction of a distinct set of disulfide bridges as described in the previous Chapter. On the basis of the crystal structure we assumed that out of the four Trp residues two residues, Trp60 and Trp118, are responsible for the photo-induced rupture of these disulfide bridges. To acquire a better insight in the impact of the individual Trp residues, we constructed three mutants in which Trp60 and/or Trp118 are replaced by phenylalanine. Before the illumination experiments on these mutants were started, we compared the spectral characteristics of the native and denatured mutants and tested the occurrence of local particularities during their unfolding. These results are presented in this Chapter. Later on, two additional mutants, W26F and W104F, were produced and their physico-chemical properties are described in the addendum of this Chapter.

In contrast with alternative studies, our recombinant α -lactalbumins are expressed in *Pichia pastoris* and do not contain the extra N-terminal methionine. The substitution of Trp60 leads to a reduction of the global stability. The effect of the Trp118Phe substitution on the conformation and stability of the mutant, however, is negligible. Comparison of the fluorescence spectra of these mutants makes clear that Trp60 and -118 are strongly quenched in the native state. They both contribute to the quenching of Trp26 and -104 emission. By the interplay of these quenching effects, the fluorescence intensity changes upon thermal unfolding of the mutants behave very differently. This is the reason for a discrepancy of the apparent transition temperatures derived from the shift of the emission maxima ($T_{m,Fl\lambda}$) and those derived from DSC ($T_{m,DSC}$). However, the transition temperatures derived from fluorescence intensity ($T_{m,Fl\text{int}}$) and from DSC ($T_{m,DSC}$), respectively, are quite similar and thus, no local rearrangements are observed upon heat-induced unfolding. At room temperature, the occurrence of specific local rearrangements upon GdnHCl-induced denaturation of the different mutants is deduced from the apparent free energies of their transition state obtained from stopped-flow fluorescence measurements. By ϕ^\ddagger -value analysis it appears that, while the surroundings of Trp118 are exposed in the kinetic transition state, the surroundings of Trp60 remain native.

4.2 Introduction

α -Lactalbumin (LA) performs an important function in mammary secretory cells as it acts as a regulatory subunit of the lactose synthase system (1). In complex with galactosyltransferase LA modifies the specificity of the enzyme so that it can catalyse the transfer of galactose to glucose (2). Most LAs, including human, bovine and goat LA, consist of 123 amino acid residues. X-ray crystallographic analysis has shown that the three-dimensional structure of LA is very similar to that of c-type lysozymes (3). Although the native proteins are compact, their structure consists of two clearly distinct parts: an α - and a β -domain. The two domains are divided by a deep cleft which in the homologous lysozyme represents the substrate binding site. Ca^{2+} ions bind to all LAs and stabilize the protein against denaturation (4). The Ca^{2+} -binding loop connects both domains and is absent in most lysozymes (3,5).

LA exhibits a partially unfolded state, the molten globule, which is stably populated at equilibrium under various mildly denaturing conditions (6,7). The molten globule conformer is characterized by a native-like α -domain, while the β -domain (residues 35-85) is largely unstructured (8). The similarity of the LA molten globule conformer to an early intermediate on the folding pathway has led to extensive study of LA as a model for protein folding (9,10). Other conformers that are intermediate between the native and the molten globule state also have been reported (11,12). An aggregated, misfolded form of LA causes apoptosis in tumor but not in normal cells (13), indicating that some of the partially folded states of LA may be biologically important.

Besides the major part of the β -domain, also the sequences 105-110 and 112-119 at the surface of the α -helical domain are characterized by high flexibility and conformational variability (14). The side chains of Gln117 and Trp118 are essential for efficient binding with galactosyltransferase (15-17). The vicinal sequence 105-110, although itself not in contact with the enzyme, is also important for the formation of the lactose synthase complex (17,18). This flexible region adopts either a loop or a helix conformation, depending on the pH of the medium (14). Ramakrishnan et al. (19,20) showed that, in mouse LA, this region adopts a helical conformation when bound in the lactose synthase complex.

In the present study we replaced Trp60 and Trp118 in goat LA, either one or both, by Phe. As mentioned above, Trp60 as well as Trp118 are surrounded by flexible sequences. Both sequences are, however, located in different regions. Figure 1 in Chapter 3 represents the structure of GLA and indicates the sites of the Trp residues. Trp60 is located in the β -domain, near the cleft region. Trp118 is located near the C-terminus, in a flexible region of the α -domain. This study aims to obtain information on local aspects of organization and of destabilization within the LA molecule. This is accessed by comparing the spectral characteristics deduced from emission fluorescence and from near-UV CD spectroscopy with the DSC scans of the various mutants.

Emission fluorescence and near-UV CD spectroscopy are two commonly used techniques for the observation of conformational changes in proteins. Both techniques make use of Trp as a reporter and are very sensitive to the local environment of the Trp groups (21,22). As LAs generally have four Trp residues, the observed fluorescence and CD signals are a superposition of the individual signals. In order to study the proper contribution of a specific Trp, the other Trp groups can be substituted with non-fluorescent amino acids as was done by Chakraborty et al. for human LA (23). We, on the other hand, followed an alternative way in which we substituted a single Trp with a non-fluorescent amino acid and from the difference spectrum of the mutant with respect to the wild type protein, we deduced the specific contribution of the substituted Trp. Such single point mutations minimize the direct disturbance of protein biophysical properties such as stability, flexibility and folding kinetics. We measured fluorescence to follow thermal as well as GdnHCl-induced unfolding. The fluorescence data of wild type and mutant GLA were compared to detect local effects on the stability, kinetics and enzymatic activity. In order to distinguish between local and global effects we compared fluorescence and near-UV CD data, which are specifically Trp-related, with data obtained from DSC and from far-UV CD measurements, that are not directly associated with Trp residues. In the kinetic experiments, local and global effects are distinguished by comparing the respective apparent free energies of the kinetic transition state that were obtained on the basis of stopped-flow fluorescence data.

It is worth to mention that the present study, to our knowledge for the first time, deals with recombinant LA expressed in *Pichia pastoris*. The expression of LA in yeast has important advantages over the use of *E. coli*, which was up to now the preferential host for the production of recombinant LA (15, 24-26). *P. pastoris* secretes natively folded GLA, and the extra N-terminal methionine is absent. This is important, as it has been shown that methionyl-LA has more solvent-accessible Trp residues, lower stability and decreased calcium affinity compared to

the authentic protein (24,26). As will be shown further, the wild type GLA expressed in *P. pastoris* has properties identical to those of authentic GLA from milk whey.

4.3 Materials and Methods

4.3.1 Materials

Authentic goat α -lactalbumin (GLA) was prepared from fresh milk whey (27). Restriction endonucleases, Klenow polymerase, T4 DNA ligase and calf intestinal alkaline phosphatase were purchased from Boehringer-Mannheim or Promega. Primers were synthesized by Invitrogen. MES was obtained from Sigma. Bovine galactosyltransferase and UDP-galactose were from Sigma and ^3H -labeled UDP-galactose from Amersham.

4.3.2 Strains and Media

Escherichia coli DH5 α (*supE44* Δ *lacU169*(ϕ 80*lacZ* Δ *M15*) *hsdR17* *endA1* *recA1* *gyrA96* *thi-1* *relA1*) used as host strain for bacterial transformations and routine plasmid preparations was grown in Luria broth (28).

For the expression of GLA mutants in *P. pastoris* the GS115 (*his4*, Mut⁺) strain of the Pichia Expression Kit (Invitrogen[®]) was cultivated on RDB plates and YPD media as described by the manufacturer. For large scale expression YPMG and YPMM (1 % yeast extract, 2 % peptone, 0.1 M MES, 0.1 % threonine, 0.003 % myoinositol, 0.003 % pantothenate, 0.0225 % leucine, 0.0045 % adenine and uridine, 0.00227 % amino-acids: L-Trp, His, Arg, Met, Tyr, Lys, Phe and 5% glycerol or 0.5 % methanol, respectively) were used. The pH was adjusted at pH 7.

4.3.3 Construction of wild type and mutant GLA genes

The pTZsA1T(ZSS)-plasmid containing the wild type bovine α -lactalbumin gene (BLA gene) was constructed from the pTZs31T-plasmid (29) to allow the transfer of the BLA gene and its mutants, together with the prepro- α -mating factor, to the yeast vector pPIC9K (Pichia Expression Kit, Invitrogen®). Construction of the GLA gene from BLA was carried out in 4 subsequent steps using the QuikChange™ Site-Directed Mutagenesis Kit (Stratagene®, La Jolla, CA, USA) as described by the manufacturer. The resulting plasmid, called pTZsA1TGLA(ZSS), was used as a template to construct two plasmids containing either the W60F or the W118F mutation. The double mutant W60/118F was constructed by ligation of the appropriate fragments resulting from the cleavage with *AvaI* and *XbaI* of the two plasmids containing the W60F or the W118F mutation. The correct construction of all the plasmids was verified by restriction digestion and sequence analysis. Plasmid DNA, used for DNA sequence analysis and for transformation was prepared with the QIAGEN Plasmid Purification Kit (Qiagen, Westburg, Hilden, Germany). DNA sequence analysis was performed by Genome Express (Labo Grenoble, Meylan, France). The shuttle vector pPIC9K was opened up by a double digestion with *BamHI* and *EcoRI*, with the loss of the α -mating factor preprosequence as a consequence. It was ligated to the *BamHI-EcoRI* fragment of pTZsA1TGLA(ZSS) vector, which consisted of the α -mating factor preprosequence and the wild type or the mutant GLA gene. The DNA sequence was analyzed to confirm the correct sequence of the inserts.

4.3.4 Transformation, Expression and Purification

The recombinant plasmids were linearized with either *BglII*, *SacI* or *SallI*. The linearized plasmids were used to transform *P. pastoris* cells according to the sferoplast method of Hinnen et al.(30). His⁻ RDB plates were used to screen for plasmid containing cells. After a qualitative pre-screening, the best producing clones were grown in YPD at 28°C in shaker culture for 2 days (31). The cells were resuspended in YPMG and incubated for 3 days at 28 °C with shaking. Methanol induction started by changing the YPMG for YPMM-medium. To maintain induction the cells were supplied with methanol added to a final concentration of 1%. The culture was harvested after 5 days of growth and a RIA was used to estimate the expression yield of the

recombinant protein (28). The proteins were purified from the culture supernatant by means of hydrophobic interaction chromatography (27), dialyzed and lyophilized. As *P. pastoris* secretes a certain percentage of glycosylated LA (32) the samples were further purified by affinity chromatography on a Con A Sepharose 4B column (Pharmacia). The non-glycosylated fraction was lyophilized.

4.3.5 Protein characterisation

The protein samples were run on a 10-20% tricine gradient gel (Invitrogen) in a Tris-tricine buffer. After fixation, the protein was detected with Coomassie PhastGel[®]Blue R (Pharmacia).

The proteins were subjected to electrospray ionization mass spectrometry (ESI-MS) on a Q-TOF mass spectrometer (Micromass, Manchester, U.K.) equipped with a nanoESI source, NanoMate100 (Advion Biosciences).

All experiments were performed in 10 mM Tris-HCl buffer, pH 7.5, containing 2 mM Ca^{2+} . The GLA concentration was determined by spectrophotometry using $\epsilon_{280} = 28840 \text{ (mol/l)}^{-1} \text{ cm}^{-1}$ for authentic and wild type GLA, $\epsilon_{280} = 23150 \text{ (mol/l)}^{-1} \text{ cm}^{-1}$ for the W60F and W118F mutants and $\epsilon_{280} = 17460 \text{ (mol/l)}^{-1} \text{ cm}^{-1}$ for the double mutant W60/118F of GLA. The values of the molar extinction coefficients were calculated from the number of Trp, Tyr and Cys residues (33).

4.3.6 Spectroscopic Equilibrium Measurements

Circular dichroism measurements were made on a Jasco J-810 spectropolarimeter (Jasco, Tokyo, Japan), using an optical cell with path length of 0.02 cm for measurements in the far-UV region and 0.2 cm for measurements in the near-UV region. The GLA concentration used was approximately 30 μM .

Steady state fluorescence was measured with a Perkin Elmer LS55 Luminescence Spectrometer. The GLA concentration used was approximately 5 μM . Amounts of 3 ml of the degassed protein solutions were transferred into a 10 x 10 mm cell for fluorescence spectroscopy. The excitation wavelength was 280 nm, the bandpass for the excitation and emission slits was 5 nm and 3 nm, respectively. The fluorimeter was equipped with a magnetic stirrer mounted under the cell

holder. The cell holder was thermostatted by circulating water from an external water bath. By means of a PID-control algorithm (Labviewild type^M) we imposed a stepwise heating program to the circulator thermostat: every 8th minute the temperature was increased by 3 °C. Adjustment of the imposed temperature was controlled by a Pt100 sensor dipped in the solution. The registration of each fluorescence spectrum started 6 min after a new temperature was applied, 3 min after temperature equilibration of the sample is reached. The temperature did not vary more than 0.2 °C during the registration of the spectrum. The temperature halfway this scan is noted.

The fractional change of the emission wavelength ($f_{fl,\lambda}$), used to plot apparent thermal transition curves, was defined as:

$$f_{fl,\lambda} = (\lambda_{obs} - \lambda_N) / (\lambda_U - \lambda_N) \quad (1)$$

where λ_{obs} is the observed wavelength of the emission maximum. At each temperature within the transition range the wavelengths of the emission maximum of native and unfolded LA, λ_N and λ_U , are extrapolated from the baselines before and after the thermal transition.

The fractional change of the fluorescence intensity ($f_{fl,int}$) was obtained by replacing the wavelengths by the corresponding intensities in the above equation.

4.3.7 Differential Scanning Calorimetry

Calorimetric scans were carried out on a MicroCal VP-DSC differential scanning calorimeter, using the software supplied by the manufacturer for data collection and analysis. The reference and the sample solutions were degassed for 15 min at room temperature prior to scanning at rates of 60 °C/h. The protein concentration in the sample solutions was about 30 μ M. The heat capacity of the sample protein was obtained by subtraction of a reference scan from the scan of the sample solution. Each heat capacity scan was normalized by dividing the heat capacity scan of the sample by the number of moles of protein in the sample. The excess heat capacity function related to the protein unfolding was determined after subtraction of the baseline that takes into account the sigmoidal progression of the unfolding process.

4.3.8 Stopped-flow fluorescence experiments

Folding and unfolding experiments were performed on a SX.18MV sequential mixing stopped-flow fluorescence spectrometer from Applied Photophysics (Leatherhead, U.K.). The stopped-flow unit and the observation cell with 2 mm path length were thermostated by circulating water from a temperature-controlled bath. A monochromator was used for excitation at 280 nm and the fluorescence emission was measured using a high-pass filter with 320 nm cutoff. The dead-time of the instrument was estimated to be about 2 ms. Typically, kinetics were measured 10-12 times, averaged and analysed as a sum of exponential functions by using the manufacturer's software. Chevron plots were constructed by plotting the logarithm of the rate constant as a function of denaturant concentration. All measurements were done at 25 °C and pH 7.5 in 10 mM Tris and 2 mM Ca^{2+} . In the refolding experiments a solution of 0.5 mg/ml unfolded protein in 6 M GdnHCl was diluted 11-fold with refolding buffer containing various concentrations of GdnHCl. In unfolding experiments native protein (0.5 mg/ml) in buffer was diluted 11-fold with GdnHCl solutions of varying concentrations to give a final concentration between 2.8 and 6 M GdnHCl.

4.3.9 Kinetic data analysis

The transition curve expressed by the fraction of unfolded LA, f_{unf} , as a function of the concentration of denaturant, c , was obtained from the final fluorescence signal of the individual stopped-flow traces for refolding and unfolding experiments. The fractions for different mutants were fitted to the equation:

$$f_{\text{unf}} = \frac{\exp(-(\Delta G_{\text{unf}}^{\text{H}_2\text{O}} - m_{\text{unf}}c))}{1 + \exp(-(\Delta G_{\text{unf}}^{\text{H}_2\text{O}} - m_{\text{unf}}c))} \quad (2)$$

The fitting provides the numeric values of the unfolding free energy in the absence of denaturant, $\Delta G_{\text{unf}}^{\text{H}_2\text{O}}$, and of the cooperativity index for the transition, m_{unf} (34).

The unfolding free energy in presence of denaturant, ΔG_{unf} , is linearly dependent on GdnHCl concentration, c :

$$\Delta G_{\text{unf}} = \Delta G_{\text{unf}}^{\text{H}_2\text{O}} - m_{\text{unf}}c \quad (3)$$

The difference in the Gibbs free energy between the wild type and a particular mutant at a given GdnHCl concentration is defined as:

$$\Delta\Delta G_{\text{unf}} = \Delta G_{\text{unf}}^{\text{wt}} - \Delta G_{\text{unf}}^{\text{mut}} \quad (4)$$

The ϕ^\ddagger -value of the transition state was calculated using the unfolding rates as follows:

$$\phi^\ddagger = 1 - \frac{\Delta\Delta G_{\text{unf}}^\ddagger}{\Delta\Delta G_{\text{unf}}} = 1 - \frac{RT \ln \left(\frac{k_{\text{unf}}^{\text{mut}}}{k_{\text{unf}}^{\text{wt}}} \right)}{\Delta\Delta G_{\text{unf}}} \quad (5)$$

where $k_{\text{unf}}^{\text{mut}}$ and $k_{\text{unf}}^{\text{wt}}$ are the unfolding rates of the mutant and the wild type protein, respectively, at a given GdnHCl concentration. The ϕ^\ddagger -values are summarized in Table 5.

4.3.10 Lactose synthase assays

The lactose synthesis regulatory activities of the recombinant LAs were compared with the activity of authentic GLA using bovine β -galactosyltransferase (GT) and UDP-galactose according to Brew et al. (35). The assays were performed in 200 μ l of 50 mM Tris-HCl buffer (pH 7.5), 20 mM MnCl_2 , 40 mM glucose, 0.3 mM UDP-galactose, 0.4 μ Ci UDP-[6- ^3H]-galactose, 6mU GT and 4-40 μ g of recombinant protein. Anion exchange (0.6 ml of Dowex-1x4) was used to separate synthesized [^3H]-glucose from the unreacted UDP-[6- ^3H]-galactose. The amount of eluted lactose was measured with the aid of a liquid scintillation counter (Packard Tri-Carb[®] 1900TR).

4.4 Results

4.4.1 Characterization of GLA mutants

Wild type GLA and the three Trp mutants were expressed in transformed *P. pastoris*. The level of expression of the recombinant proteins in the culture supernatant was measured by a RIA and amounts to about 40 mg.l⁻¹ for both wild type GLA and mutant W118F. The yield of W60F and W60/118F was in the range of 7 mg.l⁻¹. The recombinant proteins were purified from their respective supernatants by hydrophobic interaction chromatography. About 20% of wild type GLA as well as of W118F obtained after this step was glycosylated. The mutants W60F and W60/118F were glycosylated for up to 40%. The non-glycosylated proteins were isolated by chromatography on a concanavalin A column. The purity of the final products was assayed by SDS-PAGE under reducing and non-reducing conditions. Under non-reducing conditions a small band at about 30kDa revealed the existence of a small fraction of dimeric GLA (~5%).

The recombinant proteins were further characterized by mass spectrometry. The mass spectrum of wild type GLA exhibited a peak at 14186 Da in correspondence with the mass of GLA purified from milk whey. The peaks for the mutants W60F and W118F were both at 14148 Da. The double mutant W60/118F exhibited a peak at 14109 Da. All masses agree with the respective theoretical amino acid composition and indicate that the obtained proteins are free of glycosylation and of any other expression-related modification.

Equal rates of synthesis of lactose are observed when authentic GLA, wild type GLA and the W60F mutant were used as activator of lactose synthesis. Only 4% of this rate is obtained when either W118F or W60/118F was assayed as activator. The latter result confirms previous observations indicating that the substitution of Trp118 always leads to a major reduction of the lactose synthase activity (15).

4.4.2 CD measurements

The secondary and tertiary structure of the authentic and the recombinant GLA was characterized by far- and near- UV CD spectroscopy in 10 mM Tris-HCl, 2 mM Ca²⁺ at pH 7.5 and 25°C. Under these conditions GLA is known to adopt the native conformation. The far-UV CD spectra of authentic and of wild type GLA coincide with each other (Figure 2A, ■). They show a broad band with two minima near 207 and near 224 nm, respectively, the first minimum having a lower intensity than the second one. The spectra also show a positive band near 190 nm. The observed spectral characteristics are typical for proteins with α / β character (36). The substitution of Trp118 by Phe does not significantly alter the far-UV CD spectrum (Figure 2A, □). In contrast, upon substitution of Trp60 by Phe, the positive band near 190 nm decreases in intensity (Figure 2A, ○ and △). Also the bands with negative ellipticity are less intense and the λ_{min} values shifted from 206.4 nm and 224 nm (Figure 2A, ■ and □) to 208.6 nm and 221 nm, respectively (Figure 2A, ○ and △). The CD difference spectra between the various mutants and wild type GLA (Figure 2B) confirm earlier observations that the contributions of Trp60 are more complex than those of Trp118 (23,54). The difference may, at least partly, result from coupled oscillator interactions between Trp60 and neighbouring chromophores (37). Indeed, crystal structure analysis of LA has revealed that Trp60 forms an aromatic cluster with Tyr103 and Trp104 (3,5). This aromatic cluster is part of the interaction interface between the two lobes of LA. As the interactions between the subdomains are of great importance for the formation of a fixed native structure (38,39), the substitution of Trp60 by Phe might influence the secondary structure of GLA, too. In the difference spectra (Figure 2B, ○ and △) the bands with opposite signs could also be interpreted as a decrease of the α - or 3_{10} -helix content in the W60F and W60/118F mutants relative to the wild type LA. Assuming that the ellipticity changes result exclusively from secondary structure changes, one can estimate the fractions of the different types of secondary structure from the CD spectra using specific deconvolution programs (37). The results of a secondary structure calculation using the CDNN-program (40) show that, in so far as coupled oscillator interactions between Trp60 and the vicinal aromatic rings would not affect the far-UV CD signal, the α -helix content would decrease by about 8% while that of the β -sheet structure would increase by 8-10% upon substitution of Trp60 by Phe.

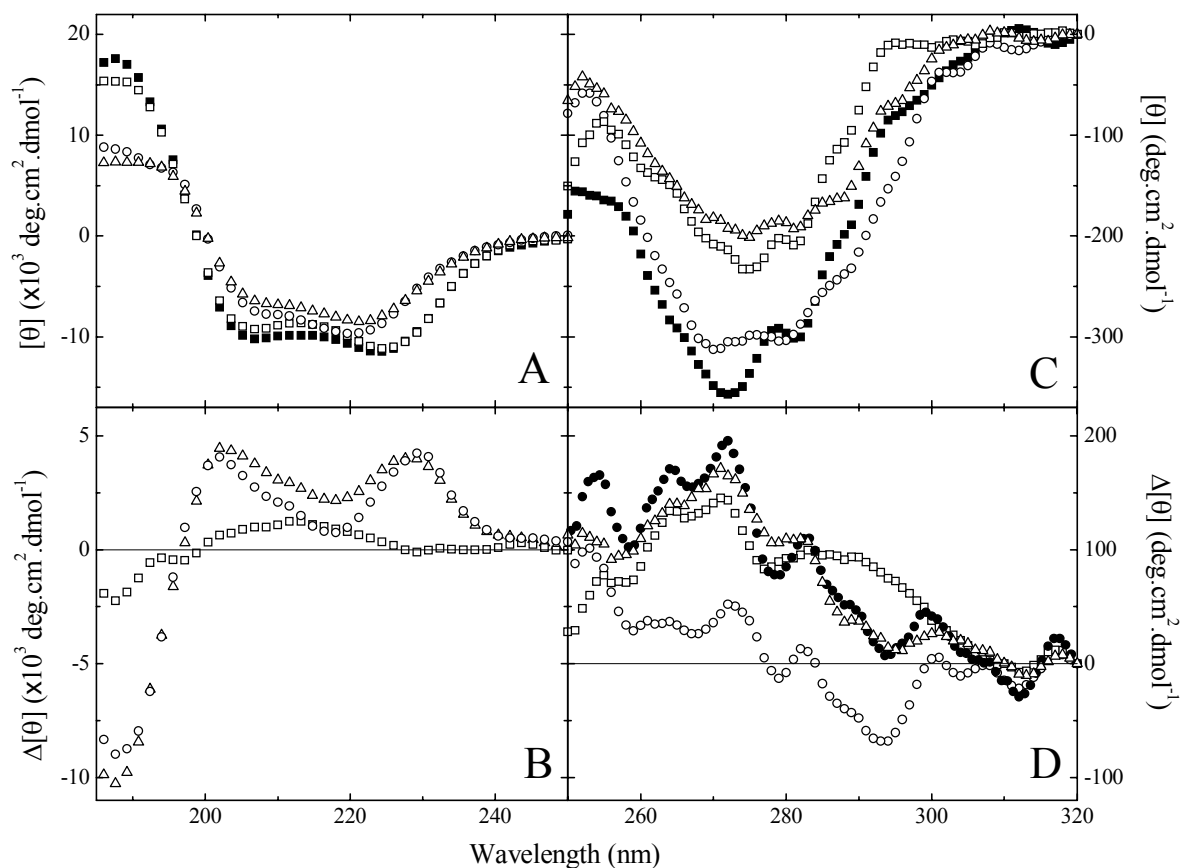


Figure 2: (A) Far- and (C) near-UV CD spectra of wild type GLA (■) and of the mutants W118F (□), W60F (○) and W60/118F (△) measured in 10 mM Tris-HCl, 2 mM CaCl₂, at pH 7.5 and 25 °C. (B) Far- and (D) near-UV CD difference spectra between mutant W60F and wild type (○), mutant W118F and wild type (□) and between mutant W60/118F and wild type (△). In (D) the curve with symbol (●) corresponds to the sum of the near-UV CD difference spectra of which mutants W60F and W118F are involved.

In the near-UV region, the ellipticity data are more specifically related with aromatic contributions than in the far-UV. The negative ellipticity band near 270 nm is most pronounced for wild type GLA (Figure 2C, ■). This indicates that, at this wavelength, each Trp residue contributes to the near-UV CD signal by a negative ellipticity value. Similar observations were made by Chakraborty et al. on substitution of Trp by Phe in human LA (23). In contrast, in the range 285-295 nm the ellipticity for wild type GLA is less negative than for W60F (Figure 2C, ○) indicating that Trp60 contributes by a positive ellipticity band within this wavelength region. In order to illustrate clearly the specific contribution caused by the substitution of Trp60, we calculated the difference spectrum between W60F and wild type GLA (Figure 2D, ○). Figure 2D also shows the difference spectrum between mutant W118F and wild type GLA (Figure 2D, □). The substitution of Trp118 clearly results in two peaks of positive ellipticity: a first maximum is found near 270 nm, the second is near 290 nm. The positive difference peaks refer

to negative contributions of Trp118. The calculated sum of both previous difference spectra (presented by ● in Figure 2D) is in good accordance with the directly measured difference spectrum obtained by subtracting the spectrum of wild type from that of W60/118F GLA (Figure 2D, △). This fair accordance suggests that the differences in the near-UV CD spectra of the various LA mutants are related to localized interactions of the aromatic residues rather than to long range conformational changes. The simultaneous introduction of two mutations does not result in enhanced structural changes within the mutants: they behave as additive, which points to strictly localized effects in a globally conserved matrix.

4.4.3 Fluorescence data

The fluorescence emission spectra of authentic and recombinant GLAs measured under conditions where they adopt the native state are presented in Figure 3. The excitation wavelength was 280 nm. To compensate for inner filter effects, the absorbance at 280 nm of the different solutions was adjusted at 0.150. Besides the Trp residues also Phe, Tyr and Cys absorb some light at 280 nm (33). However, the shape of the different fluorescence spectra corresponds to that of Trp residues in an apolar medium. Also, upon unfolding of LA the emission maximum of the different spectra shifts to about 350 nm (Figure 4A) as is expected for Trp residues that enter in aqueous medium. Therefore, the observed spectra of the different mutants can be attributed mainly to their Trp residues. For each LA mutant we calculated which fraction of light is absorbed by the Trp residues using extinction coefficients reported in (33) and we adjusted the spectra in Figure 3 so as to represent intensities measured for equal Trp concentrations (2.1×10^{-5} mol/l). The integrated fluorescence intensities per unit of Trp are collected in Table 1. These values times the number of Trp residues in the considered mutant, represent the fluorescence per LA molecule (Table 1, column 4). Mutant W60/118F with two residual Trp residues (Trp26 and -104), fluoresces more strongly than each of the mutants W60F and W118F that possess three residual Trps. In turn the three Trps of W60F and W118F fluoresce more strongly than the four Trps of wild type GLA. In a fluorescence study on mutants of human LA containing a single residual Trp, Chakraborty et al. (23) observed that, under native conditions, the fluorescence yield of the mutants with Trp60 and Trp118 is small compared to the fluorescence yield of mutants with Trp104. This was explained as due to the presence of strong quenchers nearby the former Trp residues. They also observed that the fluorescence yield of wild type human LA is

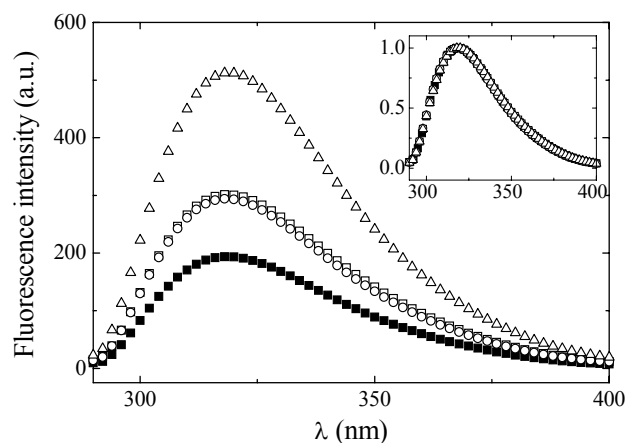


Figure 3: Relative fluorescence intensity of wild type GLA (■) and of the mutants W118F (□), W60F (○) and W60/118F (△) measured in 10 mM Tris-HCl, 2 mM CaCl₂, at pH 7.5 and 25°C. The excitation is at 280 nm and for each protein A_{280} equals 0.15, due to Trp absorption only as explained in the text. The inset shows the normalized fluorescence spectra of the different proteins.

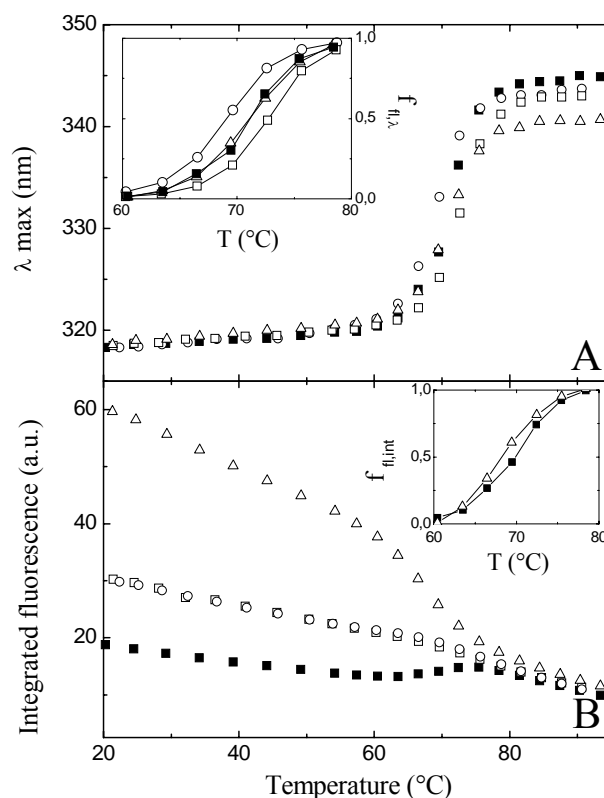


Figure 4: (A) λ_{\max} and (B) integrated fluorescence intensity as a function of temperature for wild type GLA (■) and for the mutants W118F (□), W60F (○) and W60/118F (△) measured under the solvent conditions mentioned earlier. The inset of (A) shows in detail the fractional shift of the fluorescence ($f_{fl,\lambda}$) deduced from the change of λ_{\max} . The inset of (B) shows in detail the fraction of apparently unfolded GLA ($f_{fl,int}$) derived from the change of fluorescence intensity.

Table 1: Integrated fluorescence intensity (arbitrary units) of wild type GLA and of its mutants at comparable concentrations, at 25°C and pH 7.5, in 10 mM Tris-HCl containing 2 mM CaCl₂

Mutant	Residual Trp residues	Integrated Fluorescence/Trp	Integrated Fluorescence/GLA
Wild type	26, 60, 104, 118	18.0	72.0
W60F	26, 104, 118	29.2	87.6
W118F	26, 60, 104	30.2	90.6
W60/118F	26, 104	58.2	116.4

smaller than that of the mutant containing the single Trp104. This phenomenon was considered to be mediated by energy transfer between Trp104 and a Trp residue that undergoes further quenching. Trp60 was designated as the mediator for this indirect quenching in accordance with an earlier report (41). Our data (Table 1, column 4) indicate that both Trp118 and Trp60 are about equally effective in the quenching of the fluorescence of both Trp26 and -104.

Starting from W60/118F, the integrated fluorescence intensity per protein molecule is reduced by 26 to 29 arbitrary units by the addition of the first supplemental Trp (in W60F or W118F) and only by 15 to 18 arbitrary units by the addition of the second supplemental Trp (wild type GLA). This decrease of increment of the quenching effect supports the idea that in native LA, Trp26-104 behaves as a resonance couple and not as two individually emitting units. Indeed, if Trp26 and Trp104 would behave as two separate emission units, the quenching effect mediated by the introduction of one of the vicinal Trps, Trp60 or Trp118 (Trp60 is vicinal to Trp104 and Trp118 is vicinal to Trp26) would not be influenced by the addition of the other vicinal Trp (Trp118 or Trp 60 respectively).

It is worth noticing that, although the emission intensities of the native GLA mutants are very different, the shape of the different spectra is very similar (Figure 3). To better visualize the latter property the different spectra are rescaled to the same maximum (inset of Figure 3). The excellent similarity is readily explained by the fact that each spectrum reflects fluorescence of the same Trp residues. As mentioned previously, Trp60 and -118 do not importantly contribute to the fluorescence of native W118F, nor of native W60F or wild type GLA. Therefore, in each of these molecules the fluorescence mainly results from Trp26 and/or -104. The fluorescence of

those buried Trp residues is at the short wavelength side of the emission spectrum and exhibits a maximum near 320 nm.

Figure 4A shows the change of wavelength of the emission maximum for GLA and its mutants as a function of temperature. For the reasons mentioned above, the emission maximum of all GLA mutants is near 320 nm at temperatures below the transition temperature, $T_{m,Fl}$. At temperatures above $T_{m,Fl}$ the emission maximum of the different mutants and of wild type GLA shifts to longer wavelengths (340-345 nm) and finally differ mutually by several nm (Figure 4A). It is worth to notice that in the thermally unfolded state, especially the double mutant W60/118F has a lower λ_{max} (340nm) than authentic and wild type GLA (345 nm). This suggests that, in the unfolded form, the Trp26 and Trp104 residues remain somewhat more protected from solvent than Trp60 and/or Trp118 which are additionally present in the other constructs. Indeed Trp26 and -104 belong to the α -helical domain of GLA. Moreover, Trp26 belongs to one of the major α -helices (helix 23-34). α -Helices are known to resist strongly denaturing conditions.

The fractional change of the wavelength maximum upon transition is easily determined with good accuracy for the various recombinant LA mutants. The resultant curves (Figure 4A, inset) show symmetry. The midpoints represent the apparent transition temperatures ($T_{m, Fl\lambda}$) and are listed in Table 2.

Table 2 : Unfolding temperature (°C) deduced from the transition midpoint of thermal unfolding of GLA and its Trp mutants

	$T_{m,Fl\lambda}$	$T_{m,Fl\ int}$	$T_{m,DSC}$	$T_{m,Fl\lambda} - T_{m,DSC}$
Authentic	70.7 ± 0.4		71.0 ± 0.2	- 0.3
Wild type	71.2 ± 0.2	69.9 *	71.1 ± 0.2	+ 0.1
W118F	73.0 ± 0.2	/	71.5 ± 0.2	+ 1.5
W60F	69.2 ± 0.2	/	67.9 ± 0.2	+ 1.3
W60/118F	71.0 ± 0.3	68.0 ± 0.3	68.1 ± 0.2	+ 2.9

The unfolding temperature is deduced from shifts of the fluorescence wavelength ($T_{m,Fl\lambda}$), the fluorescence intensity ($T_{m,Fl\ int}$) and from heat capacity changes ($T_{m,DSC}$), respectively.

* the transition curve from which this value is deduced did not fit to the van 't Hoff equation

Below the transition temperature, the integrated fluorescence intensity of all types of recombinant GLA studied decreases upon heating (Figure 4B). The decrease corresponds with

the expected thermal quenching. Within the domain of the thermal transition the fluorescence of wild type GLA shows a sigmoid increase, while the transition curve of the W60/118F mutant is characterized by an enhanced, sigmoid decrease. The effect of thermal transition on the fluorescence intensity of authentic and of wild type GLA is dominated by a strong reduction of the close contact between Trp60 and -118, respectively, and their putative quenchers. Also, the indirect quenching of Trp26 and -104 which is mediated by the former Trps decreases when the compact protein loses its native tertiary structure. In contrast, due to the absence of quenching effects in native W60/118F, the effect of the thermal transition on the fluorescence intensity of this mutant is dominated by the loss of apolar environment of Trp26 and -104 and, therefore, by an increase of contact quenching by the polar medium. The fractional changes within the transition region are presented in the inset of Figure 4B. The midpoints ($T_{mFl,int}$) are listed in Table 2.

4.4.4 DSC

The molar heat capacity of GLA and its mutants as a function of temperature is shown in Figure 5. After subtraction of the respective baselines, which take into account the progression of the denaturation process, the profiles of the excess heat capacity as a function of temperature result in symmetric Gauss curves with maxima at the respective transition midpoint temperatures, $T_{m,DSC}$ (Table 2). Due to their perfect symmetry the curves fit the van t' Hoff equation for a two-state transition. The related molar enthalpy (ΔH_{unf}) and entropy changes (ΔS_{unf}) are derived from the curves using software for data analysis provided by the manufacturer. The respective ΔH_{unf} and ΔS_{unf} values are collected in Table 3. Under the conditions of our experiments (Tris-HCl buffer of pH 7.5 at 25°C in the presence of 2 mM Ca^{2+}) the $T_{m,DSC}$ and ΔH_{unf} values of authentic and wild type GLA are 71.1 ± 0.1 °C and 351 ± 1 kJ.mol⁻¹, respectively. These values are clearly higher than the corresponding ones of bovine LA (BLA). Under identical conditions $T_{m,DSC}$ and ΔH_{unf} of BLA is 68.7 °C and 318 kJ.mol⁻¹, respectively (42, 43, 44). In previous work we already observed that at 25 °C the ΔH values for the unfolding of Ca^{2+} -bound GLA are larger than those of BLA: 216 kJ.mol⁻¹ and 196 kJ.mol⁻¹, respectively (45). Visibly, the higher enthalpy of unfolding of GLA compared to that of BLA is a stabilizing factor over the whole temperature range.

The substitution of Trp60 by Phe reduces ΔH_{unf} by about 20-30 $\text{kJ}\cdot\text{mol}^{-1}$ and shifts $T_{\text{m,DSC}}$ of GLA from 71.1 to 67.9 $^{\circ}\text{C}$; the influence of the Trp118 substitution on $T_{\text{m,DSC}}$ and on ΔH_{unf} is clearly smaller.

Table 3 : Thermodynamic parameters for thermal unfolding of authentic and of recombinant GLA in the presence of 2 mM Ca^{2+} and 10 mM Tris-HCl at pH 7.5.

	$T_{\text{m,DSC}}$ ($^{\circ}\text{C}$)	ΔH_{unf} ($\text{kJ}\cdot\text{mol}^{-1}$)	ΔS_{unf} ($\text{kJ}\cdot\text{mol}^{-1}\cdot\text{K}^{-1}$)
Authentic	71.0 ± 0.2	351.5 ± 1.7	1.021 ± 0.006
Wild type	71.1 ± 0.2	349.4 ± 0.9	1.015 ± 0.003
W118F	71.5 ± 0.2	344.4 ± 0.8	0.999 ± 0.003
W60F	67.9 ± 0.2	320.2 ± 0.6	0.939 ± 0.002
W60/118F	68.1 ± 0.2	324.0 ± 1.0	0.949 ± 0.004

The parameters are obtained by fitting the curves of the excess heat capacity (DSC) to the van 't Hoff equation for a two-state transition.

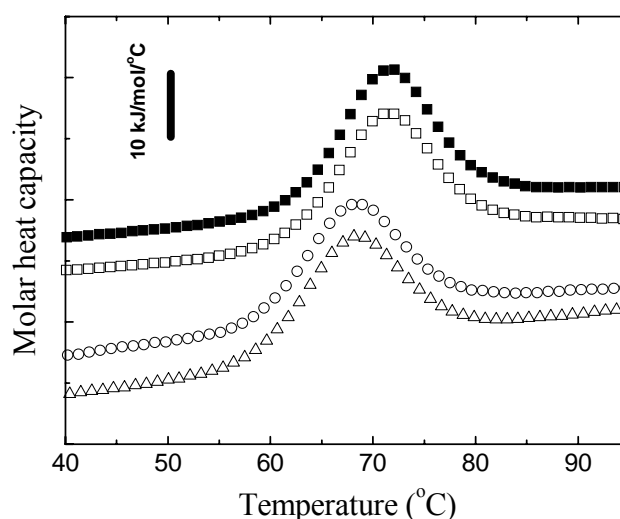


Figure 5: Molar heat capacity as a function of temperature for wild type GLA (■) and for the mutants W118F (□), W60F (○) and W60/118F (△) measured under the solvent conditions mentioned earlier.

4.4.5 Refolding and unfolding kinetics

Figure 6A shows the kinetic traces obtained in a refolding buffer without additional denaturant leading to a final concentration of 0.54 M GdnHCl. For each of the proteins, a substantial fluorescence intensity change (33-41%) occurs during the dead-time of the instrument (2 ms).

The observable part of the signal evolves according to a bi-exponential function with rate constants k_1 and k_2 (Table 4). In absolute terms the fluorescence intensity change during refolding is largest in the wild type sample, the fluorescence of which is largely quenched in the native state as has been concluded previously from the static fluorescence spectra (Figure 4). As can be derived from the different final intensity levels of the native protein (Figure 6A), the fluorescence intensity change during refolding is smaller in both single mutants and is the smallest in the double mutant.

For the wild type protein, the bi-exponential fit gives refolding rates of $k_1 = 20.8 \pm 0.5 \text{ s}^{-1}$ and $k_2 = 2.06 \pm 0.1 \text{ s}^{-1}$ with fractional amplitudes of 90.4% and 9.6% of the observed signal changes. The mutation of Trp118 leaves these parameters practically unchanged. Mutation of Trp 60, however, reduces k_1 to $11.9 \pm 0.5 \text{ s}^{-1}$ without significant change of k_2 and of the contributions of the respective amplitudes. The double mutant W60/118F conserves the k_1 value ($12.8 \pm 0.5 \text{ s}^{-1}$) of W60F but shows a modified distribution of the amplitudes. It must be remarked, however, that in this case, the calculated fractions refer to a much smaller total amplitude and, therefore, are less precise.

In panel B of Figure 6, the normalized fluorescence intensity is depicted for the unfolding process to a final concentration of 5.05 M GdnHCl. In general, when a protein unfolds, Trp residues become increasingly water accessible and the intensity of the fluorescence emission of the unfolded protein decreases due to a higher rate of internal conversion (46).

Table 4 : Refolding and unfolding parameters of GLA and its Trp mutants at pH 7.5, 2 mM CaCl₂ and 25°C

Mutant	A_1 (%)	k_1 (s ⁻¹)	A_2 (%)	k_2 (s ⁻¹)	k_{unf} (s ⁻¹)
Authentic	88.5	19.5	11.5	2.21	0.54
Wild type	90.4	20.8	9.6	2.06	0.68
W118F	89.3	21.7	10.7	2.86	1.23
W60F	86.7	11.9	13.3	2.01	0.65
W60/118F	80.5	12.8	19.5	2.05	1.33

The refolding parameters are obtained in 0.54 M GdnHCl. A_1 and A_2 represent the fractional amplitudes of the signal observed after dead time, k_1 and k_2 are the respective refolding rate constants. The unfolding rate constant k_{unf} is obtained in 5.05 M GdnHCl. The unfolding fits a mono-exponential decay. No burst-phase intermediate has been observed upon unfolding.

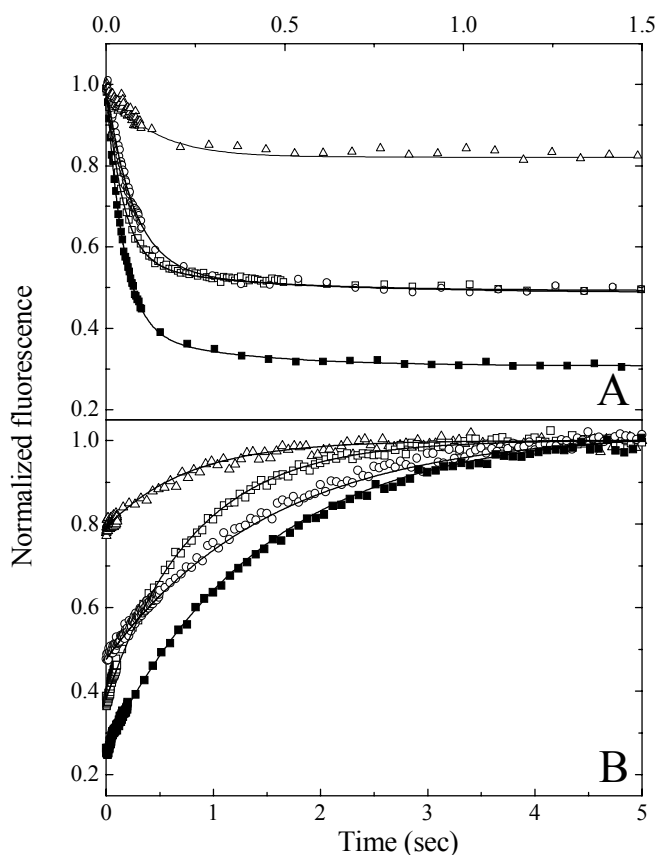


Figure 6: Time course of (A) kinetic refolding after dilution from 6 M to 0.54 M GdnHCl and of (B) kinetic unfolding after addition of GdnHCl to a final concentration of 5.05 M for wild type GLA (■) and for the mutants W118F (□), W60F (○) and W60/118F (△) monitored by stopped-flow fluorescence. The other environmental conditions are: pH 7.5, 25 °C and 2 mM CaCl₂. The continuous line represents a double (A) and a single (B) exponential fit through the experimental data. For each mutant the fluorescence values are relative to those of the unfolded state, the fluorescence of which has been set to unity.

This is not the case in GLA and its Trp mutants; the intensity observed in the unfolded state increases with respect to the intensity in the native state. This effect can be interpreted as resulting from the loss of internal quenching by surrounding His residues (His32, His68 and His107) and disulfide bridges (Cys6-Cys120, Cys28-Cys111, Cys61-Cys77 and Cys73-Cys91) upon unfolding of the protein (47). Interestingly, when Trp118 and Trp60 are mutated, the difference in fluorescence level between the native and unfolded state decreases. This means, that the remaining Trp residues (Trp26 and Trp104) are probably quenched by the neighbouring His residues (His32 and His107) as it has been reported that both residues are somewhat shielded from solvent at high pH (6.5 – 8) (14,48).

For all samples, the evolution towards the unfolded state, that is set to show the same final fluorescence intensity, can be described by a single exponential function (Table 4). Mutation of Trp 118 causes a nearly doubling of the speed of the unfolding process which is also observed in the double mutant, while the replacement of Trp 60 has practically no effect.

4.4.6 Chevron plots

The kinetics of folding and unfolding of authentic GLA has recently been studied extensively (56). In this work, the refolding and unfolding kinetics of wild type GLA and the different mutants were measured at various concentrations of GdnHCl. In all cases, the major rate constant k_1 shows a V-shaped dependence on GdnHCl concentration (Figure 7). The minimum of this chevron plot corresponds with the midpoint of transition upon chemical denaturation as it can be derived from equilibrium measurements. In this way, the c_m was determined to be 3.6 M GdnHCl for wild type GLA. The replacement of Trp118 does not significantly affect this value (Figure 7), indicating that the stability towards chemical denaturation of the protein has not been changed by this mutation. This observation is in accordance with our previous results on the thermal stability obtained by DSC (Figure 5). In W60F and in the double mutant (Table 5), on the other hand, the minimum shifts to 3.1 M, referring to a lower stability of these proteins. These observations correspond with the DSC results, where for both these mutants $T_{m,DSC}$ also shifts to a lower value.

The thermodynamic parameters can be calculated from the N→U transition curves resulting from the kinetic measurements that are depicted in Figure 8. These values are brought together in Table 5. The continuous lines in Figure 8 are the curves theoretically drawn with the parameters obtained from the fit. In all cases the m_{unf} -values determined from the kinetic data are very similar, indicating that the degree of solvent exposure of the native and denaturated states has not been significantly altered by the respective mutations.

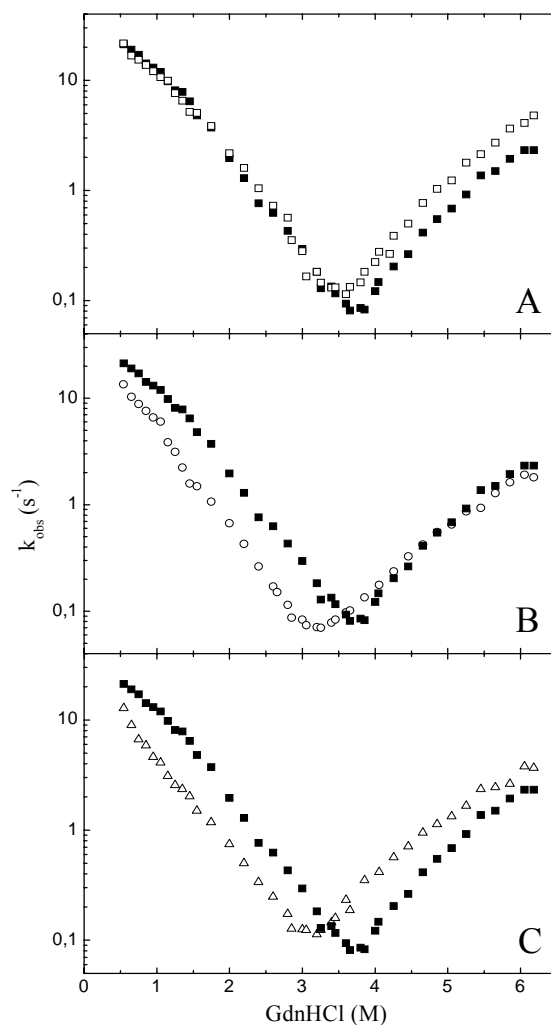


Figure 7: Observed rate constants of refolding (left branch) and unfolding (right branch) for wild type GLA (■) with respect to the mutant (A) W118F (□), (B) W60F (○) and (C) W60/118F (△) as a function of the denaturant concentration at pH 7.5, 25 °C and 2mM CaCl_2 .

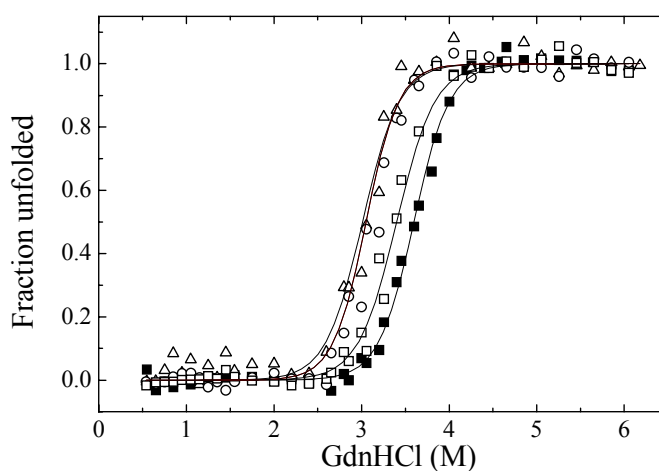


Figure 8: Unfolded fraction of wild type GLA (■) and of the mutants W118F (□), W60F (○) and W60/118F (△) as a function of the denaturant concentration at pH 7.5, 25 °C and 2mM CaCl_2 . The data are calculated from the final values of the fluorescence intensity measured during folding and unfolding. The solid lines represent fits based on a two state model.

Table 5 : Thermodynamic parameters for the GdnHCl-induced unfolding of wild type GLA and its mutants at 25°C, pH 7.5, in 10 mM Tris-HCl containing 2 mM CaCl₂

	c_m (mol.l ⁻¹)	$\Delta G_{\text{unf}}^{\text{H}_2\text{O}}$ (kJ·mol ⁻¹)	m_{unf} (kJ·mol ⁻¹ ·M ⁻¹)	$\Delta G_{\text{unf}}^{5.05\text{GdnHCl}}$ (kJ·mol ⁻¹)	$\Delta\Delta G_{\text{unf}}^{5.05\text{GdnHCl}}$ (kJ·mol ⁻¹)	ϕ^\ddagger
Wild type	3.6 ± 0.1	44.2 ± 2.5	12.2 ± 1.2	-17.6	-	-
W118F	3.5 ± 0.1	44.0 ± 2.0	12.6 ± 1.4	-19.8	2.2	0.07
W60F	3.1 ± 0.1	41.2 ± 1.6	13.1 ± 1.2	-25.1	7.5	0.94
W60/118F	3.0 ± 0.1	40.4 ± 1.3	13.2 ± 1.1	-26.4	8.8	0.97*

c_m is the midpoint concentration of the GdnHCl-induced unfolding, $\Delta G_{\text{unf}}^{\text{H}_2\text{O}}$ and $\Delta G_{\text{unf}}^{5.05\text{GdnHCl}}$ are free energies for unfolding in the absence of denaturant and in 5.05 M GdnHCl, respectively. $\Delta\Delta G_{\text{unf}}^{5.05\text{GdnHCl}}$ is the difference between the unfolding free energy of wild type and mutant GLA in 5.05 M GdnHCl. m_{unf} is the cooperativity index. The ϕ^\ddagger -values are calculated as described in Materials and Methods.

*this value has been calculated in relation to k_{unf} and to ΔG_{unf} of mutant W118F and thus is illustrative for the influence of the mutation of Trp60.

4.5 Discussion

In GLA we substituted Trp60 and -118, respectively, by Phe. Both Trps are located in flexible but different regions of the protein. As Trp residues are extremely sensitive reporters in near-UV CD and fluorescence spectroscopy, we expected that comparison of the characteristics derived from these spectra under equilibrium and kinetic conditions would supply information on local organization and stability within the LA molecule. In order to judge whether the changes induced by thermal or chemical denaturation are local or global, we also used techniques that are not directly Trp-related such as far-UV CD and DSC.

The substitution of Trp118 by Phe, which occurs in a flexible region of the α -helical domain, strongly inhibits the ability of LA to act as a lactose synthase modulator. This result perfectly agrees with observations of Grobler *et al.* (15) who found that mutation of residue 118 reduces the affinity for galactosyltransferase. The former substitution does not influence the far-UV CD spectrum (Figure 2A) indicating that the secondary structure of LA is not affected. Also, as can be derived from DSC, the thermodynamic characteristics (ΔH_{unf} and ΔS_{unf}) and the associated transition temperature ($T_{\text{m,DSC}}$) of GLA are hardly affected by this mutation (Table 3).

The β -domain of LA is known to represent another region of relatively poor stability and high flexibility (8). The substitution within that region of Trp60 by Phe has no measurable effect on the lactose synthase activation by GLA, indicating that at least the region that interacts with galactosyl transferase conserves its native conformation. As mentioned above, the latter region is located at the surface of the α -helical domain. A second indication that the α -helical domains of W60F and of W60/118F mainly conserve their native structure comes from the shape of the fluorescence spectrum (inset of Figure 3). The fact that neither the positions nor the shapes of these spectra differ, is a strong indication that the structure around Trp26 and -104 is conserved. These residues are located within the α -domain. Therefore, the differences between the far-UV CD spectrum of W60F and that of wild type GLA (Figures 2A and 2B) must be interpreted as mainly due to coupled oscillator interactions between Trp60 and the neighbouring Tyr103 and Trp104 (23,54).

The results from DSC scans indicate that substitution of Trp60 by Phe leads to a decrease of the global stability. Indeed, the transition temperature (Table 3) has decreased from about 71.1 °C for wild type GLA to 67.9 °C for W60F and to 68.1 °C for W60/118F. The loss of stability is interpreted as due to the weakened interactions in the aromatic cluster rather than to changes in the secondary structure. From the thermodynamic point of view, this decrease of $T_{m,DSC}$ is effectuated by a reduction of ΔH_{unf} and is not compensated by the associated reduction of ΔS_{unf} (Table 3).

The question remains to what degree the differences between T_m values derived from fluorescence measurements and from DSC are indicative for local versus global conformational changes. In answer to that question, we compared the transition temperature deduced from DSC ($T_{m,DSC}$) with that deduced from fluorescence wavelength shift ($T_{m,Fl \lambda}$) and fluorescence intensity ($T_{m,Fl int}$), respectively. As mentioned earlier, the thermal denaturation of each LA mutant results in a pronounced shift of its Trp emission maximum towards longer wavelengths (Figure 4A). Its evolution as a function of temperature can be easily derived. Each of the obtained transition curves (Figure 4A, inset) could be fitted to the van 't Hoff equation and the deduced ΔH -values (not shown) correspond with those of DSC. Therefore, the midpoints of these transition curves, referred to as $T_{m,Fl \lambda}$ in Table 2, are frequently used as reliable transition temperatures (57,58). The calculated temperature differences ($T_{m,Fl \lambda} - T_{m,DSC}$) amount to +0.1 °C for wild type GLA, +1.3 °C for W60F, +1.5 °C for W118F and +2.9 °C for the double mutant W60/118F (Table 2).

Seemingly, the differences could refer to a retarded exposure to solvent of the two remaining Trp residues, Trp26 and Trp104, at the core of the α -domain. However, the above conclusion assumes that additivity exists for the shift of the wavelength maximum, i.e. that the observed wavelength maximum equals the sum of the wavelength maximum for the fractions of protein in the native and that for protein in the unfolded state. This consideration obliged us to search for the possible causes of non-additive behavior and to examine other, more reliable reasons why $(T_{m,Fl \lambda} - T_{m,DSC})$ increases when Trp60 and Trp118 are mutated in GLA. The solution of the problem is given by the observation that the increase of the value $(T_{m,Fl \lambda} - T_{m,DSC})$ (Table 2) also follows the increase of the difference between the fluorescence intensity of the native and that of the unfolded state (Figure 4B). As has been stated by Eftink (46), the emission maximum of a mixture of overlapping fluorescence spectra will be weighted toward the dominantly emitting species. Therefore, by their larger fluorescence intensities in the native state than in the unfolded state, the mutants W60F and W118F have to unfold to a larger extent than wild type GLA in order to realize a shift of the wavelength maximum. For the same reason mutant W60/118F has to unfold to a larger extent than these single mutants. Thus, the value $(T_{m,Fl \lambda} - T_{m,DSC})$ for a Trp mutant of GLA is, at least partially, related with the difference between the fluorescence intensity of the native and the unfolded state.

In contrast to the wavelength shift, the global fluorescence intensity is the sum of all fractional contributions. Therefore, the value $(T_{m,Fl \text{ int}} - T_{m,DSC})$ may offer a better indication for the occurrence of local rearrangements upon thermal unfolding than $(T_{m,Fl \lambda} - T_{m,DSC})$. When looking at the change of the fluorescence intensity, only in the case of wild type GLA and of W60/118F a clear transition is observed (Figure 4B). For both these LAs, $T_{m,Fl \text{ int}}$ -values (Table 2) are obtained at the midpoints of the corresponding transition curves (Figure 4B, inset). Actually, only the $T_{m,Fl \text{ int}}$ of W60/118F could be determined with satisfactory confidence. Indeed, only for that mutant the transition curve could be fitted to the van 't Hoff equation and the deduced ΔH -value corresponds with that of DSC. The resulting $(T_{m,Fl \text{ int}} - T_{m,DSC})$ -value is nearly zero. As a consequence no intermediate state with locally rearranged Trp residues can be detected upon thermal unfolding. However, it is worth to remember that, above 70 °C, the unfolded LA keeps a nucleus containing of Trp26 and -104 that is partly protected from solvent as has been concluded from the incomplete fluorescence shift of W60/118F (Figure 4A).

The refolding and unfolding kinetics of wild type GLA and of the Trp mutants upon dilution with or addition of GdnHCl (Figures 6 and 7) as well as the associated equilibria between the

folded and the unfolded state (Figure 8) have been followed by measuring the evolution of the fluorescence intensity as a function of time. At 25°C, 2 mM Ca^{2+} and 0.54 M GdnHCl, the respective rate constants for the biphasic refolding reactions of mutant W118F and of wild type GLA are very similar (Table 4), while the unfolding reaction of the mutant in 5.05 M GdnHCl is nearly twice as fast (Table 4). This suggests that, at room temperature, the stability difference can be related to the increased unfolding rate of W118F. The difference in activation free energy between the wild type and the mutant, $\Delta\Delta G_{\text{unf}}^{\ddagger}$, is known to be given by the ratio of the unfolding rate constants as:

$$\Delta\Delta G_{\text{unf}}^{\ddagger} = RT \ln \left(\frac{k_{\text{unf}}^{\text{mut}}}{k_{\text{unf}}^{\text{wt}}} \right) \quad (6)$$

where $k_{\text{unf}}^{\text{mut}}$ and $k_{\text{unf}}^{\text{wt}}$ represent the unfolding rate constants for the mutant and wild type GLA, respectively. Since $k_{\text{unf}}^{\text{mut}}$ is nearly 2 times larger than $k_{\text{unf}}^{\text{wt}}$ at 5.05 M GdnHCl, $\Delta\Delta G_{\text{unf}}^{\ddagger}$ is estimated to be 1.8 kJ/mol, and this value is nearly identical with the $\Delta\Delta G_{\text{unf}}$ (2.2 kJ/mol) at the same concentration of denaturant (Table 5). Equivalent results are obtained with other GdnHCl concentrations. The fact that identical values are obtained for $\Delta\Delta G_{\text{unf}}^{\ddagger}$ and for $\Delta\Delta G_{\text{unf}}$ on substitution of Trp118 by Phe ($\phi^{\ddagger} = 0.07$), means that in the transition state the structure around the mutation site is identical with that in the denatured state, i.e. not organized (49-51). This result also indicates that the initiation site for refolding of GLA is not located in the region near Trp118. It is in agreement with previous studies on bovine LA in which it has been shown that the structure around the 6-120 disulfide bond, which is vicinal to Trp118, is not yet organized in the transition state of refolding (52).

In contrast with W118F, the $\Delta\Delta G_{\text{unf}}^{\ddagger}$ of the W60F variant is estimated to be 0 kJ/mol since its unfolding rate remains unchanged by the latter mutation (Table 4, Figure 7B) whereas $\Delta\Delta G_{\text{unf}}$ amounts to 7.5 kJ/mol (Table 5). The corresponding ϕ^{\ddagger} -value equals 0.94. This means that the structure around the mutation site is similarly organized in the native state and in the transition state. The findings strongly indicate that the interface between the α and β -domain is organized in the transition state (53).

Recently *Saeki et al.* (54) studied a large number of GLA mutants, including W60A, all of them carrying an N-terminal methionine. They followed the GdnHCl-induced unfolding of the recombinant proteins with equilibrium and stopped-flow CD techniques. The similarity of the $\Delta\Delta G_{\text{unf}}^{\ddagger}$ and $\Delta\Delta G_{\text{unf}}$ values for their mutant W60A indicates that the mutation site is not involved in the formation of an intermediately folded state. Their results furthermore demonstrate that the native structure around the Ca^{2+} -binding site of mutant D87N is fully formed in the transition state and that the mutation sites of I55V, I89V, V90A and I95V are partly organized. The latter mutations are located in the interface between the H3-helix and the β -domain. Trp60 is similarly located in the β -domain and keeps contact with the H3-helix (3). According to *Saeki et al.* (54) the mutation site of their protein, W60A, is not organized in the transition state, whereas in our mutant, W60F, the similar region has native-like structure. A possible reason for this striking difference in unfolding behavior of these two mutants could reside in the difference in steric properties and hydrophobic character of Phe and Ala. Indeed, Trp60 is part of the aromatic cluster II (3,15) and the propensity to form hydrophobic clusters has been designated as being important for the initial collapse upon protein folding and for the retention of an intermediately folded structure upon unfolding (55). Obviously, in contrast to Phe, the hydrophobic character of Ala in W60A is not strong enough to take over the role of Trp during the unfolding process. The marked difference of $\Delta\Delta G_{\text{unf}}^{\ddagger} / \Delta\Delta G_{\text{unf}}$ between W60F and W60A indicates that the nature of the involved amino acids strongly determines the extent and the tightness of packing of the intermediately formed folding nuclei. This result demonstrates that the role of these amino acids is not limited to the final docking processes resulting in the native state, but also involves the earlier phases of folding.

4.6 Conclusion

In GLA, which contains four Trps, the mutation of Trp60 and/or Trp118 by Phe has allowed us to observe that these Trp residues are both quenched in native GLA. Moreover, both residues equally contribute to the quenching of Trp26 and Trp104, which behave as a resonance couple. In our search to discriminate between global and local rearrangements upon thermal denaturation we demonstrated that the differences between the mutants, which were obtained from measurements of the value $(T_{\text{m,Fl}} - T_{\text{m,DSC}})$, are related to differences in quenching and,

therefore, to the different fluorescence intensities of the Trp residues. The fact that equal values were obtained for $T_{m,Fl\ int}$ and $T_{m,DSC}$ of the W60/118F mutant, allowed us to conclude that no local folding events occurred upon thermally induced unfolding of this Ca^{2+} -bound mutant. In addition, this mutant allowed us to observe that unfolded GLA, above 70°C, conserves a nucleus consisting of Trp26/104 that is partly protected from solvent.

In contrast, stopped-flow fluorescence measurements of chemically induced folding/unfolding reactions of these mutants have shown the direct behaviour of the intermediate environments of Trp60 and -118. Short range rearrangements are indeed deduced by ϕ^\ddagger -value analysis, i.e. by comparing the apparent free energy changes needed to reach the kinetic transition and the unfolded state, respectively. Specifically, our findings indicate that in the kinetic transition state the mutation site of W118F loses its native conformation while the mutation site of W60F is conserved.

4.7 Acknowledgment

We thank Wim Noppe, Linda Desender, Christiane Duportail and Nicole Holvoet for their help with construction, expression and purification of mutant α -lactalbumins. We are grateful to Bart Devreese and Kris De Vriendt of the laboratory for Protein Biochemistry and Protein Engineering of the University of Ghent, for molecular mass determinations. This work was supported by grant G-0180-03 from the Flemish Fund for Scientific Research and by grant OTKA T 037719 from the Hungarian Scientific Research Foundation.

4.8 References

1. Hill, R.L. and Brew K. (1975) Lactose synthetase. *Adv. Enzymol.* 43, 411-490.
2. Bell, J.E., Beyer, T.A. and Hill R.L. (1976) Kinetic mechanism of bovine milk galactosyltransferase - role of alpha-lactalbumin. *J. Biol. Chem.* 251, 3003-3013.
3. Acharya, K.R., Stuart, D.I., Walker, N.P.C., Lewis, M. and Phillips, D.C. (1989) Refined structure of baboon alpha-lactalbumin at 1.7-Å resolution - comparison with c-type lysozyme. *J. Mol. Biol.*

- 208, 99-127.
4. Kronman, M.J., Sinha, S.K. and Brew, K. (1981) Characteristics of the binding of Ca^{2+} and other divalent metal-ions to bovine alpha-lactalbumin. *J. Biol. Chem.* 256, 8582-8587.
 5. Chrysina, E.D., Brew, K., and Acharya, K.R. (2000) Crystal structures of apo- and holo-bovine alpha-lactalbumin at 2.2-Å resolution reveal an effect of calcium on inter-lobe interactions. *J. Biol. Chem.* 275, 37021-37029.
 6. Kronman, M.J. (1989) Metal-ion binding and the molecular conformational properties of alpha-lactalbumin. *Crit. Rev. Biochem. Mol. Biol.* 24, 565-667.
 7. Kuwajima, K. (1996) The molten globule state of alpha-lactalbumin. *FASEB J.* 10, 102-109.
 8. Wu, L.C., Schulman, B.A., Peng, Z.Y., and Kim, P.S. (1996) Disulfide determinants of calcium-induced packing in alpha-lactalbumin. *Biochemistry* 35, 859-863.
 9. Kuwajima, K. (1989) The molten globule state as a clue for understanding the folding and cooperativity of globular-protein structure. *Proteins* 6, 87-103.
 10. Arai, M. and Kuwajima, K. (2000) Role of the molten globule state in protein folding. *Adv. Prot. Chem.* 53, 209-282.
 11. Lala, A.K. and Kaul, P. (1992) Increased exposure of hydrophobic surface in molten globule state of alpha-lactalbumin - fluorescence and hydrophobic photolabeling studies. *J. Biol. Chem.* 267, 19914-19918.
 12. Gussakovsky, E.E. and Haas, E. (1995) 2 steps in the transition between the native and acid states of bovine alpha-lactalbumin detected by circular polarization of luminescence - evidence for a premolten globule state. *Protein Sci.* 4, 2319-2326.
 13. Svensson, M., Sabharwal, H., Hakansson, A., Mossberg, A.K., Lipniunas, P., Leffler, H., Svanborg, C. and Linse, S. (1999) Molecular characterization of alpha-lactalbumin folding variants that induce apoptosis in tumor cells. *J. Biol Chem.* 274, 6388-6396.
 14. Pike, A.C.W., Brew, K. and Acharya, K.R. (1996) Crystal structures of guinea-pig, goat and bovine alpha-lactalbumin highlight the enhanced conformational flexibility of regions that are significant for its action in lactose synthase. *Structure* 4, 691-703.
 15. Grobler, J.A., Wang, M., Pike, A.C.W. and Brew, K. (1994) Study by mutagenesis of the roles of 2 aromatic clusters of alpha-lactalbumin in aspects of its action in the lactose synthase system. *J. Biol. Chem.* 269, 5106-5114.
 16. Joniau, M., Pardon, E., Maisonneuve, J.F., Haezebrouck, P., Desmet, J., Van Dael, H. and De Baetselier, A. (1996) Site directed mutants of bovine alpha-lactalbumin with reduced capacity to activate lactose synthesis. *In: Perspectives on Protein Engineering* (CD ROM, ISBN 0-9529015-0-1). Geisow, MJ, Editor. Biodigm, UK.
 17. Malinovskii, V.A., Tian, J., Grobler, J.A. and Brew, K. (1996) Functional site in alpha-lactalbumin encompasses a region corresponding to a subsite in lysozyme and parts of two adjacent flexible substructures. *Biochemistry* 35, 9710-9715.

18. Greene, L.H., Grobler, J.A., Malinovskii, V.A., Tian, J., Acharya, K.R. and Brew, K. (1999) Stability, activity and flexibility in alpha-lactalbumin. *Protein Eng.* 12, 581-587.
19. Ramakrishnan, B. and Qasba, P.K. (2001) Crystal structure of lactose synthase reveals a large conformational change in its catalytic component, the beta 1,4-galactosyltransferase-I. *J. Mol. Biol.* 310, 205-218.
20. Ramakrishnan, B., Shah, P.S. and Qasba, P.K. (2001) alpha-Lactalbumin (LA) stimulates milk beta-1,4-galactosyltransferase I (beta 4GAL-T1) to transfer glucose from UDP-glucose to N-acetylglucosamine - crystal structure of beta 4GAL-T1-LA complex with UDP-Glc. *J. Biol. Chem.* 276, 37665-37671.
21. Clark, P.L., Liu, Z.P., Zhang, J.H. and Gierasch, L.M. (1996) Intrinsic tryptophans of crabpi as probes of structure and folding. *Protein Sci.* 5, 1108-1117.
22. Wang, W.Q., Xu, Q., Shan, Y.F. and Xu, G.J. (2001) Probing local conformational changes during equilibrium unfolding of firefly luciferase: fluorescence and circular dichroism studies of single tryptophan mutants. *Biochem. Biophys. Res. Commun.* 282, 28-33.
23. Chakraborty, S., Ittah, V., Bai, P., Luo L., Haas, E. and Peng, Z.Y. (2001) Structure and dynamics of the alpha-lactalbumin molten globule: fluorescence studies using proteins containing a single tryptophan residue. *Biochemistry* 40, 7228-7238.
24. Chaudhuri, T.K., Horii, K., Yoda, T., Arai, M., Nagata, S., Terada, T.P., Uchiyama, H., Ikura, T., Tsumoto, K., Kataoka, H., Matushima, M., Kuwajima, K. and Kumagai, I. (1999) Effect of the extra N-terminal methionine residue on the stability and folding of recombinant alpha-lactalbumin expressed in *Escherichia coli*. *J. Mol. Biol.* 285, 1179-1194.
25. Chaudhuri, T.K., Arai, M., Terada, T.P., Ikura, T. and Kuwajima, K. (2000) Equilibrium and kinetic studies on folding of the authentic and recombinant forms of human alpha-lactalbumin by circular dichroism spectroscopy. *Biochemistry* 39, 15643-15651.
26. Ishikawa, N., Chiba, T., Chen, L.T., Shimizu, A., Ikeguchi, M. and Sugai, S. (1998) Remarkable destabilization of recombinant alpha-lactalbumin by an extraneous N-terminal methionyl residue. *Protein Eng.* 11, 333-335.
27. Noppe, W., Haezebrouck, P., Hanssens, I. and De Cuyper, M. (1998) A simplified purification procedure of alpha-lactalbumin from milk using Ca^{2+} -dependent adsorption in hydrophobic expanded bed chromatography. *Bioseparation* 8, 153-158.
28. Viaene, A., Volckaert, G., Joniau, M., Debaetselier, A. and Vancauwelaert, F. (1991) Efficient expression of bovine alpha-lactalbumin in *Saccharomyces cerevisiae*. *Eur. J. Biochem.* 202, 471-477.
29. Pardon, E., Haezebrouck, P., Debaetselier, A., Hooke, S.D., Fancourt, K.T., Desmet, J., Dobson, C.M., Van Dael, H. and Joniau, M. (1995) A Ca^{2+} -binding chimera of human lysozyme and bovine alpha-lactalbumin that can form a molten globule. *J. Biol. Chem.* 270, 10514-10524.
30. Hinnen, A., Hicks, J.B. and Fink, G.R. (1978) Transformation of yeast. *Proc. Natl. Acad. Sci. USA*

- 75, 1929-1933.
31. Laroche, Y., Storme, V., Demeutter, J., Messens, J. and Lauwereys, M. (1994) High-level secretion and very efficient isotopic labeling of tick anticoagulant peptide (TAP) expressed in the methylotrophic yeast, *Pichia pastoris*. *Bio-Technology* 12, 1119-1124.
 32. Saito, A., Usui, M., Song, Y., Azakami, H., and Kato, A. (2002) Secretion of glycosylated alpha-lactalbumin in yeast *Pichia pastoris*. *J. Biol. Chem.* 132, 77-82.
 33. Gill, S.C. and von Hippel, P.H. (1989) Calculation of protein extinction coefficients from amino-acid sequence data. *Anal. Biochem.* 182, 319-26.
 34. Pace, C.N. (1986) Determination of urea and guanidine hydrochloride denaturation curves. *Meth. Enzymol.* 4, 2411-2423.
 35. Brew, K., Vanaman, T.C. and Hill, R.L. The role of alpha-lactalbumin and the A protein in lactose synthetase: a unique mechanism for the control of a biological reaction. *Proc. Natl. Acad. Sci. USA* 59, 491-497.
 36. Venyaminov, S.Y. and Yang, J.Y. (1996) Determination of protein secondary structure. *In: Circular dichroism and the conformational analysis of biomolecules*. Fasman GD, editor. Plenum Press, New York. 69-107.
 37. Woody, R.W. and Dunker, A.K. (1996) Aromatic and cystine side-chain circular dichroism in proteins. *In: Circular dichroism and the conformational analysis of biomolecules*. Fasman GD, editor. Plenum Press, New York. 109-157.
 38. Peng, Z.Y. and Kim, P.S. (1994) A Protein dissection study of a molten globule. *Biochemistry* 33, 2136-41.
 39. Wu L.C., Peng Z.Y. and Kim, P.S. (1995) Bipartite structure of the alpha-lactalbumin molten globule. *Nat. Struct. Biol.* 2, 281-286.
 40. Böhm, G., Muhr, R. and Jaenicke, R. (1992) Quantitative-analysis of protein far-UV Circular-Dichroism spectra by neural networks. *Protein Eng.* 5, 191-195.
 41. Sommers, P.B. and Kronman, M.J. (1980) Intermolecular and intramolecular interactions of alpha-lactalbumin - comparative fluorescence properties of bovine, goat, human and guinea-pig alpha-lactalbumin - characterization of the environments of individual tryptophan residues in partially folded conformers. *Biophys. Chem.* 11, 217-232.
 42. Hendrix, T.M., Griko, Y.V. and Privalov, P.L. (1996) Energetics of structural domains in alpha-lactalbumin. *Protein Sci.* 5, 923-931.
 43. Vanderheeren, G., Hanssens, I., Meijberg, W. and Van Aerschot, A. (1996) Thermodynamic characterization of the partially unfolded state of Ca²⁺-loaded bovine alpha-lactalbumin: evidence that partial unfolding can precede Ca²⁺ release. *Biochemistry* 35, 16753-16759.
 44. Hendrix, T., Griko, Y.V. and Privalov, P.L. (2000) A calorimetric study of the influence of calcium on the stability of bovine alpha-lactalbumin. *Biophys. Chem.* 84, 27-34.
 45. Vanhooren, A., Vanhee, K., Noyelle, K., Majer, Z., Joniau, M. and Hanssens, I. (2002) Structural

- basis for difference in heat capacity increments for Ca^{2+} binding to two α -lactalbumins. *Biophys. J.* 82, 407-417.
46. Eftink, M.R. (2000) Use of fluorescence spectroscopy as thermodynamics tool. *Methods Enzymol.* 323, 459-473.
 47. Vanhooren, A., Devreese, B., Vanhee, K., Van Beeumen, J. and Hanssens, I. (2002) Photoexcitation of tryptophan groups induces reduction of two disulfide bonds in goat α -lactalbumin. *Biochemistry* 41, 11035-11043.
 48. Harata, K. and Muraki, M. (1992) X-ray structural evidence for a local helix-loop transition in α -lactalbumin. *J. Biol. Chem.* 267, 1419-1421.
 49. Kuwajima, K., Mitani, M. and Sugai, S. (1989) Characterization of the critical state in protein folding - effects of guanidine-hydrochloride and specific Ca^{2+} binding on the folding kinetics of α -lactalbumin. *J. Mol. Biol.* 206, 547-5461.
 50. Matouschek, A., Kellis, J.T., Serrano, L. and Fersht, A.R. (1989) Mapping the transition-state and pathway of protein folding by protein engineering. *Nature* 340, 122-126.
 51. Serrano, L., Matouschek, A. and Fersht, A.R. (1992) The folding of an enzyme .3. Structure of the transition-state for unfolding of barnase analyzed by a protein engineering procedure. *J. Mol. Biol.* 224, 805-818.
 52. Ikeguchi, M., Fujino, M., Kato, M., Kuwajima, K. and Sugai, S. (1998) Transition state in the folding of α -lactalbumin probed by the 6-120 disulfide bond. *Protein Sci.* 7, 1564-1574.
 53. Schulman, B.A., Redfield, C., Peng, Z.Y., Dobson, C.M. and Kim, P.S. (1995) Different subdomains are most protected from hydrogen-exchange in the molten globule and native states of human α -lactalbumin. *J. Mol. Biol.* 253, 651-657.
 54. Saeki, K., Arai, M., Yoda, T., Nakao, M. and Kuwajima, K. (2004) Localized nature of the transition-state structure in goat α -lactalbumin folding. *J. Mol. Biol.* 341, 589-604.
 55. Demarest, S.J., Boice, J.A., Fairman, R. and Raleigh, D.P. (1999) Defining the core structure of the α -lactalbumin molten globule state. *J. Mol. Biol.* 294, 213-221.
 56. Chedad, A. and Van Dael, H. (2004) Kinetics of the folding and unfolding of goat α -lactalbumin. *Proteins* 57, 345-356.
 57. Veprintsev, D.B., Permyakov, S.E., Permyakov, E.A., Rogov, V.V., Cawild typehern, K.M. and Berliner, L.J. (1997) Cooperative thermal transitions of bovine and human apo- α -lactalbumins: evidence for a new intermediate state. *FEBS Lett.* 412, 625-628.
 58. Markovic-Housley, Z., Stolz, B., Lanz, R. and Erni, B. (1999) Effect of tryptophan to phenylalanine substitutions on the structure, stability and enzyme activity of the IIAB subunit of the mannose transporter of *Escherichia coli*. *Protein Sci.* 8, 1530-1535.

4.9 Addendum

4.9.1 Introduction

In order to test the contribution of all Trp residues to the fluorescence of GLA, we also replaced Trp26 and 104 by Phe (Fig 1, Chapter 3). Both Trp 26 and 104, together with Phe53, Trp60 and Tyr103, belong to aromatic cluster II in the α -helical domain of GLA. Trp26 belongs to one of the major α -helices (Helix 2: 23-34) while Trp104 -conserved in all known LA's- is positioned in a loop between Helix 3 (residues 86-98) and the flexible loop/helix region (residues 105-111) (1-3).

Mutants W26F and W104F were expressed in *Pichia pastoris* and the mutants were studied with emission fluorescence, CD spectroscopy, differential scanning and lactose synthesis assay as described in Vanhooren et al. (4).

4.9.2 Results and discussion

Characterization of GLA mutants

The level of expression for W26F and W104F, measured with RIA, was in the range of 6 mg.l⁻¹. About 40 % of the protein was glycosylated. The non-glycosylated protein was further purified and characterized with SDS-PAGE and mass spectrometry. When W26F was used as an activator of lactose synthesis, equal rates as authentic GLA were observed. Only 30% of this rate is obtained when W104F was used as an activator. The result of W104F is not unexpected because Grobler et al. (5) found that the substitution of Trp104 by tyrosine in bovine LA also causes a reduction of the activity. On the basis of an energy minimization study, these authors suggest that the reduced activity of W104Y results from a localized conformational change rather than Trp104 being part of the functional site. However, when Trp is replaced by phenylalanine, the changes in the CD spectra are not more pronounced than the changes caused by the substitution of Trp60 or Trp118.

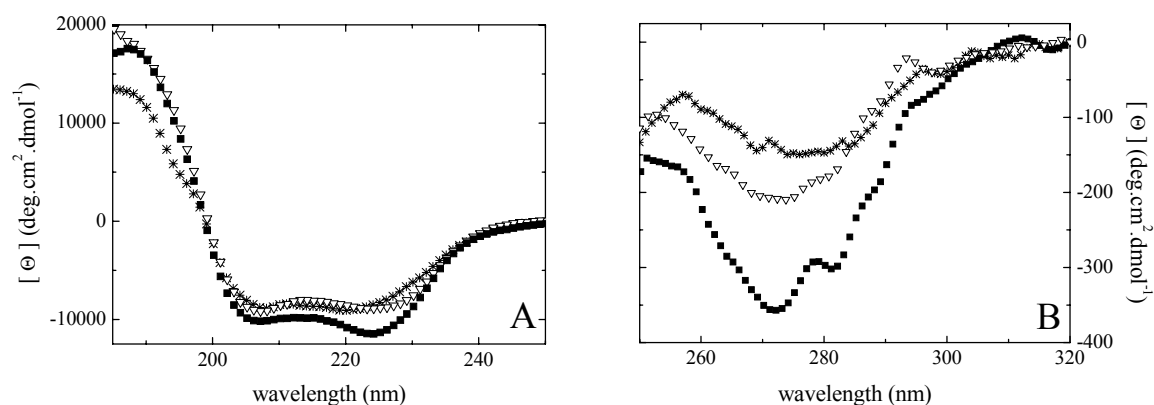


Figure 1: (A) Far- and (B) near-UV CD spectra of wild type GLA (■) and of the mutants W26F (▽) and W104F (✱) measured in 10 mM Tris-HCl, 2 mM CaCl₂, at pH 7.5 and 25°C.

Figure 1 shows the far- and near-UV CD spectra of wild type GLA and the two mutants W26F and W104F. The two mutants have a pronounced far-UV CD spectrum of similar magnitude to wild type GLA, referring to the same secondary structure (Fig 1A). The spectra of both mutants differ slightly from that of wild type GLA in the region 220-230 nm as in that wavelength region aromatic side chains contribute to the global spectrum (6). The depth of the shoulder around 230 nm diminishes when Trp26 and Trp104 are mutated for Phe. Additionally for Trp104 the ellipticity minimum shifts from 224 to 220 nm.

The most remarkable feature in the near-UV CD spectrum of all lactalbumins is the deep trough near 270 nm. Its amplitude, being the largest for wild type GLA with four Trp residues, diminishes whenever a Trp residue is mutated (4,7). The strongest reduction is observed in W104F, a smaller one in W26F.

Fluorescence and DSC data

The fluorescence spectra of the two mutant proteins under native conditions at 20 °C are presented in Fig. 2. Mutant W104F fluoresces more strongly than wild type GLA, whereas the integrated fluorescence yield from W26F is almost identical as wild type GLA. The emission maximum for W104F is similar to that of wild type whereas the λ_{\max} value for W26F is red-shifted with respect to that of wild type and W104F.

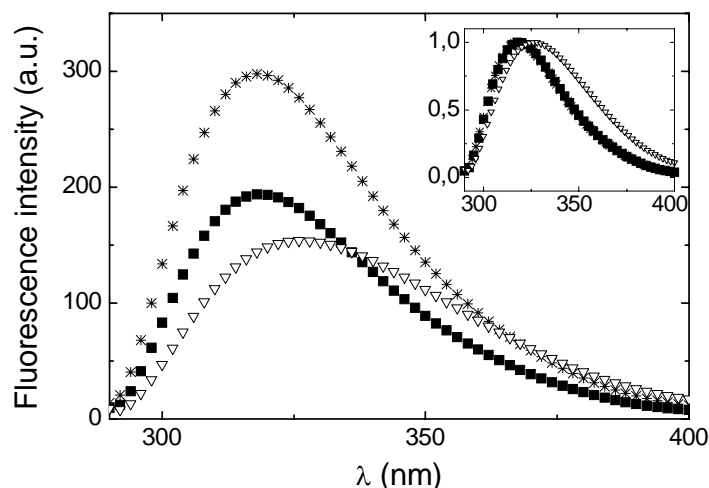


Figure 2: Relative fluorescence intensity of wild type GLA (■) and of the mutants W26F (▽) and W104F (✱) measured in 10 mM Tris-HCl, 2 mM CaCl₂, at pH 7.5 and 25°C. The excitation is at 280 nm and for each protein A_{280} equals 0.15, due to Trp absorption only as explained in Vanhooren et al. (4). The inset shows the normalized fluorescence spectra of the different proteins.

Previously in this Chapter (4), we found evidence that the fluorescence in GLA mainly results from Trp26 and from Trp104 which behave as a resonance couple and are partly quenched by Trp60 and Trp118. The fluorescence of this buried couple is at the short wavelength side of the emission spectrum and exhibits a maximum near 320 nm. The differences between the present fluorescence spectra of W104F and of W26F indicate that the individual Trp residues, Trp26 and Trp104, do not equally contribute to the fluorescence yield of wild type GLA. Mutant W104F containing the Trp residues 60, 118 and 26 fluoresces more intensily than mutant W26F containing the Trp residues 60, 118 and 104 indicating that Trp 104 is quenched more than Trp 26. As the resonance couple Trp26-Trp104 is quenched equally by Trp60 and by Trp118 (4) the result indicates that Trp104 is more intensily quenched in a direct way than Trp26 is. According to Chakraborty et al. (7) two residues, Asp102 and Tyr103, may serve as potential quenchers for Trp104. Furthermore, the red shift of W26F may suggest that this Trp 26 dominates the fluorescence spectrum and is responsible for the emission maximum near 320 nm of native GLA. This may be due to its apolar environment as well as to its high fluorescence yield. Possibly the red shift may be induced by a slight rearrangement of part of the α -domain hydrophobic core. Indeed, in HLA where Trp26 is replaced by a leucine, the side-chain packing is subtly changed and the hydrophobic core is less tightly packed (8).

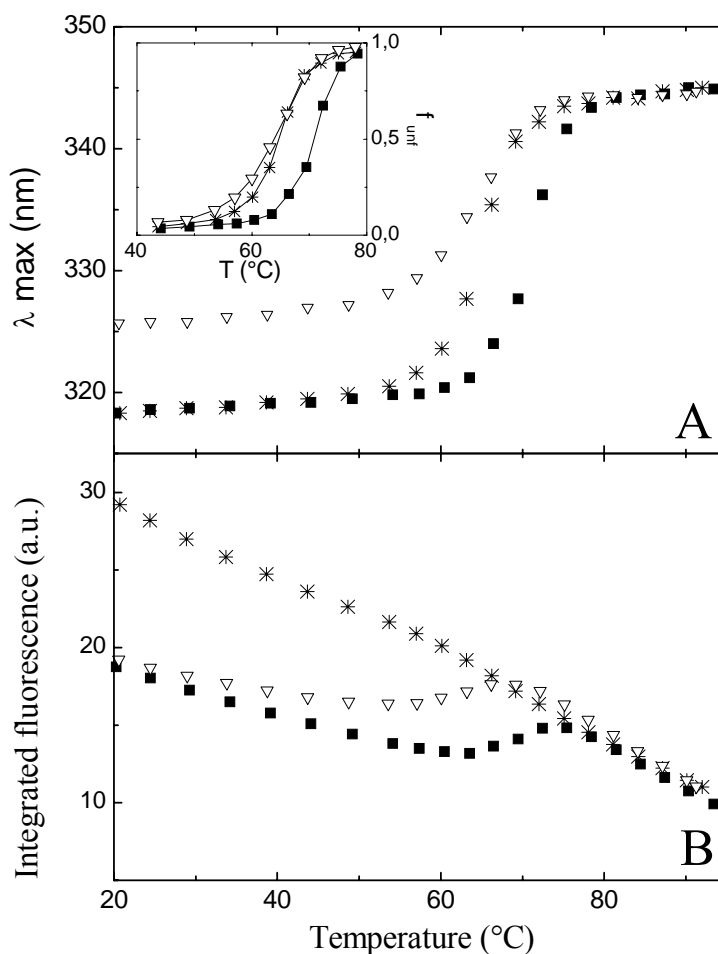


Figure 3: (A) λ_{\max} and (B) integrated fluorescence intensity as a function of temperature for wild type GLA (■) and for the mutants W26F (▽) and W104F (*) measured under the solvent conditions mentioned in Fig. 2. The inset of (A) shows in detail the fractional shift of the fluorescence ($f_{fl,\lambda}$) deduced from the change of λ_{\max} .

Figure 3 shows the wavelength of the emission maximum (A) and the integrated fluorescence intensity (B) as a function of temperature for wild type GLA, W26F and W104F. The transition temperature derived from the fractional wavelength shift (inset of Fig. 3A) clearly shows that the mutants W26F and W104F are less stable than wild type GLA and unfold at an about 6 °C lower temperature than wild type GLA does. In agreement with this, the transition temperature derived from DSC scans (Fig. 4) has decreased from about 71,7 °C for wild type GLA to 65,8 °C for W26F and 63.9 °C for W104F. These results indicate that the removal of Trp 26 or Trp104 leads to a decrease of global stability.

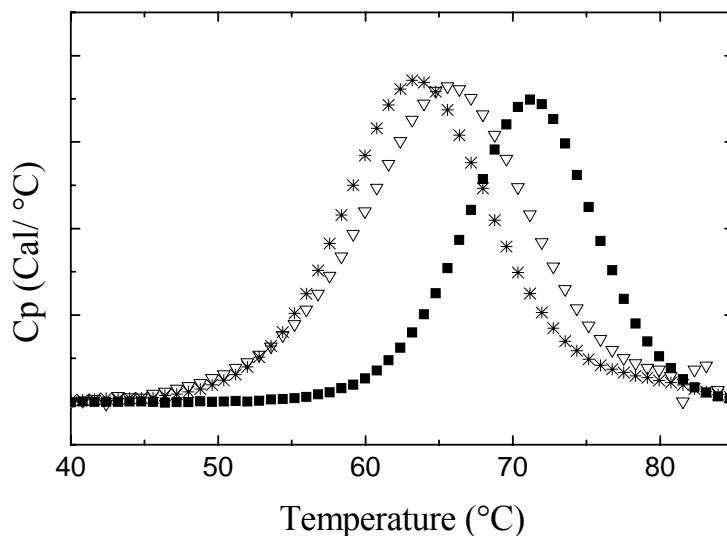


Figure 4: Heat capacity as a function of temperature for wild type GLA (■) and for the mutants W26F (▽), W104F (✱) measured under the solvent conditions mentioned earlier. For all recombinant proteins the concentration was approximately 40 μ M.

4.9.3 Conclusion

Comparison of the fluorescence spectra of wild type, W60F, W118F and W60/118F has demonstrated that Trp26 and Trp104 behave as a resonance couple of which the fluorescence is partly quenched by resonance energy transfer mediated by Trp60 and Trp118. Furthermore, the spectra of W26F and W104F evidence that Trp26 and Trp104 do not equally contribute to the fluorescence yield of wild type GLA. Especially Trp104 is clearly quenched by an additional residue other than tryptophan.

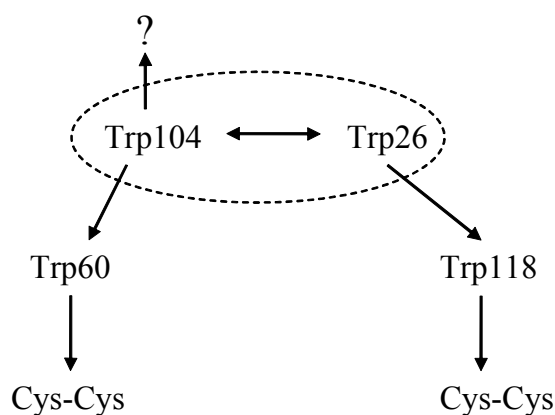


Figure 5: Schematic drawing of the quenching of Trp residues within LA represented by arrows (see text for details). A nucleus which is conserved at high temperatures during unfolding is indicated by dashed lines.

Earlier in this chapter we demonstrated that the effect of the W118F substitution on the conformation and global stability of the mutant is negligible. Substitution of Trp60, 26 or 104 by a Phe decreases the transition temperature from 71.0 °C to respectively 67.9, 65.8 and 63.9 °C. While Trp118 is part of aromatic cluster I, the three other Trp residues belong to aromatic cluster II, located in the core of the protein. The conservation of this core is important. The high impact of Trp104 and Trp26 on the hydrophobic core is demonstrated by the shift of the T_m -values upon substitution of these latter residues. We also observed that in unfolded W60/118F the aromatic nucleus with Trp26 and Trp104 is partly protected from solvent. The impact of these latter Trp residues is also indicated by slight conformational changes which are expressed by a shift of the emission maximum in native W26F and by a decrease in lactose synthase activity and far-UV CD changes in W104F.

4.9.4 References

1. Acharya, K.R., Stuart, D.I., Walker, N.P.C., Lewis, M. and Phillips, D.C. (1989) Refined structure of baboon alpha-lactalbumin at 1.7-Å resolution - Comparison with c-type lysozyme. *J. Mol. Biol.* 208, 99-127.
2. Chrysina, E.D., Brew, K. and Acharya, K.R. (2000) Crystal structures of apo- and holo-bovine alpha-lactalbumin at 2.2-Å resolution reveal an effect of calcium on inter-lobe interactions. *J. Biol. Chem.* 275, 37021-37029.
3. Koga, K. and Berliner, L.J. (1985) Structural elucidation of a hydrophobic box in bovine alpha-lactalbumin by NMR - nuclear Overhauser effects. *Biochemistry* 24, 7257-7262.
4. Vanhooren, A., Chedad, A., Farkas, V., Majer, Z., Van Dael, H., Joniau, M. and Hanssens, I. (2005) Tryptophan to phenylalanine substitution allows to differentiate between short and long range conformational changes during denaturation of goat alpha-lactalbumin. *Proteins* 60, 118-130.
5. Grobler, J.A., Wang, M., Pike, A.C.W. and Brew, K. (1994) Study by mutagenesis of the roles of 2 aromatic clusters of alpha-lactalbumin in aspects of its action in the lactose synthase system. *J. Biol. Chem.* 269, 5106-5114.
6. Woody R.W. and Dunker A.K. (1996) Aromatic and cystine side chain circular dichroism in proteins. In: *Circular dichroism and the conformational analysis of biomolecules*. Plenum Press, New York. 109-157.

7. Chakraborty, S., Ittah, V., Bai, P., Luo, L., Haas, E. and Peng, Z.Y. (2001) Structure and dynamics of the alpha-lactalbumin molten globule: fluorescence studies using proteins containing a single tryptophan residue. *Biochemistry* 40, 7228-7238.
8. Pike, A.C.W., Brew, K. and Acharya, K.R. (1996) Crystal structures of guinea-pig, goat and bovine alpha-lactalbumin highlight the enhanced conformational flexibility of regions that are significant for its action in lactose synthase. *Structure* 4, 691-703.

Selectivity of tryptophan residues in mediating photolytic cleavage of disulfide bridges in goat α -lactalbumin

A. Vanhooren, K. De Vriendt¹, A. Chedad, H. Van Dael, B. Devreese¹ and I. Hanssens

Interdisciplinary Research Center, Katholieke Universiteit Leuven Campus Kortrijk, Kortrijk, Belgium

¹Laboratory for Protein Biochemistry and Protein Engineering, University of Ghent, Belgium

5.1 Abstract

GLA comprises four Trp residues and four disulfide bonds. As discussed in Chapter 3, upon illumination of GLA with near-UV light, we observed cleavage of the disulfide bridges (Cys6-Cys120 and Cys73-Cys91). The photo-reduction of a disulfide bridge results in the formation of one free cysteine, suggesting that a large number of the intermediately formed thiyl radicals are involved in the creation of new bonds. In the tryptic digest of irradiated GLA we also observed a fragment of 1553 Da which, on the basis of the available MS data, has been interpreted as being composed of a dipeptide in which the disulfide bridge Cys73-Cys91 was conserved and in which a thioether linkage was formed between Cys73 and Trp60. Upon illumination of human LA Permyakov et al. (8) also observed the cleavage of Cys73-Cys91. Remarkably these authors also report the rupture of Cys61-Cys77 while the Cys6-Cys120 in HLA remains intact.

The first goal of this study is to obtain more information about the small number of free thiols formed in each disrupted disulfide bond, the possible thioether linkage and the discrepancies between the results of goat and human LA. For this cause, illuminated wild type GLA was carbamidomethylated, fragmented with trypsin and extensively analyze by two new mass spectrometric devices, MALDI-TOF-TOF-MS and a chip-based nano-ESI device. Peptide fragments containing Cys120Cam, Cys61Cam and Cys91Cam are detected as well as two dipeptides containing a new Cys-Lys crosslink. In one dipeptide Cys6 is crosslinked with Lys122. The exact nature of the crosslink (either Cys91-Lys79 or Cys73-Lys93) in the second dipeptide could not be defined. The results refer to photolytic cleavage of Cys6-Cys120, Cys61-Cys77 and Cys73-Cys91. While the cleavage of Cys6-Cys120 and of Cys73-Cys91 was found in our earlier work, the cleavage of Cys61-Cys77 was not detected previously in GLA. In contrast to the other disulfide bonds, Cys28-Cys111 seems to resist the photolytic cleavage.

The second goal of this chapter is to examine the impact of the individual Trp residues on the reduction of disulfide bridges. For this cause we constructed the GLA mutants W26F, W60F, W104F and W118F by replacing a single Trp residue by Phe. The progress of the photolysis is followed by the determination of free thiols. The substitution of each Trp led to a lesser thiol production than in wild type GLA. This reduction is clearly more significant upon substitution of Trp60 than upon substitution of each other Trp residue. The reduction in thiol production of W118F only becomes significant in an advanced stage of the photolysis. The formation of

Cys61Cam containing peptide was observed upon illumination of each mutant. In contrast, upon illumination of mutant W26F neither Cys120Cam, nor Cys6-Lys122 could be detected. Moreover, neither Cys91Cam, nor the dipeptide containing either Cys91-Lys79 or Cys73-Lys93 was detected in illuminated W26F and W104F. These results indicate that each individual Trp residue of LA has a unique impact on the photolytic cleavage of disulfide bridges.

5.2 Introduction

The presence of endogenous chromophores makes proteins sensitive for photo-induced degradation. The major chromophoric amino acids are tryptophan (Trp), tyrosine (Tyr), phenylalanine (Phe), histidine (His), cysteine (Cys) and cystine. The absorption of UV light can give excited state species and radicals which both initiate various degradation processes (1-3)

In the near-UV, the indolic side-chain of Trp has a significantly greater molar absorption coefficient than the other amino acid side chains. This makes Trp the primary component in the mediation of protein photodegradation. The triplet state of Trp (^3Trp) can undergo electron transfer with suitable acceptors. Disulfides, such as cystine, readily accept an electron leading to formation of the disulfide radical anion which in turn can readily dissociate (4). The electron transfer from excited Trp with cystine and the subsequent reductive splitting of this disulfide bond in proteins has been postulated decades ago (5). However, a first unambiguous example of such a Trp mediated photoreduction has been demonstrated only recently in *Fusarium solani pisi* cutinase (5,6). Meanwhile, strong indication for Trp mediated degradation of cystine bonds has been observed in goat and human α -lactalbumin (7,8) and in bovine somatotropin (9).

As *Fusarium solani pisi* cutinase contains a single Trp residue the interaction between the excited and the disrupted disulfide bond could be easily identified. α -Lactalbumins (LAs) contain four disulfide bridges and, dependent upon the animal species, they also contain three or four Trp residues. It makes the photolytic process more complicated. Goat α -lactalbumin (GLA), which is used in our study, contains four Trp residues. The structure of GLA is homologous to that of other types. The protein, 123 amino-acids long, consists of two lobes separated by a cleft (Fig. 1).

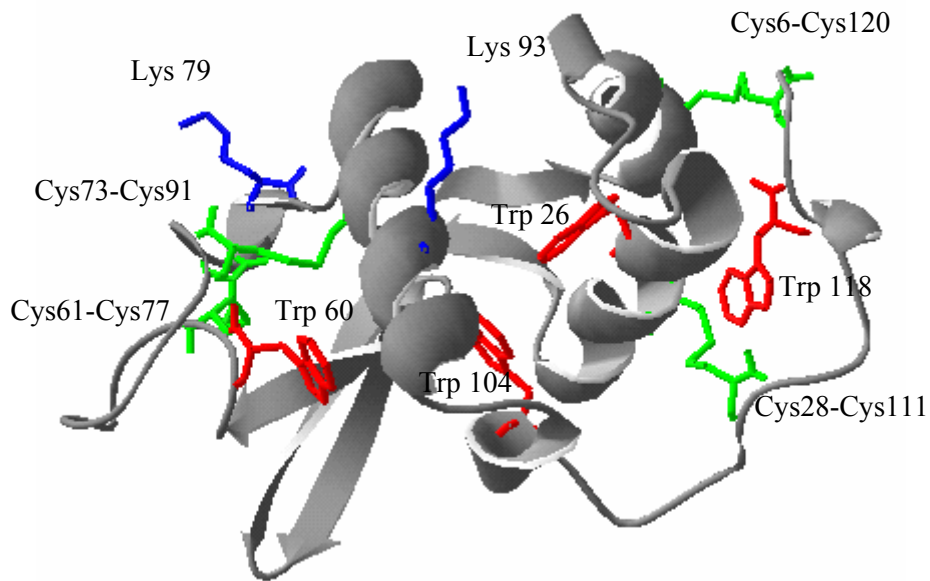
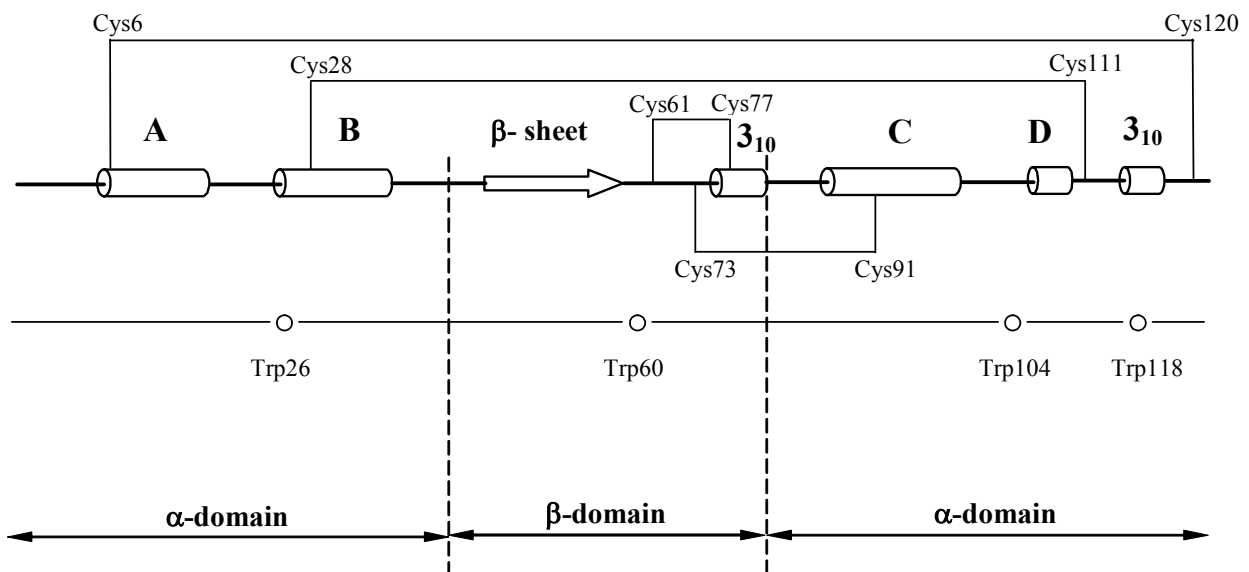
A**B**

Figure 1: (A) Crystal structure of goat α -lactalbumin generated from coordinates disposed in the Brookhaven Protein Data Bank, ref 1HFY using the program SWISS-MODEL (27). The side chains of the four Trp residues (red), the disulfide bonds (green) and two lysine residues (Lys 79 and 93, blue) are represented by sticks. Lys 122 is not represented as it is not possible to define the conformation of residues 121-123 due to the poor definition of the electron density maps in these regions (23). (B) Schematic representation of GLA. Secondary structure elements and the disulfide bonds in native GLA are indicated at the top. The domain boundaries are shown as dotted lines. The tryptophan residues (O) are indicated at their positions in the sequence.

The larger lobe, formed by the amino- and carboxyl-terminal sections of the polypeptide chain (residues 1-34 and 86-123), mainly contains helical structures including the α -helices H1, H2 and H3 (Fig. 1B), the flexible loop/helix H4 and a 3_{10} helix. The smaller lobe, formed by the central section of the polypeptide chain (residues 35-85), encompasses a small three-stranded antiparallel β -sheet, a small 3_{10} helix and a large part of non-structured loops. Two disulfide bridges (Cys6-Cys120 and Cys28-Cys111) are located in the α -helical lobe. Cys61-Cys77, located in the smaller lobe, connects non-structured loops. Cys73-Cys91 makes a bridge between both lobes.

The LA structure is characterized by the presence of two hydrophobic clusters (10,11). Hydrophobic cluster I, to which Trp 118 belongs, is part of the active site. Hydrophobic cluster II, located near the cleft, encompasses parts of both lobes. Three of the four Trp residues of GLA (Trp26, Trp 60 and Trp104) participate to that cluster. In Chapter 4 we showed important energy transfer among the several Trp residues in native GLA (12). Moreover, Trp60 and -118 are strongly quenched and, as a result of resonance energy transfer among Trp residues, both contribute to the quenching of Trp26 and -104. In Chapter 3 (7), upon analysis of the reaction products of illuminated GLA we observed photolytic cleavage of Cys6-Cys120 and of Cys73-Cys91. Trp118 is close to the former disulfide bridge and Trp60 is close to the latter bridge, therefore, a direct relationship between the excitation of both individual Trp residues and the reduction of their nearby disulfide bridge was postulated. Nevertheless, a number of questions arise. Trp118 is closer to the sulphur atoms of Cys28-Cys111 (3.4 Å) than to those of Cys6-Cys120 (9.8 Å). Therefore, we rather expected the photoreduction of Cys28-Cys111 than of Cys6-Cys120. Furthermore, upon illumination of human α -lactalbumin (HLA), in which Trp26 is substituted, no reduction of Cys6-Cys120 is observed (8). This suggests that the even more distant Trp26 (at 13.6 Å) might mediate the photolysis of Cys6-Cys120 rather than Trp118. Lastly, Permyakov et al. (8) observed the photolytic cleavage of Cys61-Cys77, which was not observed in our work.

In order to examine more accurately which relationships exists between the photoexcitation of a particular Trp and the combined reduction of disulfide bridges we constructed four GLA mutants by replacing successively a single Trp residue for a phenylalanine. The recombinant LAs (W26F, W60F, W104F and W118F) were expressed in *Pichia pastoris* and we mutually compared the photolytic degradation products of each mutant with that of wild type GLA. The photolytic degradation is investigated by measuring the number of free thiol groups as a function of the

light energy absorbed and by MALDI MS/MS and nano-ESI MS/MS analysis of fragments obtained after carbamidomethylation and trypsin digestion of the photolyzed proteins. We also followed the effect of the photolysis on the conformation and on the enzymatic activity of the protein.

5.3 Materials and Methods

5.3.1 Protein expression and purification

Trp mutants of GLA were constructed as described in Chapter 4 (12). The Trp mutants were expressed in *P. pastoris* and purified by hydrophobic interaction chromatography and affinity chromatography (12,13). The identity of all proteins was confirmed by electrospray ionization mass spectrometry (ESI-MS). Protein concentrations were determined from the optical density at 280 nm (14). Calculated extinction coefficients were: 28840 (mol/l)⁻¹cm⁻¹ for the wild type GLA and 23150 (mol/l)⁻¹cm⁻¹ for the single mutants (W26F, W60F, W104F, W118F). All experiments were performed in 10 mM Tris-HCl buffer (pH 7.5) containing 2 mM Ca²⁺.

5.3.2 Illumination of GLA

Wild type GLA or its Trp mutants were illuminated with an Aminco-Bowman Series 2 spectrofluorimeter (Rochester, N.Y.) as described in Chapter 3 (7). The excitation wavelength was centered at 290 nm with a bandpass of 16 nm, in contrast to previous illumination at 280 nm (7). We chose this different wavelength to reduce the possibility of interference of tyrosine excitation. A 2 ml sample of a protein solution in 2 mM Ca²⁺ and 10 mM Tris-HCl at pH 7.5 was illuminated in the cuvette holder of a spectrofluorimeter. The protein concentration was 30 μM and the temperature was kept at 4 °C. During illumination, the solution was stirred with a magnetic stirring bar at 120 rpm. To avoid air oxidation, all solutions were thoroughly degassed prior to use and kept under N₂ atmosphere during illumination. The number of free thiol groups was determined with DTNB using a molar extinction coefficient of 13600 (mol/l)⁻¹ cm⁻¹ for

TNB⁻ (15,16). The lactose synthesis regulatory activity of the illuminated and non-illuminated recombinant proteins was compared with the activity of authentic LA.

5.3.3 Spectroscopic measurements

Fluorescence, circular dichroism and absorption measurements were carried out immediately after illumination as described in Chapter 3 (7). In short, steady state fluorescence spectra were acquired at 4 °C using an Aminco-Bowman Series 2 spectrofluorimeter (Rochester, N.Y.). The CD measurements were performed at 25 °C on a Jasco J-600 spectropolarimeter (Tokyo, Japan). Cuvettes of 10 mm and 1 mm were used for the near-UV and far-UV region, respectively. The absorption measurements were performed on an Uvikon 933 double beam UV/VIS spectrophotometer (Kontron Instruments, Milano, Italy) at room temperature.

5.3.4 Peptide characterization

Mass spectrometry was carried out with the iodoacetamide-treated samples of illuminated proteins as described in Chapter 3 (7). Compared to this earlier study, however, novel mass spectrometric approaches have been introduced. The protein was digested using trypsin and the resulting peptides analyzed using MALDI-TOF-TOF-MS (4700 Proteomics Analyzer, Applied Biosystems). Previously, we used a single MALDI-TOF instrument, which did not allow us to perform MS/MS on MALDI generated ions. In the current setup, for MS data acquisition, a total of 2000 shots were collected (40 sub-spectra accumulated from 50 laser shots each). All MS/MS data was acquired in the 1keV MS/MS mode using air as the collision gas (1.2×10^{-7} torr). A total of 3000 shots (40 sub-spectra accumulated from 75 laser shots each) were acquired and the timed-ion-selector window was set to 250 resolution (FWHM). Electrospray MS and MS/MS were performed as described on a Q-TOF mass spectrometer (Micromass) except that the original nano-electrospray source was replaced by a chip-based nano-ESI device (NanoMate 100, Advion Biosciences).

5.4 Results

5.4.1 Disulfide bond cleavage in Trp mutants

Wild type GLA and four single Trp mutants (W26F, W60F, W104F and W118F) were excited with light of 282-298 nm to investigate whether the replacement of the various Trp residues into Phe affects the photo-induced cleavage of disulfide bonds. The amount of free thiols generated per protein molecule (F_{th}) was detected with Ellman's reagents and plotted as a function of irradiation time (Figure 2A). The evolution of the number of free thiols for wild type GLA is in good agreement with these for authentic GLA under the same conditions (7), indicating that the behavior of wild type and authentic GLA upon irradiation is analogous. For all recombinant proteins –wild type and mutants– the rate with which free thiols are formed during the illumination experiment gradually decreases as is expected for a reaction with decreasing availability of disulfide bonds. Interestingly, the saturation in thiol formation is reached more quickly for the mutants W60F and W118F than for W26F, W104F or wild type GLA. The different lengths of time needed to obtain the limit of free thiol content, is a first clear indication that the various Trp residues direct the photolytic cleavage of disulfide bonds in a different way. The fact that the mutants W60F and W118F, lacking Trp 60 and Trp 118 respectively, reach this limit more rapidly indicates that those disulfide groups which are potential targets for photolytic cleavage mediated by Trp 26 and by Trp 104 become exhausted more rapidly than those of which the photolysis is mediated by Trp 60 and by Trp 118.

In order to obtain a more quantitative estimation of the impact of the different Trp groups on disulfide rupture, we calculated the difference of the amount of thiols formed in wild type and mutant GLA after 3 hours of illumination. The data collected in Figure 2B clearly illustrate to what degree each replacement of Trp residue with Phe decreases the progress of the photolytic degradation process. In comparison with wild type, 3 hours of irradiation of W60F decreases the amount of free thiols by $0.43 (\pm 0.06)$ thiols /LA unit. The substitution of Trp 26 decreased the thiol production by about $0.24 (\pm 0.06)$ thiols /LA unit. When replacing Trp104 or Trp 118 by Phe the protein forms $0.18 (\pm 0.08)$ thiols /LA unit less than wild type GLA does. The sum of the individual numbers of all four Trp single mutants is $1.03 (\pm 0.14)$ and approaches very well the number of free thiols obtained while illuminating wild type GLA (1.22 ± 0.05). This observation

suggests that each Trp residue has an independent impact on the photolytic degradation process. These data also show that the potential photolytic cleavage of disulfide bonds that is not mediated by Trp residues is negligible compared to the cleavage mediated by Trp.

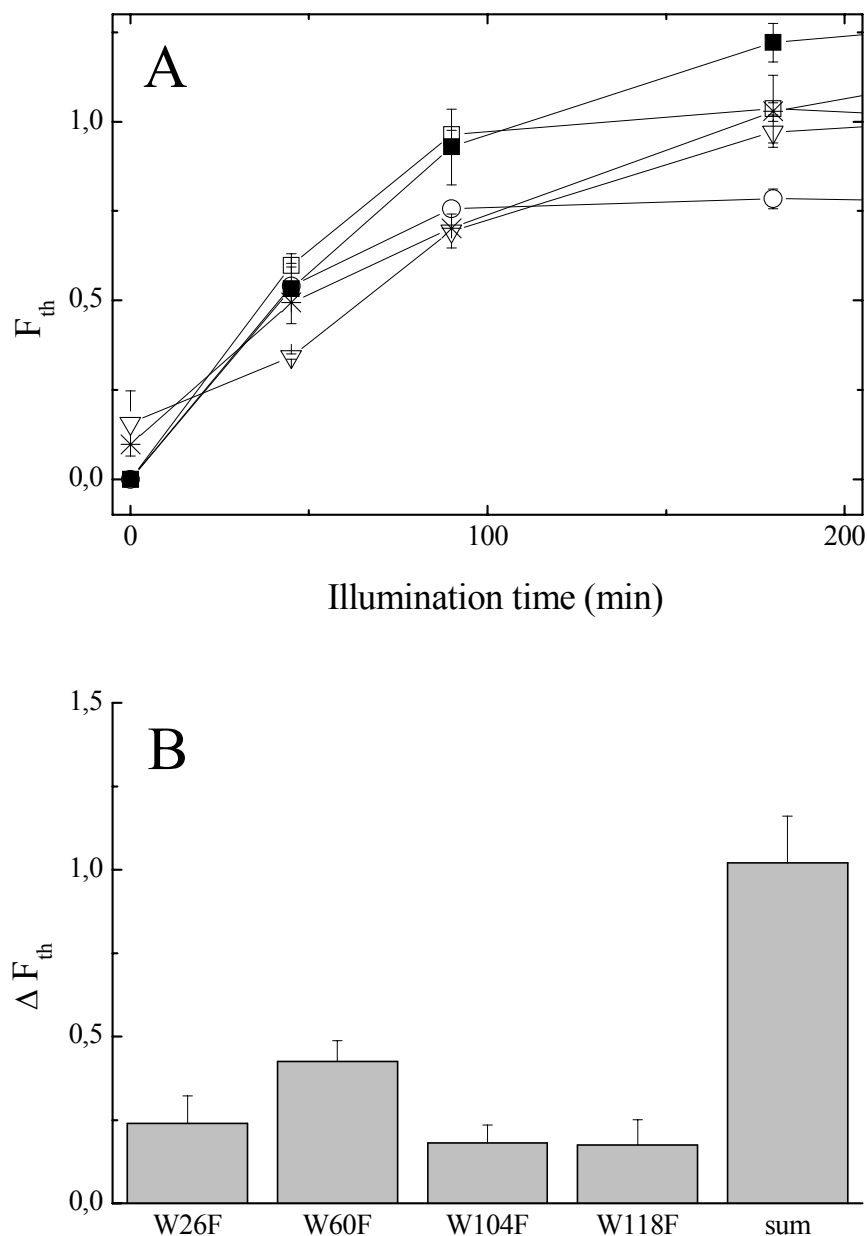


Figure 2: (A) Number of free thiol groups per recombinant GLA (wild type GLA ■, W118F □, W60F ○, W26F ▽ and W104F *) as a function of illumination time measured with Ellman's reagent. The samples were illuminated under the conditions mentioned in Materials and Methods: Illumination of GLA. The error bars represent experimental divergences. (B) Difference of the amount of thiols per LA unit formed in wild type and in mutant GLA (W26F, W60F, W104F or W118F) after 3 hours of illumination. The sum of the differences for all Trp mutants is indicated in the last column.

5.4.2 Spectroscopic studies

Emission fluorescence and near-UV CD spectroscopy were used to observe the conformational changes caused by the disulfide bond cleavage in the illuminated proteins. In general, the partial unfolding of LA effects a change of two characteristics of its fluorescence spectrum (17). On the one hand, unfolding of LA evokes an increase in fluorescence intensity as the contacts of Trp with quenching residues are reduced in the expanded state. On the other hand, a red shift of the maximum wavelength is caused by the enhanced solvent accessibility of the Trp residues in the partially unfolded state.

Figure 3A shows the percentage evolution of the integrated fluorescence as a function of the irradiation time. For all recombinant proteins the fluorescence increases during the first 100 min of illumination and this is followed by a loss of yield. The first phenomenon corresponds to the loosening of the tertiary structure of wild type GLA and of its mutants upon illumination. The subsequent loss of fluorescence yield probably refers to photo-destruction of Trp residues.

As shown in Fig. 3B, all recombinant proteins show a continuous red shift of the fluorescence upon irradiation. This refers to a continuous progress of the unfolding induced by irradiation. The limit of the emission maximum (λ_{\max}) obtained after 6 hours of illumination strives for 340 nm. However, an emission maximum (λ_{\max}) of 348 nm is found for the amino acid Trp in water (18) and the λ_{\max} of wild type GLA in 6 M GndHCl occurs at 345 nm (19). None of the recombinant proteins reach that fluorescence wavelength; this may be an indication that parts of the native structure are conserved in the illuminated GLA or that a fraction of the proteins is still native.

The near-UV ellipticity signal at 270 nm of recombinant GLA as a function of irradiation time (Fig. 3C), gives similar information on the progress of protein unfolding as the data obtained from fluorescence wavelength shift. All illuminated recombinant proteins display signals that are weak compared to those of the non illuminated proteins. This loss of near-UV CD signal arises from the loss of fixed tertiary interactions for the aromatic amino acids. For all recombinant proteins, the time courses for the fractional reduction of the CD signal and of the fractional shift of λ_{\max} are fairly similar.

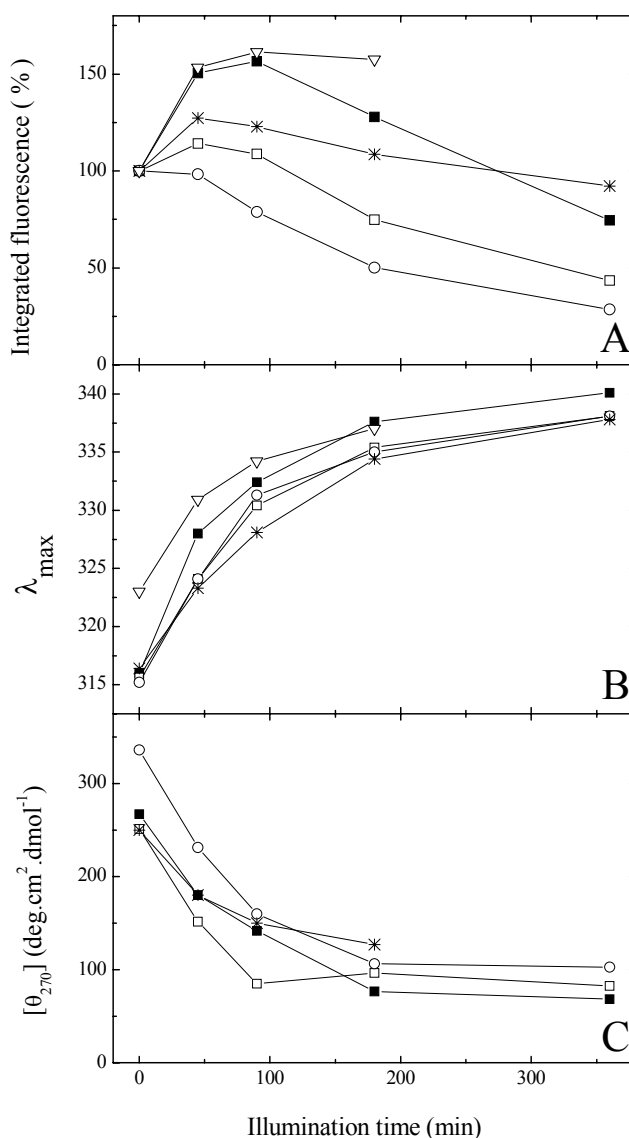


Figure 3: (A) Percentage of the integrated fluorescence, (B) λ_{\max} and (C) ellipticity at 270 nm for wild type GLA (■) and for the mutants W118F □, W60F ○, W26F ▽ and W104F * as a function of illumination time.

5.4.3 Lactose synthesis

The influence of irradiation on the ability of LA to act as a stimulator of lactose synthase activity was investigated. For wild type GLA about 35% of the original activity of lactose synthetase is conserved after 3 hours of illumination. The two mutants, W26F and W60F, also stimulate the activity of lactose synthase to the same degree as wild type GLA before illumination and 35% of the original activity after irradiation. Replacing Trp118 into a Phe causes a nearly complete

reduction of the lactose synthesis as this Trp is part of the catalytic cluster in lactose synthase (see Chapter 4; 20). In the addendum of Chapter 4 the replacement of Trp104 was found to reduce the lactose synthase activity to 20% of that of wild type GLA. As a consequence of the poor yield, no relevant data are found to determine the influence of irradiation on the rate of lactose synthesis of W118F and of W104F.

5.4.4 Mass spectrometry

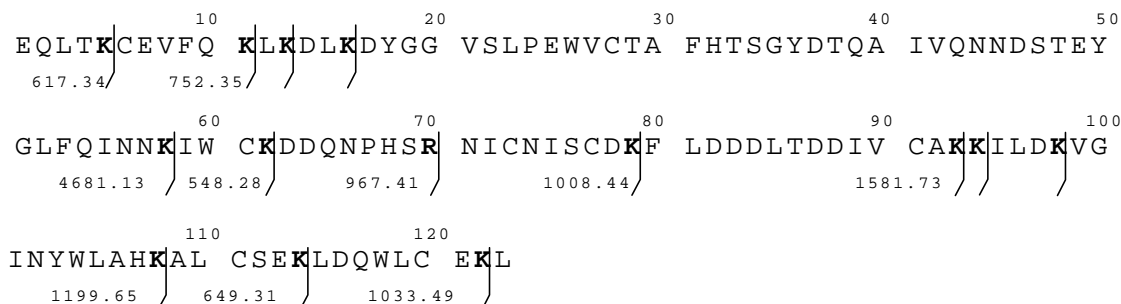
Wild type GLA and its mutants were exposed to UV irradiation at 282-298 nm for 180 min. The free thiol groups were carbamidomethylated with iodoacetamide. The proteins were digested with trypsin and the resulting peptides were analyzed using MALDI-TOF-TOF-MS and nano-ESI-MS. The amino acid sequence of GLA and the sites suited for digestion with trypsin are presented in Table 1A. An overview of the peptides resulting from intact wild type GLA is shown in Table 1B. The differences in the spectra of the intact recombinant GLA and the irradiated and carbamidomethylated GLA were further analyzed by a combination of MALDI-MS/MS and nano-ESI MS/MS.

Mass spectra of wild type GLA

Comparison of the MS spectrum of the digest of carbamidomethylated intact wild type GLA with the spectrum of the digest of the irradiated protein reveals significant differences. The spectrum of the illuminated wild type GLA shows a decrease of two peaks: at 1784.80 Da and 3135.38 Da, respectively. These masses account for two fragments containing peptides with intact disulfide bridges (Table 1B). The disappearance of these peaks suggests that disulfide bridges are ruptured within those fragments. In addition to the decrease of two peaks, four new peaks (1553.70 Da, 1639.0 Da, 1841.80 Da and 3192.49 Da) appear in the spectrum of illuminated and digested wild type GLA. The sequence of all peptides was investigated using MS/MS analysis, which selects a precursor ion for low-energy gas-phase collisional activation and subjects the resulting product ions to MS (Fig. 4).

Table 1: (A) Amino acid sequence of wild type GLA. Trypsin digestion sites and masses of the peptides in a tryptic digest that would not contain disulfide bridges, are indicated. (B) Overview of the peptides, derived from wild type GLA after digestion with trypsin, containing intact disulfide bridges.

A



B

Disulfide bridge	Peptide sequence	Mass [M+H] ⁺
6-120	$L^{115}DQWLC^{120}EK^{122}$ C^6EVFQK^{11}	1784.84
61-77 73-91	$F^{80}LDDDLTDDIVC^{91}AK^{93}$ $N^{71}IC^{73}NISC^{77}DK^{79}$ $I^{59}WC^{61}K^{62}$	3135.38
28-111	$D^{17}YGGVSLPEWVC^{28}TAFH(\dots)NK^{58}$ $A^{109}LC^{111}SEK^{114}$	5329.44

Under these conditions, peptide ions fragment primarily at the amide bond, yielding a ladder of sequence ions. Retention of charge on the N-terminal portion of the peptide ion yields a b-type ion; retention on the C-terminal portion of the peptide ion yields a y-type ion. Subtracting the masses of adjacent ions reveals the amino acid sequence. MALDI TOF MS/MS of disulfide bonded peptides yields specific fragments due to disruption of the C-S-S-C linkage at any of the 3 bonds (21). We designated these as F-fragments as shown in Fig. 4A and 4B.

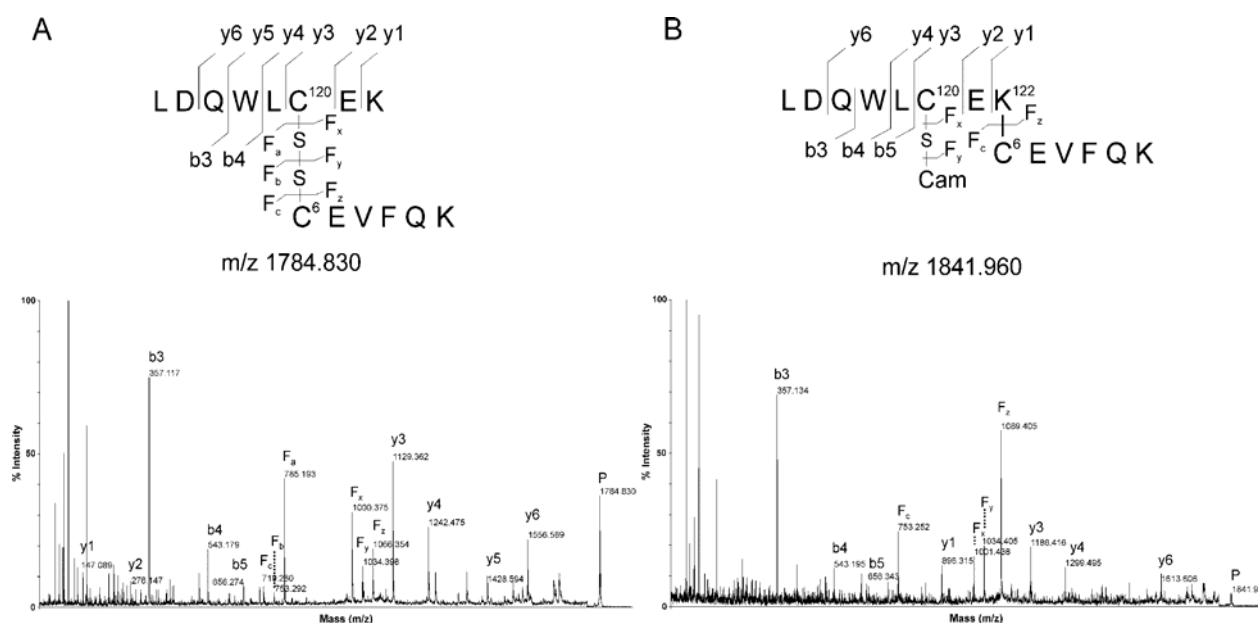


Figure 4: MALDI-MS/MS spectra of (A) the dipeptide (m/z 1784.80) derived from intact wild type GLA containing the intact disulfide bridge Cys6-Cys120 and of (B) the dipeptide (m/z 1841.80) linked by a Cys6-Lys122 bond from irradiated and carbamidomethylated wild type GLA.

The MS/MS analysis of the fragments at m/z 1784.80 and m/z 1841.80 are illustrated in Figure 4. For non illuminated GLA, the series of b-type ions, y-type ions and F-type ions, generated in the analysis of the m/z 1784.80 ion ($[\text{peptide} + \text{H}]^{1+}$) (Fig. 4A) is consistent with the sequence of the dipeptide containing the intact bridge Cys6-Cys120. After UV exposure this peptide at 1784.80 Da reduces in height, suggesting that Cys6-Cys120 is broken. An additional peak at m/z 1841.80 is detected. MALDI-MS/MS (Fig. 4B) as well as ESI-MS/MS (data not shown) suggest that this peak accounts for a complex peptide formed by a novel cross-link between Cys6 and Lys122 and containing a carbamidomethyl group (Cam) at Cys120.

The MS/MS analysis of the peptide at 1553.70 ($[\text{M} + \text{H}]^{1+}$), appearing after UV irradiation, reveals that it is the Ile59-Arg70 peptide, having a carbamidomethyl group at Cys61 (Fig 5). Clearly this carbamidomethylated fragment results from the rupture of disulfide bridge Cys61-Cys77. However, the appearance of the Ile59-Arg70 peptide was unusual as digestion with trypsin would normally lead to the Ile59-Lys62 peptide due to the typical cleavage after a Lys residue (Table 1A). Moreover, the theoretical mass of Ile59-Arg70 is 1555.67 Da instead of the observed 1553.70, suggesting a loss of 2 protons after UV exposure. Indeed, the mass difference between the y-ions in the MALDI-MS/MS and ESI-MS/MS spectra confirms that the Cys61-Cam has a

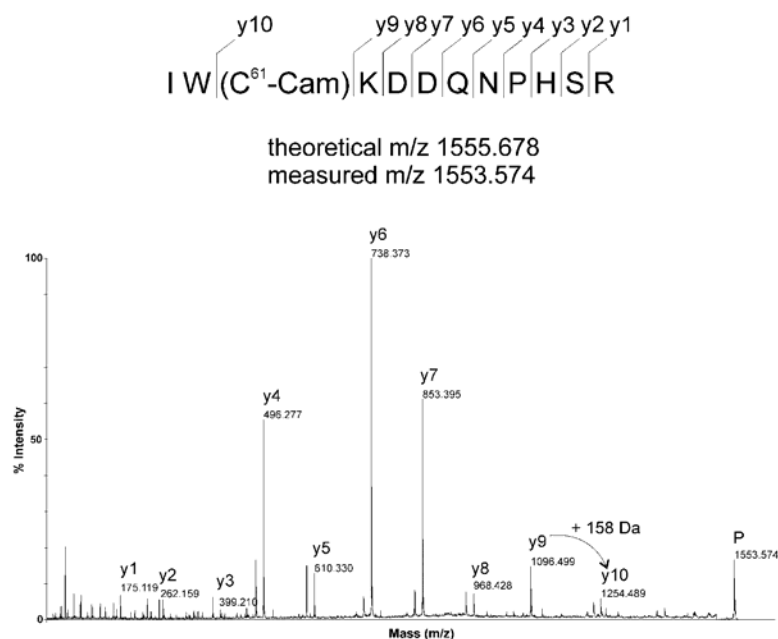


Figure 5: MALDI-MS/MS spectrum of a new peptide at m/z 1553.7 originating from the trypsin digest of irradiated and carbamidomethylated wild type GLA. In particular, a fragmentation ion with 2 Da difference between theoretical and measured mass is indicated with an arrow.

mass of 158 Da, instead of the expected 160 Da (Fig5). This suggests the formation of a double bond between C α and C β of the cysteine residue, probably as a result of a radical reaction following UV-induced disulfide bridge cleavage.

The MS/MS data of the new peaks at 3192.49 Da and at 1639.0 Da, both contain evidence of the cleavage of disulfide bridge Cys73-Cys91. Indeed, the new peak with a mass of 1639.0 Da correlates with a peptide Phe80-Lys93 containing the carbamidomethylated Cys91 (affirmed with ESI MS/MS in Chapter 3; 7). The appearance of a peak at 3192.49 Da reveals that a peculiar observation can be related with the reduction of this disulfide bond. In the intact protein a tripeptide containing two disulfide bridges (Cys61-Cys77 and Cys73-Cys91) is found at 3135.38 Da (Table 1B). After UV exposure, ESI-MS reveals that this fragment has gained 57 Da due to a carbamidomethylated thiol. The fact that the tripeptide is still present, although one of the cysteins is carbamidomethylated, suggests that a second Cys-Lys bond, similar to Cys6-Lys122 is formed. To confirm this hypothesis, the peptide was further purified and reduced with DTT, resulting in a new peptide at 882.60 [M+3H]³⁺. This mass corresponds to a fragment composed of a Phe80-Lys93 peptide being linked to an Asn71-Lys79 peptide with either a Cys91-Lys79 bond and carbamidomethylation at Cys73 or a Cys73-Lys93 bond and carbamidomethylation at Cys91. Both possibilities are presented in Figure 6.



Figure 6: Possible structures of the dipeptide at 882.60 [M+3H⁺]. After consecutive UV exposure, treatment with iodoacetamide and trypsin digestion of wild type GLA a complex carbamidomethylated peptide of 3192.49 Da is obtained. Upon treatment with DTT, this complex peptide is further reduced to the above dipeptide.

ESI-MS/MS confirmed the nature of this dipeptide, but could not distinguish the linkage between the two peptides.

In conclusion, the MS analysis of illuminated wild type GLA reveals the reduction of 3 disulfide bonds (Cys6-Cys120, Cys73-Cys91 and Cys61-Cys77) accompanied with 2 peculiar phenomena. These phenomena include the formation of at least one Cys-Lys bond and a remarkable 2 Da loss at the carbamidomethylated Cys61.

Mass spectra of tryptophan mutants

Analogous experiments were performed on the Trp mutants to define which of the four Trp residues within GLA are essential for inducing photoreduction of disulfide bonds. For wild type GLA and its mutants, Table 2 summarizes whether a particular disulfide bridge (6-120, 28-111, 61-77 and 73-91) is cleaved by irradiation or not. For each disulfide bond broken, all carbamidomethylated thiols (Cys-Cam) identified with MS/MS are indicated. Also, for each recombinant protein, Table 2 indicates whether prove of two new linkages between a cysteine and a lysine (Cys6-Lys122 and Cys91-Lys79 or Cys73-Lys93) could be found.

Below we underline some striking results which will be discussed in the next section. For each broken disulfide bridge only one carbamidomethyl group was found. In none of the recombinant proteins, Cys28-Cys111 is affected by UV radiation. By contrast, in all proteins UV illumination results in the disruption of the disulfide bridge Cys61-Cys77. Evidence for the cleavage of Cys6-Cys120 could be found for all proteins except for mutant W26F. Furthermore, in mutant W26F and in W104F no evidence for the disruption of Cys73-Cys91 was found.

Table 2: Rearrangements of disulfide bridges in UV exposed WT GLA or its mutants. The formation of all carbamidomethylated cysteins is indicated and evidences the cleavage of the disulfide bond. Not detected (ND) indicates that no evidence for the cleavage of the disulfide bridge could be found.

	Cys6-Cys120	Cys28-Cys111	Cys61-Cys77	Cys73-Cys91	Cys6-Lys122 ^a	Cys91-Lys79 or Cys73-Lys93 ^b
Wild type	Cys120Cam	ND	Cys61Cam	Cys91Cam	yes	yes
W26F	ND	ND	Cys61Cam	ND	no	no
W60F	Cys120Cam	ND	Cys61Cam	Cys91Cam	yes	yes
W104F	Cys120Cam	ND	Cys61Cam	ND	no	no
W118F	Cys120Cam	ND	Cys61Cam	Cys91Cam	yes	yes

^a Formation of Cys6-Lys122 bond evidenced by an important fragment in MALDI MS/MS
^b Involvement of a second Cys-Lys bond with either Cys73 or Cys91

5.5 Discussion

In order to study the effect of individual Trp residues on the photoinduced degradation of disulfide bonds in GLA, we constructed the mutants in which the four Trp residues are successively substituted by a Phe (W26F, W60F, W104F and W118F). In a first step, the number of free thiol groups created upon the photolysis of the different recombinant proteins was followed as function of the amount of incident light (Fig. 2A). The substitution of any Trp led to a smaller thiol production in the mutant than in wild type GLA. Interestingly, after a fixed length of time the sum of the diminutions observed for the four different Trp mutants approximates the amount of thiols created in the wild type protein (Fig. 2B). This finding provides evidence that Trp mediated cleavage represents nearly the total amount of photolytic cleaved disulfide bridges in GLA. After three hours, the amount of thiol groups created by mediation of Trp60 is clearly higher than that of each other Trp residue. This is expected as the fluorescence emission of Trp60 is strongly quenched. Nearby disulfide bridges, responsible for the quenching effects, are primary candidates for undergoing cleavage. For this reason we are surprised to observe a clearly smaller effect of Trp118 on the thiol formation (Fig. 2B). Indeed, also Trp118 is strongly quenched in GLA (12). At least in the crystal structure, the indole group of Trp118 is in direct contact with the disulfide bridge of Cys28-Cys111 (at 3.4 Å) in the way that considerable

transfer of energy or of electrons from photo-excited Trp118 to Cys28-Cys111 looks inevitable. A plausible reason for the poor contribution of Trp118 to mediation of disulfide cleavage may result from the fact that Cys28-Cys111 is situated in a very stable protein region. Indeed, Peng et al. (22) found that the region surrounding the Cys28-Cys111 disulfide bond has very high preference for adopting a native-like structure. Therefore, this activated disulfide bond does not tend to cleave. Even upon possible cleavage, the resulting thiyl radicals do not tend to migrate from each other and the disulfide bond may repair before cross reactions are enabled. This idea is in agreement with the fact that Cys28-Cys111 is the only disulfide bridge in GLA which does not experience cleavage (Table 2). Finally, Figure 2B shows that also Trp26 and -104, two Trp residues that are quenched considerably less than Trp118, importantly contribute to the photolytic reduction of disulfide bridges. Especially, the contribution of Trp104 has not been expected in the previous papers dealing with the photolytic cleavage of disulfide bridges in LA (7,8).

For a more thorough inspection of the specific mediation of individual Trp residues, irradiated and non-irradiated samples of the various recombinant GLAs were treated with iodoacetamide and subsequently digested with trypsin. MALDI-MS/MS and nano-ESI-MS/MS analysis enabled to specify unambiguously which new peptides were created. Therefore, the analysis also revealed which disulfide bonds were cleaved, which Cys groups became carbamidomethylated and which new cross-links were formed upon photolysis. These results are summarised in Table 2. In the next discussion we overlook the summarized data.

For wild type GLA, the photo-induced cleavage of three disulfide bridges could be observed: Cys6-Cys120, Cys61-Cys77 and Cys73-Cys91. In Chapter 3 (7) we already proved the cleavage of the Cys6-Cys120 and Cys73-Cys91 bonds. In this earlier study we also pointed to the creation of a peptide fragment of 1553.0 Da, containing Ile-Trp at the N-terminal. On the basis of this mass and of these terminal amino acids the peptide has been interpreted to consist of the linked GLA fragments 59-62 and 71-79 (Table 1B). Consequently, the bond Cys61-Cys77 was considered to resist photolysis. However, the present MALDI-MS/MS spectrum allows a far more thorough analysis of the 1553.0 Da peptide. The extended data provide evidence that it consists of the GLA sequence 59-70 having a carbamidomethyl group at Cys61 and consequently, point to photolysis of the Cys61-Cys77 bond (Fig. 5). In Chapter 3 this eventuality was not considered as we expected that the peptide consisting of the GLA sequence 59-70 would hydrolyze at Lys62 upon trypsin digestion which then yields a peptide with the same mass. The

ESI MS/MS spectrum, moreover, provided rather poor information in the lower molecular weight part of the spectrum leaving some uncertainty on the C-terminal part of the spectrum. In addition the peptide representing the carbamidomethylated 59-70 sequence of GLA has a deficient of 2 Da, resulting from a double bond formed by the subtraction of two hydrogens in the side chain of Cys61, a phenomenon that was previously ignored.

The summary of data collected in the various columns of Table 2 gives insight in the specificity with which some Trp residues mediate the photoactivation of a disulfide bond. At first, mutant W26F is the only mutant in which neither a peptide with carbamidomethylated Cys120 nor a peptide with cross-link between Cys6 and Lys122 has been found. This indicates that the photolysis of the Cys6-Cys120 bond is exclusively mediated by photoexcitation of Trp26. In our earlier study (7) we assumed that Trp118 should mediate the photolysis of this bond. Indeed, the shortest distance between the indole ring of Trp118 and the Cys6-Cys120 disulfides is about 9.8 Å, while the distance of these disulfides to Trp26 amounts to 14.5 Å (23). However, Permyakov et al. (8) studied the photoreduction of the disulfide bonds in HLA possessing the same Trp residues as the W26F mutant of GLA. They observed photolysis of Cys61-Cys77 and of Cys73-Cys91 but could not detect photoreduction of Cys6-Cys120. Therefore, they at first postulated the mediation of Trp26 for the photolysis of Cys6-Cys120. In an attempt to explain this preferential impact, Permyakov et al. (8) suggest that Trp26 may exist in the different rotamer forms by which the inter-residue distance with Cys6-Cys120 could be shortened as low as 8.0 Å. The present study offers an alternative reason why Trp26 rather than Trp118 mediates the photolysis of the Cys6-Cys120 disulfide bond. As mentioned above, photo-excited Trp118 readily transfers energy or electrons to the Cys28-Cys111 bond which does not tend to undergo net cleavage. Furthermore, the fact that a new Cys-Lys crosslink is detected upon photolysis Cys6-Cys120 as well as upon photolysis of Cys73-Cys91 (Table2, column 5) is an indication that also the mediation of Lys group can be important in the cleavage of disulfide bonds. Hawkins and Davies (1) stated that the one-electron oxidations of free amine groups give rise to nitrogen-centered radicals: aminium radical cations ($\text{RNH}_2^{+\bullet}$) or neutral aminyl radicals (RNH^\bullet). These authors also mentioned that the side chain aminyl radicals formed from the ϵ -amino group of Lys side chains generate radicals at either C-3 or at the α -carbon (24). Conversely, Fu et al. (25) observed that Cys residues in peptides form intramolecular and intermolecular -S-NH-bridges with lysine and arginine residues when radicals are created by excitation of HOCl. Although our analysis does not demonstrate which atoms of the Cys6 and the Lys122 side chains

are involved in the cross-links, the generation of such sulfenamide bonds looks very acceptable when dealing with radical reactions initiated by photo-excitation of Trp.

The results summarized in the third column of Table 2 evidence that, in none of the recombinant GLAs, a peptide could be detected with fragments referring to split Cys28-Cys111. In contrast, a peptide of mass 5329.4 Da (1333.4 [M+4H⁺]), referring to the linked GLA fragments 17-58 and 109-114, has been observed before and after illumination. These findings suggest that Cys28-Cys111 resist the Trp mediated photoexcitation. This observation may astonish as, in the crystal structure of GLA, the considered S-S bond is in very close contact with Trp118 (3.4 Å) and is also nearby Trp26 (8.9 Å) and Trp104 (9.0 Å). A plausible reason for the high resistance of this disulfide bond may result from the fact that Cys28-Cys111 is situated in a very stable protein region. As mentioned above, Peng et al. (22) found that the region surrounding the Cys28-Cys111 disulfide bond has very high preference for adopting a native-like structure. Therefore, upon eventual cleavage of the disulfide bond Cys28-Cys111 the resulting radicals do not tend to migrate from each other and the disulfide bond may repair before cross reactions are enabled.

In contrast to the stable Cys28-Cys111 binding, the disulfide bond Cys61-Cys77 has been photolyzed in all recombinant proteins (Table 2, next column). This indicates that none of the substituted Trp residues in an exclusive way mediates the photoreduction of Cys61-Cys77. The distance between this disulfide bridge and Trp60 amounts to 6.4 Å. The distance with Trp104 amounts to 11.7 Å. Both other Trps are clearly more distant from this disulfide bond. Therefore, the most plausible explanation for the observed persistence of the reactivity of the Cys61-Cys77 bond over the series of single Trp mutants seems to be that the two vicinal Trp residues, Trp60 as well as Trp104, are able to mediate photolysis of this bond. An indication in favor of this hypothesis is given by the fact that Trp60 strongly enhances the production of free thiols upon illumination (Figure 2B) while no unique mediation of this Trp has been found (Table 2). For an unambiguous verification of the hypothesis a double mutant with substituted Trp60 and -104 should be constructed.

Another intriguing observation evidenced in Table 2, is that the Cys73-Cys91 is protected against photolytic cleavage when Trp104 is replaced as well as when Trp26 is substituted. The peptide fragment that should refer to the disrupted Cys73-Cys91 disulfide bond is well defined from the corresponding analysis of the other GLA mutants and, therefore, it can be traced accurately. As a consequence, the fact that no peaks of 3192.49 Da, nor of 1639.0 Da are

detected in the peptide digest of photolyzed W26F and of photolyzed W104F is a strong indication that the photolysis of the Cys73-Cys91 bond did not happen in either of these mutants. For the explanation of these results we have to assume that in one mutant the photolysis pathway has been interrupted in a direct way, while in the other mutant the mechanism is interrupted in an indirect way. The sulfur atoms of Cys73-Cys91 are most near to Trp104 (7.7 Å). Therefore, the photolysis of this disulfide bridge seems most readily mediated by Trp104 and the substitution of this Trp may directly interrupt the photolysis pathway. The indirect interruption of this photolysis pathway then should result from a displacement of one of the interacting agents upon substitution of Trp26. In favour of this possibility, the λ_{\max} of the fluorescence spectrum shifted from 318nm to 326 nm upon mutation of Trp26 to Phe (data not shown). This indicates that subtle conformational changes may happen upon substitution of Trp26. Also, Pike et al. (23) noticed that in HLA, where Trp26 is replaced by a leucine, the 3_{10} helix at position 13-15 does not pack as close as in GLA. As Trp104 is located nearby this 3_{10} helix, the substitution of Trp26 may also effect a reorientation of Trp104 and, therefore, disable the transfer of an electron to the Cys73-Cys91 disulfide bond. Finally, at the end of this paragraph it is worth to remember that Cys73-Cys91 is the second disulfide bond in GLA of which the photolytic disruption may result in the formation of a new Cys-Lys crosslink. The analysis of our ESI-MS/MS spectra does not allow discrimination between a Cys91-Lys79 and a Cys73-Lys93 crosslink. However, an inspection of the crystal structure (23) indicates that in native GLA neither Cys91 keeps contact with Lys79 nor Cys73 keeps contact with Lys93. As a consequence, the formation of the Cys-Lys bond requires some reorganisation in GLA following on the cleavage of Cys73-Cys91. In addition, Cys73 and Lys93 are located at opposite sites of helix H3 and any linkage of those residues will require an important displacement of this central helix. Therefore, the creation of a Cys91-Lys79 crosslink seems far more probable than a Cys73-Lys93 linkage.

To finish this overview of results we ought to give some comments on the fact that no relation has been found between the photolysis mediated by Trp118 and a specific disulfide bond (Table 2). This agrees with the low contribution of Trp118 to this type of photolysis (Fig. 2B). Also, the contribution of Trp118 is expressed in a late stadium of the photolysis (Fig. 2A) when GLA has lost native structure (Fig. 3A, B and C). In order to explain this we remember that the poor mediation results from important energy and electron transfer from Trp118 to the fairly stable Cys28-Cys111 bond. In partially unfolded GLA, the direct contact between Trp118 and the disulfide bond of Cys28-Cys111 will loose and the aromatic residue may enter in contact with a

large number of other substructures. In this state, the potential products of the Trp mediated photolysis may be numerous, each at difficult detectable amounts.

With regard to the resulting catalytic activity after 3 hours of photolysis, a considerable amount of protein ($\pm 35\%$) keeps its ability to act as activator of the lactose synthesis. This high percentage is surprising as near-UV CD (Fig. 3C) and emission wavelength shifts (Fig. 3B) indicate that the tertiary structure in the irradiated protein sample is importantly disrupted. However, in none of the recombinant proteins evidence for the reduction of the disulfide bridge Cys28-Cys111 was found. This may be important for the functional properties of irradiated GLA as Cys111 is located in a region which is known to be involved in the β -galactosyltransferase binding (26).

5.6 References

1. Hawkins, C.L. and Davies, M.J. (2001) Generation and propagation of radical reactions on proteins. *Biochimica et Biophysica Acta-Bioenergetics* 1504, 196-219.
2. Davies, M.J. (2003) Singlet oxygen-mediated damage to proteins and its consequences. *Biochemical and Biophysical Research Communications* 305, 761-770.
3. Davies, M.J. and Truscott, R.J.W. (2001) Photo-oxidation of proteins and its role in cataractogenesis. *Journal of Photochemistry and Photobiology B-Biology* 63, 114-125.
4. Creed, D. (1984) The Photophysics and Photochemistry of the near-UV absorbing amino-acids .1. Tryptophan and its simple derivatives. *Photochemistry and Photobiology* 39, 537-562.
5. Dose, K. (1968) The photolysis of free cystine in the presence of aromatic amino acids. *Photochemistry and Photobiology* 8, 331-335.
6. Neves-Petersen, M.T., Gryczynski, Z., Lakowicz, J., Fojan, P., Pedersen, S., Petersen, E. and Petersen, S.B. (2002) High probability of disrupting a disulfide bridge mediated by an endogenous excited tryptophan residue. *Protein Science* 11, 588-600.
7. Vanhooren, A., Devreese, B., Vanhee, K., Van Beeumen, J. and Hanssens, I. (2002) Photoexcitation of tryptophan groups induces reduction of two disulfide bonds in goat alpha-lactalbumin. *Biochemistry* 41, 11035-11043.

8. Permyakov, E.A., Permyakov, S.E., Deikus, G.Y., Morozova-Roche, L.A., Grishchenko, V.M., Kalinichenko, L.P. and Uversky, V.N. (2003) Ultraviolet illumination-induced reduction of alpha-lactalbumin disulfide bridges. *Proteins-Structure Function and Genetics* 51, 498-503.
9. Miller, B.L., Hageman, M.J., Thamann, T.J., Barron, L.B. and Schoneich, C. (2003) Solid-state photodegradation of bovine somatotropin (bovine growth hormone): Evidence for tryptophan-mediated photooxidation of disulfide bonds. *Journal of Pharmaceutical Sciences* 92, 1698-1709.
10. Chrysina, E.D., Brew, K. and Acharya, K.R. (2000) Crystal structures of apo- and holo-bovine alpha-lactalbumin at 2.2-Å resolution reveal an effect of calcium on inter-lobe interactions. *Journal of Biological Chemistry* 275, 37021-37029.
11. Chakraborty, S., Ittah, V., Bai, P., Luo, L., Haas, E. and Peng, Z.Y. (2001) Structure and dynamics of the alpha-lactalbumin molten globule: fluorescence studies using proteins containing a single tryptophan residue. *Biochemistry* 40, 7228-7238.
12. Vanhooren, A., Chedad, A., Farkas, V., Majer Z., Van Dael, H., Joniau, M. and Hanssens, I. (2005) Tryptophan to phenylalanine substitution allows to differentiate between short and long range conformational changes during denaturation of goat α -lactalbumin. *Proteins-Structure Function and Genetics* 60, 118-130.
13. Noppe, W., Haezebrouck, P., Hanssens, I. and De Cuyper, M. (1998) A simplified purification procedure of alpha-lactalbumin from milk using Ca^{2+} -dependent adsorption in hydrophobic expanded bed chromatography. *Bioseparation* 8, 153-158.
14. Gill, S.C. and Vonhippel, P.H. (1989) Calculation of protein extinction coefficients from amino-acid sequence data. *Analytical Biochemistry* 182, 319-326.
15. Ellman, G.L. (1959) Tissue sulfhydryl groups. *Arch.Biochem.Biophys.* 82, 70-77..
16. Parker, A. and Engel, P.C. (1999) 5,5'-dithiobis-(2-nitrobenzoic acid) as a probe for a non-essential cysteine residue at the medium chain acyl-coenzyme A dehydrogenase binding site of the human 'electron transferring flavoprotein' (ETF). *Journal of Enzyme Inhibition* 14, 381-390.
17. Sommers, P.B. and Kronman, M.J. (1980) Intermolecular and intramolecular interactions of alpha-lactalbumin - comparative fluorescence properties of bovine, goat, human and guinea-pig alpha-lactalbumin - Characterization of the environments of individual tryptophan residues in partially folded conformers. *Biophysical Chemistry* 11, 217-232.
18. Lakowicz, J. (1983) *Principles of fluorescence spectroscopy*. Plenum Press, New York and London.
19. Chedad, A. and Van Dael, H. (2004) Kinetics of folding and unfolding of goat alpha-lactalbumin. *Proteins-Structure Function and Bioinformatics* 57, 345-356.
20. Grobler, J.A., Wang, M., Pike, A.C.W. and Brew, K. (1994) Study by mutagenesis of the roles of 2 aromatic clusters of alpha-lactalbumin in aspects of its action in the lactose synthase system. *Journal of Biological Chemistry* 269, 5106-5114.

21. Schnaible, V., Wefing, S., Resemann, A., Suckau, D., Bucker, A., Wolf-Kummeth, S. and Hoffmann, D. (2002) Screening for disulfide bonds in proteins by MALDI in-source decay and LIFT-TOF/TOF-MS. *Anal Chem.* 74, 4980-8.
22. Peng, Z.Y., Wu, L.C. and Kim, P.S. (1995) Local structural preferences in the alpha-lactalbumin molten globule. *Biochemistry* 34, 3248-3252.
23. Pike, A.C.W., Brew, K. and Acharya, K.R. (1996) Crystal structures of guinea-pig, goat and bovine alpha-lactalbumin highlight the enhanced conformational flexibility of regions that are significant for its action in lactose synthase. *Structure* 4, 691-703.
24. Hawkins, C.L. and Davies, M.J. (1998) Reaction of HOCl with amino acids and peptides: EPR evidence for rapid rearrangement and fragmentation, reactions of nitrogen-centred radicals. *J. Chem. Soc. Perk. T 2* 1937-1945.
25. Fu, X.Y., Mueller, D.M. and Heinecke, J.W. (2002) Generation of intramolecular and intermolecular sulfenamides, sulfinamides, and Sulfonamides by hypochlorous acid: A potential pathway for oxidative cross-linking of low-density lipoprotein by myeloperoxidase. *Biochemistry* 41, 1293-1301.
26. Malinovskii, V.A., Tian, J., Grobler, J.A. and Brew, K. (1996) Functional site in alpha-lactalbumin encompasses a region corresponding to a subsite in lysozyme and parts of two adjacent flexible substructures. *Biochemistry* 35, 9710-9715.
27. Guex, N. and Peitsch, M.C. (1997) Swiss-model and the Swiss-PDB viewer: an environment for comparative protein modeling. *Electrophoresis* 18, 2714-2723.

Summary, conclusions and perspectives

6.1 Summary

6.2 Conclusions and future perspectives

6.1 Summary

Proteins and enzymes, the most abundant molecules in biology other than water, have a multitude of roles in biological, medical and industrial processes. However, proteins have to convert into a unique structure and remain folded to exert their biological functions. Revealing the characteristics that enhance and -on the contrary- abolish their structure and stability, is hence of particular importance.

To provide further insight in these characteristics, we have analysed the differences in stability and Ca^{2+} binding of two related proteins, goat and bovine α -lactalbumin. To elucidate the implications of UV exposure on the structure and function of proteins, we have studied the photolysis of disulfide bridges in native and recombinant goat α -lactalbumins.

In the absence of Ca^{2+} , BLA is clearly less stable than GLA although both Ca^{2+} bounded forms display similar thermal stability. The results of ITC (isothermal titration calorimetry) indicate that the heat capacity increment (ΔC_p) for the binding of Ca^{2+} is larger for BLA than for GLA. This larger ΔC_p value suggests that binding of Ca^{2+} to BLA induces larger conformational changes than Ca^{2+} binding to GLA. In BLA, 7 amino acids differ from the amino acid sequence of GLA. Inspection of the location of the differing amino acids within the spatial structure of LA reveals that in BLA, Glu 11 contributes to a larger cluster of negative charges. The cluster is composed of the Asp-residues of the calcium binding site, of Glu37 and of Glu7 and Glu11. In GLA the negativity of this region is reduced by the substitution of Glu11 by Lys. The observed difference in ΔC_p values for the binding of Ca^{2+} is presumably in part related to this difference in charge distribution.

While performing fluorescence measurements on α -lactalbumin, we observed unusual fluorescence behaviour of the protein caused by the exposure to near-UV light. Prolonged irradiation induces conformational changes diminishing the ability of LA to act as a co-factor in the lactose synthetase complex. We also observed that the inactivation of LA is accompanied by the rupture of disulfide bridges. More information on the photolyzed disulfide bonds was obtained by MALDI and ESI mass spectrometry of the illuminated, carbamidomethylated and successively digested protein. In our first experiments we could demonstrate that out of the 4 disulfide bonds present in LA, Cys6-Cys120 and Cys73-Cys91 are lysed by irradiation.

Inspection of the protein crystal structure indicated that the bond Cys73-Cys91 is in direct contact with Trp60, in such a way that a direct electron transfer from the excited indole nucleus to the disulfide bond can be realized. However, in the crystal structure, there is no direct contact between the bond of Cys6-Cys120 and the nearest Trp (Trp118). Moreover, no lysis of Cys28-Cys111, which is in direct contact with this Trp, has been found. The results indicate that Trp-mediated photolysis of disulfide bonds not only depends on the distance between Trp and the attacked bond. Stress applied to the disulfide bond may importantly influence its susceptibility for photolytic cleavage.

In order to acquire a better insight in the impact of the photo-excitation of individual Trp residues upon photolysis of disulfide bridges in goat LA, we constructed several mutants in which one Trp or more residues were replaced for a phenylalanine. The recombinant proteins were expressed in *Pichia pastoris* and the spectral characteristics were investigated to obtain information about the local aspects of organization and destabilization within the LA molecule. Comparison of the fluorescence spectra suggested that the fluorescence in GLA mainly results from Trp26 and/or Trp104, which behave as a resonance couple and which are partly quenched by mediation of Trp60 and Trp118. Furthermore, the spectra of GLA mutants with substituted Trp26 and Trp104, respectively, demonstrate that Trp26 and Trp104 do not equally contribute to the fluorescence yield. Especially Trp104 is clearly quenched by an additional residue other than tryptophan. DSC measurements demonstrate that the substitution of Trp26, 60 or 104 by a Phe leads to a lowering of the transition temperature while the effect of the W118F substitution on the conformation and global stability of the mutant is negligible. The existence of specific local rearrangements in the environment of Trp60 and of Trp118 upon GdnHCl-induced denaturation was deduced from the apparent free energies of the transition state obtained from stopped-flow fluorescence measurements. Our findings indicate that in the kinetic transition state the mutation site of W118F loses its native conformation while the native state of the mutation site of W60F is conserved in the kinetic transition state.

The impact of the individual Trp residues on the photolysis of disulfide bonds was examined by comparing the photolytic degradation products of each GLA mutant (W26F, W60F, W104F and W118F) with that of wild type GLA. The MS data of the illuminated, carbamidomethylated and successively digested proteins were obtained with new, advanced mass spectrometers. The new data reveal that besides the disulfide bonds Cys6-Cys120 and Cys73-Cys91, also the disulfide bridges Cys79-Cys93 becomes photolysed. Furthermore, the photolytic reduction of two of these

disulfide bridges leads to the formation of two new crosslinks: a Cys6-Lys122 crosslink and a crosslink between either Cys91-Lys79 or Cys73-Lys 93. The fact that no Cys6-Lys122 crosslink and no carbamidomethylated Cys120 was observed in the mutant W26F suggests that the cleavage of Cys6-Cys120 is exclusively mediated by photoexcitation of Trp26. The rupture of Cys73-Cys91 seems to be mediated in a direct way by Trp104. In all of the recombinant proteins, Cys28-Cys111 seems to resist the Trp mediated photolysis, although it is in close contact with Trp118. Moreover, the substitution of Trp118 induces a diminution in thiol production compared with wild type GLA only in advanced stage of the photolysis experiments. In contrast to the stable Cys28-Cys111 binding, the disulfide bond Cys61-Cys77 has been photolysed in all recombinant proteins indicating that none of the substituted Trp residues in an exclusive way mediates the photoreduction of Cys61-Cys77. As Trp60 strongly enhances the production of free thiols upon illumination and, as Trp60 and Trp104 are in close contact to this disulfide bond, both Trp residues are able to mediate photolysis of this bond. However, for an unambiguous verification of the hypothesis a double mutant with substituted Trp60 and -104 should be constructed.

6.2 Conclusions and future perspectives

We have indications that a region of negative charges within BLA is more sensitive to a Ca^{2+} -dependent conformational change than the corresponding region in GLA. This hypothesis provides a structural basis for the difference in stability of apo-BLA and apo-GLA. To unambiguously prove this hypothesis, we have constructed a GLA mutant in which Lys11 of GLA is mutated to Glu11 of BLA. The stability and thermodynamic parameters of this mutant will be compared with those of GLA and BLA. The study ought to present a clear example of the impact of distinctly localized charges on the thermodynamic parameters which govern protein stability.

In the second part of this thesis, we evidenced that UV illumination of LA degrades its three-dimensional structure and biological function. We have unambiguously provided evidence that the irradiation of LA leads to the Trp-mediated reduction of disulfide bridges. To reveal the impact of the individual Trp residues within this process, several Trp mutants were produced and their structural characteristics were defined. The study of the structural changes and the analysis

of the photoproducts derived from UV exposure of GLA and its mutants, demonstrates that the impact of the four excited Trp residues of GLA on the disulfide cleavage is very different. This is the first report in literature illustrating that each individual Trp residue within a single protein has a unique impact on the photolytic cleavage of disulfide bridges. This knowledge invites us to further determine the factors that govern Trp-mediated photolysis. For this research, synthetic peptides containing Trp residues and disulfide bridges in different relative positions and in presence of groups that may enhance photolysis have been constructed and photolysis experiments are ongoing. Two aspects of the photolytic reduction draw our special attention. First of all, we focus on the role of lysine in the photolytic process. Secondly, we will focus on structural stress exerted on the disulfide bridge. Indeed, the high resistance of Cys28-Cys111 toward photolysis and, conversely, the high sensitivity of Cys6-Cys120 may suggest that the photolytic cleavage strongly depends on the structural stress exerted by the conformational environment.

In addition to the research on lactalbumins and peptides, the study on Trp-mediated reduction of disulfide bridges, will be extended to other physiologically important proteins. In view of the important role played by proteins in industrial and medical practice, it is of the utmost interest to study the impact of irradiation on the functionality and the structure of proteins. In first instance, we will study the influence of illumination on an immunoglobulin. The reason for this is that the immunoglobulin folding motif is characterized by a 'triad' consisting of the two sulphur atoms of a disulfide bond and a vicinal Trp. The study will concentrate on an immunoglobulin fragment containing this folding motif and triad.

Samenvatting - Invloed van hitte en UV bestraling op geit α -lactalbumine

- 7.1 Hoofdstuk 1: Inleiding
 - 7.2 Hoofdstuk 2: Vergelijkende studie van de vouwingstoestand van BLA en GLA
 - 7.3 Hoofdstuk 3: Belichtingsproeven op authentiek geit α -lactalbumine
 - 7.4 Hoofdstuk 4: Invloed van tryptofaan mutaties op de structurele eigenschappen van geit α -lactalbumine
 - 7.5 Hoofdstuk 5: Selectiviteit bij de tryptofaan-gemedieerde reductie van disulfidebruggen
-

7.1 Hoofdstuk 1: Inleiding

Eiwitten controleren en reguleren haast alle chemische processen die deel uit maken van ons leven en liggen aan de basis van bijna alle structurelementen binnenin de cel. Om deze biologische functies te kunnen uitvoeren, moeten eiwitten zich vouwen tot een unieke compacte structuur. Vandaar dat het belangrijk is om de eigenschappen die de structuur en de stabiliteit van een eiwit versterken of vernietigen te bepalen.

De meest gedetailleerde informatie over de manier waarop een eiwit vouwt, wordt verkregen uit studies van kleine eiwitten met minder dan 100 aminozuren omdat het vouwen van deze eiwitten beschreven kan worden aan de hand van een eenvoudig tweetoestanden model. Bij grotere eiwitten wordt het vouwen tot een unieke structuur vaak vooraf gegaan door de vorming van intermediaire vouwingsvormen waarbij vooral veel interesse bestaat voor de *molten globule*. De *molten globule* is een stabiele intermediaire vouwingsvorm, die behoorlijk compact is en gekenmerkt wordt door een vrij labiele tertiaire structuur en een losse stapeling van peptidezijketens. De *molten globule* wordt waargenomen in matig denaturerend midden en werd een tijd lang aanvaard als algemeen voorkomend intermediair in eiwitvorming. Het belang van de *molten globule* tijdens de eiwitvouwing staat momenteel ter discussie. Studies van de structuur en stabiliteit van dergelijke intermediaire vormen hebben echter bijgedragen tot het inzicht dat verschillende segmenten of domeinen binnen een multidomein eiwit onafhankelijk kunnen vouwen. De overgang van de intermediaire vouwingsvorm tot de natieve conformatie, wordt gedreven door het realiseren van optimale zijketeninteracties zoals waterstofbruggen, ionische interacties, Van der Waals interacties en dipool-dipool- interacties.

Het staat vast dat de *molten globule* een belangrijke rol speelt in een hele reeks biologische functies waarbij een gedeeltelijk ontvouwen eiwit noodzakelijk is: translocatie doorheen een membraan, amyloid vorming, dissociatie van supramoleculaire complexen.

Binnenin de cel gebeurt de vouwing van eiwitten met behulp van chaperones (helpereiwitten). Een slecht of verkeerd gevouwen structuur heeft immers drastische gevolgen voor de functionaliteit van het eiwit en kan bovendien leiden tot de vorming van toxische aggregaten in de cel. Ook na de vorming van de intacte structuur, zijn eiwitten voortdurend onderhevig aan denaturerende omstandigheden die hun stabiliteit ondermijnen. In de cel zijn eiwitten immers in

contact met reactieve moleculen zoals zuurstofradicalen, reactieve suikers, enzymen en vetzuren die als detergent optreden. Buiten de cel worden eiwitten, die in de medische of industriële wereld gebruikt worden eveneens blootgesteld aan allerhande denaturerende omstandigheden, zoals hitte of koude, organische solventen en UV bestraling. Om eiwitten efficiënt te gebruiken in industriële en therapeutische toepassingen is het daarom van het grootste belang om de stabiliteit en het vouwingsgedrag te bestuderen en te leren beheersen. Om verder inzicht in deze eigenschappen te verwerven, hebben we de verschillen in stabiliteit en Ca^{2+} -binding van twee verwante eiwitten, geit en bovien α -lactalbumine (LA), bestudeerd (Hoofdstuk 2). Tijdens deze fysico-chemische studie merkten we op dat de LA bij bestraling met nabij UV-licht, structurele veranderingen ondergaat die verhinderen dat ze als co-factor kunnen werken in lactose-synthetase. In Hoofdstuk 3 tonen we aan dat het inactiveren van LA gepaard gaat met het splitsen van disulfidebruggen. De gevoelige disulfidebruggen bevinden zich in de onmiddellijke omgeving van een tryptofaan. Om de invloed van foto-excitatie van de indool-groepen van Trp op het doorbreken van disulfidebruggen nader te onderzoeken, zijn we overgegaan tot de constructie en productie van tryptofaanmutanten waarin één of meerdere tryptofanen veranderd werden in een fenylalanine. Nadat de spectrale eigenschappen van deze recombinante eiwitten bepaald werden (Hoofdstuk 4), hebben we verder nagegaan in welke mate de vier tryptofanen in LA essentieel zijn om de splitsing van deze disulfidebindingen te initiëren (Hoofdstuk 5).

7.2 Hoofdstuk 2: Vergelijkende studie van de vouwingstoestand van BLA en GLA

Lactalbumines zijn kleine globulaire eiwitten. De 2 domeinen waaruit deze globulaire eiwitten bestaan, worden door een diepe kloof van elkaar gescheiden. De variant uit geitenmelk (GLA) bestaat uit 123 aminozuren. Het α -helix domein bestaat uit de residu's 1-39 en 85-123. Het domein met de residu's 40-84 is gekenmerkt door zijn β -structuur. De lus met de residu's 79-88 verbindt beide subdomeinen en is Ca^{2+} -bindend. De ontvouwing van LA is uitvoerig bestudeerd omdat het eiwit een gemakkelijk toegankelijke, intermediair gevouwen *molten globule* toestand aanneemt in zwak denaturerende omstandigheden. GLA bevat 4 Trp-groepen en 4 disulfidebruggen. De Trp-groepen hebben de sequentiënummering 26, 60, 108 en 118. De disulfidebruggen verbinden de residu's 6-120, 28-111, 61-77 en 73-91.

De variant uit koemelk (BLA) verschilt slechts 7 aminozuren van GLA. In afwezigheid van Ca^{2+} is BLA duidelijk minder stabiel dan GLA, de Ca^{2+} -gebonden vormen zijn ongeveer even stabiel. Met behulp van ITC (*isothermal titration calorimetry*) kon aangetoond worden dat de verandering in warmtecapaciteit (ΔC_p) voor Ca^{2+} -binding duidelijk groter is voor BLA dan voor GLA. De grotere ΔC_p -waarde toont aan dat BLA een grotere conformatie-verandering ondergaat bij het binden van Ca^{2+} dan GLA. We konden verder aantonen dat hoofdzakelijk de component van ΔC_p die met Ca^{2+} -binding verbonden is, groter is in BLA dan in GLA. Daarom moet de grotere conformatie-verandering vooral in de nabijheid van de Ca^{2+} -bindende site gezocht worden. Aan de hand van de locatie van de 7 aminozuren hebben we gezocht naar een mogelijke verklaring voor de grotere conformatie-verandering. We stelden vast dat Glu11 (BLA) midden in een grote cluster van negatief geladen aminozuren ligt waar o.a. de Asp-residues van de Ca^{2+} -bindende lus (Asp83, 84, 87, 88) deel van uitmaken en waarbij ook Glu7, via Glu11, op aansluit. In GLA is de negatieve lading van deze cluster gereduceerd door substitutie van Glu11 door een Lys. We vermoeden dat deze regio meer ontvouwen is in BLA dan in GLA en daarom verantwoordelijk is voor de lagere stabiliteit van Ca^{2+} -vrij BLA. Bij het binden van Ca^{2+} zou in hoofdzaak deze regio een grotere conformatie-verandering ondergaan in BLA dan in GLA.

7.3 Hoofdstuk 3: Belichtingsproeven op authentiek geit

α -lactalbumine

Tijdens de fysico-chemische studies op natief GLA merkten we dat het eiwit een opmerkelijke toename van de fluorescentie verkrijgt bij bestraling met licht uit het golflengtegebied van 280-295 nm. We konden aantonen dat de fluorescentie-verandering gepaard gaat met het splitsen van disulfidebruggen en daarom het gevolg is van conformatie-veranderingen bij het doorbreken van de disulfidebruggen. Meer informatie over de aard van de doorbroken disulfidebruggen werd verkregen door het belichte GLA eerst te behandelen met joodacetamide waardoor de vrije thiolgroepen gecarbamidomethyleerd worden, het vervolgens te fragmenteren met trypsine om tenslotte, via MALDI- en ESI- massaspectrometrie, de aard van het bekomen fragment te analyseren. Uit deze eerste analyse kunnen we de splitsing van 2 disulfidebruggen aantonen: Cys6-Cys120 en Cys73-Cys91. Uit de kristalstructuur (PDB-code: 1HFY) blijkt dat er een direct

Van der Waals contact is tussen Trp60 en de S-atomen van de gesplitste Cys73-Cys91 brug, waardoor eventueel een directe elektron-transfer mogelijk is van de geëxciteerde Trp naar de betrokken disulfide-brug. In de kristalstructuur is er echter geen direct contact tussen de S-atomen van Cys6-Cys120 en de dichtstbij zijnde Trp (Trp118). Daarentegen is er wel een direct contact tussen Trp118 en de S-atomen van Cys28-Cys111. Dit speciaal gedrag nodigt ons uit om in de verdere studie de inbreng van de individuele Trp groepen meer gedetailleerd te onderzoeken door systematisch een Trp te muteren naar een Phe in GLA.

Bij de fotolytische splitsing van een disulfidebrug, die via een geëxciteerde Trp-groep wordt geïnduceerd, wordt telkens slechts één vrije thiol-groep gevormd. Bij de fotolytische splitsing van Cys73-Cys91, werd enkel één vrije thiol-groep op het fragment met Cys91 vastgesteld. Bij de fotolytische splitsing van Cys6-Cys120 kon alleen op het fragment met Cys120 een vrije thiol-groep worden waargenomen.

7.4 Hoofdstuk 4: Invloed van tryptofaan mutaties op de structurele eigenschappen van geit α -lactalbumine

De vorige studies laten vermoeden dat de fotolytische splitsing van disulfide-bridgen en de daaraan gekoppelde destabilisatie van GLA geïnduceerd wordt door de lichtabsorptie van Trp residuen. Vandaar dat we zijn overgegaan tot de constructie en productie van wild type GLA en van mutanten waarin telkens 1 of 2 Trp residuen vervangen werden door fenylalanine. De structurele eigenschappen van de recombinante eiwitten werden bestudeerd om de lokale organisatie en destabilisatie binnen het eiwit te verhelderen. Fluorescentie studies die op deze mutanten werden uitgevoerd maken duidelijk dat de fluorescentie van Trp60 en van Trp118 aanzienlijk gedoofd worden. De nabije disulfidebridgen lijken direct verantwoordelijk voor deze *quenching*. Trp26 en Trp104, verantwoordelijk voor de fluorescentie van *wild type* GLA, gedragen zich als een resonantiekoppel en worden beide gequencht door de overige tryptofanen. Bovendien blijkt dat Trp 104 nog door een ander aminozuur uitgedoofd wordt. Via fluorescentie, DSC- en CD-metingen konden we aantonen dat de mutatie van Trp118 naar Phe de secundaire structuur en de transitietemperatuur van het eiwit niet beïnvloedt. Daarentegen induceert de substitutie van Trp60, Trp26 of Trp104 wel een afname van de transitietemperatuur van het eiwit. Met de stopped-flow techniek werden ook de kinetische aspecten van de transitie bepaald

en vergeleken. Hieruit blijkt dat in de kinetische transitietoestand de omgeving van Trp118 ontvouwen is en de omgeving van Trp60 gevouwen is.

7.5 Hoofdstuk 5: Selectiviteit bij de tryptofaan-gemedieerde reductie van disulfidebruggen

Voor alle recombinante eiwitten hebben we verschillende karakteristieken gevolgd die een aanduiding kunnen geven over de fotolytische degradatie (o.a. vorming van thiol-groepen, fluorescentie-verandering, afname van de ellipticiteit in het nabije UV). De karakteristieken werden gevolgd in functie van de bestralingsdosis bij 290 nm. Uit de bepaling van de vrije thiolen blijkt dat in GLA, elke tryptofaan een rol heeft in het breken van disulfidebruggen. De rol van Trp 118 lijkt echter beperkt tot het doorbreken van disulfidebruggen in reeds beschadigd GLA. Massaspectrometrie wijst uit dat er geen enkele disulfidebrug is waarvan de splitsing exclusief kan toegeschreven worden aan Trp60 of aan Trp118. Daarentegen is Trp26 specifiek verantwoordelijk voor het breken van Cys6-Cys120. De fotolytische splitsing van Cys73-91 wordt geïnduceerd door lichtabsorptie van Trp104. Met de bovenstaande techniek kan eveneens aangetoond worden dat bij de fotolytische splitsing van Cys6-Cys120, alleen op het fragment met Cys120 een vrije thiol-groep kan worden waargenomen. Het tweede thiol (Cys6) gaat een verbinding aan met Lys122. Ook bij het splitsen van Cys61-Cys77 en van Cys73-Cys91 wordt enkel één vrije thiol per disulfidebrug teruggevonden nl. op Cys61 en op Cys91. Bij het splitsen van Cys73-Cys91 kan eveneens een cysteine-lysine verbinding waargenomen worden.

Publications

Vanhooren, A., Vanhee, K., Noyelle, K., Majer, Z., Joniau, M. and Hanssens, I. (2002) Structural basis for difference in heat capacity increments for Ca^{2+} binding to two α -lactalbumins. *Biophys. J.* 82, 407-417.

Vanhooren, A., Devreese, B., Vanhee, K., Van Beeumen, J. and Hanssens, I. (2002) Photo-excitation of tryptophan groups induces reduction of two disulfide bonds in goat- α -lactalbumin. *Biochemistry* 41, 11035 – 11043.

Van Dael, H., Chedad, A., **Vanhooren, A.** and Hanssens, I. (2005) Influence of experimental conditions and Trp mutations on the stability and the folding characteristics of goat α -lactalbumin. *J. Mol. Struct.* 744-747, 155-160.

Vanhooren, A., Chedad, A., Majer, Z., Joniau, M., Van Dael, H. and Hanssens, I. (2005) Tryptophan to phenylalanine substitution allows to differentiate between short and long range conformational changes during denaturation of goat α -lactalbumin. *Proteins* 60, 118-130.

Chedad, A., Van Dael, H., **Vanhooren, A.** and Hanssens, I. (2005) Influence of Trp-mutation on the native, the intermediate and the transition states of goat α -lactalbumin: an equilibrium and kinetic study. Accepted to be published in *Biochemistry*.

Dankwoord

Een doctoraat behaal je niet alleen, een heleboel mensen hebben meegeholpen om dit project tot een goed einde te brengen. Een woordje van dank is hier dus zeker op zijn plaats.

Eerst en vooral wil ik mijn promotor Prof. dr. Ignace Hanssens danken voor zijn vakkundige begeleiding, zijn enthousiasme en de vlotte samenwerking.

Eveneens een woord van dank aan de juryleden, Prof. dr. H. Deckmyn, Prof. dr. B. Devreese Prof. dr. Y. Engelborghs, Prof. dr. A. Matagne en Prof. dr. H. Van Dael, voor het kritisch nalezen van dit werk en voor de waardevolle opmerkingen.

Dank aan Prof. dr. J. Van Beeumen, Prof. dr. B. Devreese en de medewerkers van hun labo voor de vele massa-analyses die voor ons onderzoek van onschatbare waarde waren.

I would like to thank Prof. dr. Z. Majer and her staff to introduce me in the world of peptide synthesis. Moreover, I appreciate the warm welcome and friendship during my stays in Budapest.

Prof. dr. M. Joniau ben ik dankbaar voor de interessante discussies en raadgevingen.

Een speciaal woordje van dank aan Christiane, Linda, Nicole en Wim voor de enorme inzet bij de productie van onze 'mutantjes'. Dank ook aan al mijn (ex-)collega's voor de hulp bij de spectroscopische metingen en de wetenschappelijke (en minder wetenschappelijke) discussies.

Ik wil ook alle IRC-leden en andere collega's van de KULAK danken voor de praktische hulp, de interesse en de aangename babbels.

Zeker niet te vergeten zijn mijn ouders, tante, broer, schoonzus, familie en vrienden. Dank voor de steun, de interesse en de gezellige onderonsjes.

Ten slotte wil de drie personen die met het liefst zijn - Jean, Bran en Moira- bedanken voor hun steun en liefde.

Ann.